

Washington University in St. Louis

Washington University Open Scholarship

Arts & Sciences Electronic Theses and
Dissertations

Arts & Sciences

Spring 5-15-2018

Circadian Regulation of Temozolomide Sensitivity in Glioblastoma

Emily A. Slat

Washington University in St. Louis

Follow this and additional works at: https://openscholarship.wustl.edu/art_sci_etds



Part of the [Biology Commons](#), [Cell Biology Commons](#), and the [Medicine and Health Sciences Commons](#)

Recommended Citation

Slat, Emily A., "Circadian Regulation of Temozolomide Sensitivity in Glioblastoma" (2018). *Arts & Sciences Electronic Theses and Dissertations*. 1581.

https://openscholarship.wustl.edu/art_sci_etds/1581

This Dissertation is brought to you for free and open access by the Arts & Sciences at Washington University Open Scholarship. It has been accepted for inclusion in Arts & Sciences Electronic Theses and Dissertations by an authorized administrator of Washington University Open Scholarship. For more information, please contact digital@wumail.wustl.edu.

WASHINGTON UNIVERSITY IN ST. LOUIS

Division of Biology and Biomedical Sciences
Neurosciences

Dissertation Examination Committee:

Erik Herzog, Chair
Joshua Rubin, Co-Chair
Paul Taghert
Kathy Weilbaecher
Zhongsheng You

Circadian Regulation of Temozolomide Sensitivity in Glioblastoma

by

Emily Ann Slat

A dissertation presented to
The Graduate School
of Washington University in
partial fulfillment of the
requirements for the degree
of Doctor of Philosophy

May 2018
St. Louis, Missouri

© 2018, Emily Ann Slat

Table of Contents

List of Figures	iv
List of Tables	v
Acknowledgments.....	vi
Abstract	ix
Chapter 1: Introduction.....	1
Table 1.1.	4
Table 1.2.	7
Figure 1.1	18
Figure 1.2	22
Chapter 2: Characterization of circadian rhythms in gene expression and TMZ sensitivity in U87 glioma cell line <i>in vitro</i>	33
Abstract.....	34
Introduction.....	35
Materials and Methods.....	36
Results.....	38
Table 2.1	39
Figure 2.1	40
Figure 2.2	43
Figure 2.3	45
Figure 2.4	48
Discussion.....	50
References.....	55
Chapter 3: <i>Bmal1</i> -dependent rhythms in temozolomide sensitivity in Mes-GBM astrocytes <i>in vitro</i>	58
Abstract.....	59
Introduction.....	59
Materials and Methods.....	62
Results.....	68
Table 3.1	69
Figure 3.1	71
Table 3.2	74

Figure 3.2	75
Figure 3.3	79
Figure 3.4	82
Discussion	83
Acknowledgements	86
References	87
Chapter 4: Circadian clock gene expression and TMZ chronotherapy of glioblastoma models <i>in vivo</i>	94
Abstract	95
Introduction	95
Materials and Methods	99
Results	105
Figure 4.1	106
Figure 4.2	109
Figure 4.3	113
Figure 4.4	116
Figure 4.5	119
Discussion	121
Acknowledgements	125
References	126
Chapter 5: Discussion	132
Circadian oscillations in clock gene expression in GBM <i>in vitro</i> and <i>in vivo</i>	134
Time of day-dependent rhythms in response to temozolomide treatment <i>in vitro</i>	137
Where does the cell-intrinsic rhythm in TMZ response originate?	138
Role of <i>Bmal1</i> in temozolomide sensitivity	140
Role of <i>Bmal1</i> in GBM tumorigenesis <i>in vivo</i>	143
Temozolomide chronotherapy of GBM <i>in vivo</i>	143
Clinical Applications of Chronotherapy for Brain Cancer	146
Conclusions	148
References	149

List of Figures

Figure 1.1.....	18
Figure 1.2.....	22
Figure 2.1.....	40
Figure 2.2.....	43
Figure 2.3.....	45
Figure 2.4.....	48
Figure 3.1.....	71
Figure 3.2.....	75
Figure 3.3.....	79
Figure 3.4.....	82
Figure 4.1.....	106
Figure 4.2.....	109
Figure 4.3.....	113
Figure 4.4.....	116
Figure 4.5.....	119

List of Tables

Table 1.1:4
Table 1.2:7
Table 2.1:39
Table 3.1:69
Table 3.2:74

Acknowledgments

Special thanks for technical assistance from Tatiana Simon, Najla Kfoury, Nicole Warrington, Stacey Ward, Jasmin Sponagel and Andrea Binz. Constructive critiques and helpful scientific discussions were provided by many members of the Rubin and Herzog labs. Thanks to Daniel Granados-Fuentes, Tao Sun, Stacey Ward and Nicole Warrington for expert advice. Thanks to Cell-Cell Communication in Cancer, Clocksclub and Bioforum Seminars for providing scientific feedback on my project. Shondra Miller and the Genome Engineering Center for consultation and gRNA Cas9-CRISPR design and production. Andrew Liu provided the *Bmal1::dLuc* and *Per2::dLuc* lentiviruses. The caspase-3 bioluminescence reporter was provided by Dr. Alnawaz Rehemtulla (University of Michigan, Michigan, MI). Chronostar V2.0 was generously provided by B. Meier and A. Kramer.

This work was supported by funding from the Children's Discovery Institute (J.B.R. and E.D.H.) and NIGMS 9687304 (E.D.H.).

I would like to thank all of the scientific mentors I have had throughout my education and scientific training. I would like to especially thank my undergraduate mentor, Dr. Lori Isom, who helped me find my scientific path, which led me to my training here at Wash U. I am thankful to all of the people in the Isom lab, my first lab family, especially Dr. Dyke McEwen, a former graduate student in the Isom lab.

I am thankful to Dr. Erik Herzog and Dr. Josh Rubin for their time, energy, patience and enthusiasm. They have always encouraged my scientific curiosity and pushed me to think about all possible interpretations and implications of my work. Their mentorship has prepared me to become an independent scientist, which I appreciate more than words can say.

I would like to thank my thesis committee for their time, patience and helpful advice.

I am so thankful to all of my lab mates in both of my labs. Your scientific expertise has been an incredible resource to me. Critiques of my work during lab meeting presentations have improved my science and the way I present it to the scientific community. It has been a joy and an honor to work with all of you for the last four years.

Thanks to my family and friends, who have loved, supported, and encouraged me through all of the ups and downs of graduate school. Thank you from the bottom of my heart. I love you all very, very much. Finally, I thank my wonderful, supportive and loving boyfriend, Ian.

Emily Slat

Washington University in St. Louis

May 2018

This thesis is dedicated to my brother, Andy.

His determination, curiosity and passion for science inspire my every day.

ABSTRACT OF THE DISSERTATION

Circadian Regulation of Temozolomide Sensitivity in Glioblastoma

by

Emily Ann Slat

Doctor of Philosophy in Biology and Biomedical Sciences

Neurosciences

Washington University in St. Louis, 2018

Dr. Erik Herzog, Chair

Dr. Joshua Rubin, Co-Chair

The safety and efficacy of multiple cancer chemotherapeutics can vary as a function of when during the day they are delivered. This study aimed to improve the treatment of glioblastoma multiforme (GBM), the most common brain cancer, by testing the efficacy of the DNA alkylator Temozolomide (TMZ) on GBM *in vitro* and *in vivo* as a function of time of day. We found cell-intrinsic, daily rhythms in susceptibility of GBM tumor cells (mouse astrocytes deficient in NF1 and p53 signaling) to TMZ *in vitro*. The greatest TMZ-induced DNA damage response, activation of apoptosis and growth inhibition, occurred near the peak expression of the core clock gene *Bmal1* in cultured GBM cells. Deletion of *Bmal1* abolished rhythmic circadian clock gene expression and circadian rhythms in TMZ-induced activation of apoptosis and growth inhibition in GBM tumor cells *in vitro*. Taken together, these data suggest an important role for the core molecular clock in regulating the tumor cell-intrinsic response to TMZ-induced DNA damage. These results may be important broadly for how we design TMZ and other DNA damaging approaches to GBM treatment.

Chapter 1: Introduction

Overview

This thesis brings together two fields of study: neuro-oncology and chronobiology. The studies performed to complete this thesis harness the power of circadian biology to improve upon current treatments of glioblastoma multiforme (GBM). This introduction reviews the research that has illuminated the molecular biology underlying brain tumor biology. We propose that timing the delivery of chemotherapy to biological rhythms within brain tumor cells, a concept known as chronotherapy, will provide a new opportunity to improve clinical outcomes for a patient population in desperate need for improvements in current therapies. To help you understand how chronotherapy works, this introduction will describe daily rhythms in behavior, physiology and cellular processes and how they can impact the response of the tumor and the host organism to chemotherapy.

The History of Gliomas

While studying a brain tumor at gross and microscopic levels in 1863, Dr. Rudolf Virchow described similarities between the morphology of the tumor and healthy glia. He created the term “glioma” to describe these glia-like tumor cells [1]. In an effort to improve the classifications of gliomas, Dr. Percival Bailey, under the tutelage of Dr. Harvey Cushing, examined 414 pathological glioma specimens and corresponding clinical records. Bailey was able to divide these tumors into 13 categories. In 1926, Drs. Percival Bailey and Harvey Cushing published this new classification system in “A Classification of the Tumors of the Glioma Group on a Histogenetic Basis with a Correlated Study of Prognosis.” This book described a grading system for gliomas using histological characteristics of the resected tissue as well as clinical records, which provided the first demonstration of the prognostic value of microscopic histology of brain tumors[2]. This system of categorization formed the basis for all future glioma

classification systems, including the currently used classification guidelines of the World Health Organization (WHO). The WHO grading system takes into account nuclear atypia, mitotic figures, microvascular proliferation and necrosis to categorize gliomas. Astrocytic tumors are divided into 4 different grades, with the most malignant tumors in the highest grade (summarized in **Table 1.1**). Within the WHO classification system of grade IV astrocytomas, there are 3 clinico-pathological variants of glioblastoma with distinct International Classification of Diseases for Oncology (ICD-O) codes: classical, gliosarcoma and giant cell glioblastoma. There are other patterns of pathology in addition to these variants, including small cell glioblastoma and glioblastoma with oligodendroglioma component [3]. Recently recognized GBM variants include Fibrillary/epithelial GBM, Small cell astrocytoma , GBM with primitive neuroectodermal tumor , GBM with oligodendroglioma component, gemistocystic astrocytoma, granular cell astrocytoma and pediatric high grade glioma (HGG), diffuse intrinsic pontine glioma (DIPG) [4]. These emerging GBM subtypes will likely become WHO-recognized variants if the subtype has unique molecular features and prognostic value (Table 2,[4]).

Table 1.1. WHO Classification of Astrocytic Tumors (adapted from Louis, DN et al. 2007[3])

WHO Grade	I	II	III	IV
Pilocytic astrocytoma	x			
Subependymal giant cell astrocytoma	x			
Diffuse astrocytoma		x		
Pilomyxoid astrocytoma		x		
Pleomorphic xanthoastrocytoma		x		
Anaplastic astrocytoma			x	
Glioblastoma				x
Giant Cell glioblastoma				X
Gliosarcoma				X

The most aggressive astrocytoma, glioblastoma multiforme (GBM), accounts for 15.6% of all primary brain and central nervous system (CNS) tumors and 54.4% of all gliomas [5]. Neoplasms are rare in children, but brain and CNS tumors are the most common type of cancer among children and adolescents, ages 0 to 19 years, with an annual age-adjusted incidence rate of 5.42 per 100,000 in the United States [6]. Pediatric high grade gliomas (HGGs) combine GBM, anaplastic astrocytoma and diffuse intrinsic pontine gliomas (DIPGs) and occur with a frequency of 0.8 per 100,000 children diagnosed per year[7]. Pediatric GBM accounts for only approximately 3% of CNS tumors in children and adolescents, age 0 to 19 years [4, 5]. Long-term survival of pediatric GBM is greater for infants compared to older children [4, 8, 9]. Unlike adult GBM, pediatric HGGs frequently have driver mutations in key epigenetic regulators.

Mutations in the gene encoding Histone H3.3 change lysine residues in the histone tail (K27M, G34R or G34V). Mutations in histone H3.1 (K27M mutations in HIST1H3B or HIST1H3C) occur in 12-31% of pediatric HGGs, but have never been found in adult GBM [7]. These mutations alter post-translational modifications of these histone proteins, changing epigenetic regulation and causing dramatic changes in gene expression [10]. Brain and CNS tumors occur at a higher rate in adults, with an annual age-adjusted incidence rate of 27.86 per 100,000 in the United States [6]. Adult GBM can be divided into two clinical subcategories: primary and secondary GBM. Primary GBM develops *de novo* and has a mean age of onset at 62 years. Primary GBM accounts for 90-95% of all GBM and is associated with a worse prognosis. Secondary GBM arises from grade II or III astrocytomas, accounting for only 5-10% of all GBM [11-13]. Secondary GBM has a younger mean age of onset (45 years), far more frequent mutations in isocitrate dehydrogenase I (IDH1; 70% of secondary GBM versus <5% of primary GBM; [7]) and better prognosis (overall survival of 12-36 months for secondary GBM vs 6-12 months for primary GBM; [11, 13]). Across the globe, GBM affects more males than females. This is true for pediatric and adult GBM [14]. Clinical features of GBM help us predict outcomes for future patients, but we need to understand more about the underlying biology of GBM in order to create better treatments.

GBM has recently been divided into subtypes based on genetic alterations. The majority of GBM tumors occur *de novo*, classifying them as primary GBM. Gene expression profiling of GBM has led to subclassification based on dominant genetic alterations. Phillips and colleagues used DNA microarray to divide 107 high grade gliomas into three molecular subclasses: mesenchymal, proliferative and proneural [15]. Using glioma expression profiles from The Cancer Genome Atlas (TCGA) database, Verhaak and colleagues described four molecular

subtypes: classical, proneural, neural and mesenchymal [16]. There were great similarities among the proneural groups between Phillips and Verhaak. The same was true for mesenchymal subtypes created by each research group [11]. The proliferative subtype defined by Phillips and colleagues was further subdivided into classical and neural by Verhaak and colleagues. Some experts suggest these subtypes are simply mesenchymal or proneural, with higher levels of genetic alterations associated with cell cycling and proliferation [17]. When comparing the clinical features of proneural to mesenchymal in both studies, the PN subtype is more commonly associated with secondary GBM and better clinical outcomes [11]. MES subtype is associated with older patients, a worse prognosis and is more frequently seen in recurrent GBMs [11].

The subtyping created by Verhaak et al., is more frequently cited by brain tumor biologists and neuro-oncologists. According to Verhaak's study, classical was associated with amplification of chromosome 7, loss of chromosome 10 and frequent EGFR amplification and CDKN2A loss. Many tumors belonging to the proneural subtype had high expression of PDGFRA and frequent point mutations in IDH1. Neural was classified by expression of neuronal markers, like NEFL, GABRA1, SYT1 and SLC12A5. The most common genetic alterations in the mesenchymal subtype were mutation or loss of neurofibromin 1 (NF1), mutation of PTEN or TP53 [15, 16]. The genetic alterations described by the Phillips and Verhaak studies are summarized in **Table 2**. These molecular subclasses allow us to model common genetic alterations in our research in order to gain greater understanding of the molecular mechanisms driving glioma tumorigenesis and response to therapies. The murine glioblastoma model used in our studies mimics mesenchymal GBM by simulating mutations of NF1 and TP53, two of the most common genetic alterations of that subtype.

Table 1.2. Summary of molecular subtyping of gliomas, according to Phillips and Verhaak studies (modified from Morokoff et al, 2015 [11]).

Glioma Type	Glioma subtypes by Phillips et al. 2006	Glioma subtypes by Verhaak et al. 2010	Clinical Features	Genes or chromosomes amplified or overexpressed	Genes or chromosomes deleted, mutated or downregulated
Grade III glioma	Proneural (31%)	Proneural (20%)	Better prognosis, younger age	PDGFRA amplification, MYC amplification, OLIG2, PI3K/mTOR, Hedgehog, Wnt, Notch, CDK4 amplification, SOX2 amplification, DCX, DLL3, ASCL1, TCF4, CXCR4, ALT-Positive	IDH1 mutations (common), TP53 mutations, ATRX, 1p/19q loss, CIC, TERT, FUBP1, COX2, IGFBP2, Annexin1, TAZ, PIK3CAP/PIK3R1, 4EBP1
Secondary GBM					
Primary GBM					
	Neural (17%)	No data	NEFL, GABRA1, SYT1, SLC12A5 (neuronal markers)	No data	

	Mesenchymal (49%)	Mesenchymal (33%)	Worse prognosis, older age, recurrent tumors, angiogenic, necrotic, inflammatory infiltrates, MRI enhancing	EGFR, PI3K/Akt, CHI3L1, YKL40, vimentin, MET, CD44, MERTK, TGFbeta/BMP TNF Family, NF- kappaB, CXCR4, CD31, VEGFR-2, S6-kinase, Snail	NF1 loss/mutation , TP53 mutations, PTEN, TSC2, tuberin
--	----------------------	----------------------	---	---	---

As clinical treatments for gliomas have changed over time, prognosis has gradually improved. As early as 1884, neurosurgeons were removing brain tumors with very small impact on patient survival. Even Dr. Walter Dandy's radical hemispherectomies were not sufficient to eliminate GBM from the brain. The diffuse spread of GBM through the brain made it difficult to remove the tumor in its entirety. Other methods were required to eliminate the tumor cells that could not be removed surgically. In the 1950s, physicians started to use radiation therapy to treat high grade gliomas. In 1958, Frankel and German published a study demonstrating a significant increase in survival for high-grade glioma (HGG) patients who received radiation therapy after surgical resection [18]. Some of the chemotherapies originally developed for the treatment of leukemias and other solid tumors had good penetration of the blood brain barrier; these therapies were tested in high grade glioma patients [19]. Nitrosurea, a DNA alkylator, provided a modest improvement in survival to patients with grade III or IV astrocytomas, but the addition of other chemotherapies did not improve patient survival [20]. Clinicians and scientists spent decades trying to find new ways to improve upon the current treatments. Many chemotherapeutics were used, but only one blood brain barrier- permeable DNA alkylator was able to extend survival

beyond surgical resection and radiation therapy. In 2005, Stupp and colleagues ushered in a new age of glioblastoma treatment: the Temozolomide era.

The Temozolomide Era of GBM Therapy

In a landmark study published in the New England Journal of Medicine, Stupp and colleagues improved GBM outcomes by administering radiation therapy and temozolomide (TMZ) chemotherapy concomitantly, followed by a course of adjuvant TMZ therapy. The addition of the DNA alkylator TMZ extended median survival by 2.5 months compared to surgical resection and radiation therapy alone. Despite this minor lengthening of median survival, the addition of concomitant and adjuvant TMZ led to a more than two-fold increase in 2-year overall survival (10% to 27%; [21]). After decades of clinical trials providing no significant benefit to GBM patients, the seemingly modest lengthening of survival provided by temozolomide is a major advancement.

At physiologic pH, TMZ spontaneously converts to its active metabolite, monomethyl triazenoimidazole carboxamide (MTIC). MTIC methylates DNA bases at a variety of locations, including positions N7 and O6 on guanine. The O6-methyl-guanine modification is the most toxic lesion created by MTIC. Errors in repair by the mismatch repair system lead to double strand breaks, DNA damage response and apoptosis.

The most completely described mechanisms of resistance to TMZ are modifications in DNA repair. Loss of DNA mismatch repair prevents the formation of DNA double strand breaks, rendering cells resistant to TMZ therapy [22]. The DNA repair enzyme O6-methylguanine-DNA methyltransferase (MGMT) is a suicide enzyme which undergoes degradation after removing a methyl group from DNA. Overexpression of MGMT leads to resistance through a higher rate of

removal of the DNA methylation caused by MTIC. If the MGMT enzymes outnumber the O6-methylguanines, the tumor cell will avoid activation of the DNA damage response and subsequent cell death. Silencing of MGMT expression by methylation of the MGMT promoter is seen in some GBM patients. These patients derive greater benefit from radiation and TMZ concomitant therapy than patients with no methylation of the MGMT promoter [23]. Since the publication of that study, MGMT promoter methylation status has been used as a biomarker to guide treatment of GBM [24]. The human U87MG glioblastoma cell line used in this thesis has hypermethylation of the MGMT promoter, silencing expression of this enzyme and rendering these cells more susceptible to TMZ-induced cell death [25]. The MGMT promoter methylation status of our mouse model of mesenchymal GBM (Mes-GBM astrocytes) is currently unknown. Thus, two DNA repair mechanisms, MGMT and MMR activity, contribute to TMZ resistance in glioma cells.

Despite initial response to standard therapy of surgical resection, radiotherapy with TMZ and 6 cycles of adjuvant TMZ, GBM prognosis remains poor with a median survival of 14.6 months [26]. Development of new therapies is important, but equally important is the optimization of currently available therapies for patients who are fighting to survive brain tumors now.

Chronotherapy: Application to cancer patients

Chronotherapy is the improvement of treatment outcomes by minimizing treatment toxicity and/or maximizing efficacy through delivery of a medication according to biological rhythms within a patient [27]. This concept has been applied to a variety of medications, including chemotherapeutics.

The most successful application of chronotherapy was to the treatment of children with acute lymphoblastic leukemia (ALL). Between 1976 and 1984, Rivard and colleagues reviewed

the charts of 118 pediatric ALL patients receiving maintenance chemotherapy of daily 6-mercaptopurine (6-MP) and weekly methotrexate (MTX) in the morning or evening. Of the 118 patients, 82 received 6-MP and MTX in the morning, while the remaining 36 received the same medications in the evening. Disease-free survival was longer for children receiving 6-MP in the evening [28]. Based on the exciting results of this retrospective study, Schmiegelow and colleagues designed a prospective trial to examine the progression-free survival of 294 children with non-B cell ALL treated with 6-MP and MTX in the morning versus evening, or on a miscellaneous schedule. ALL patients treated in the evening had a significantly higher probability of event-free survival (0.82 evening versus 0.57 morning, $p = 0.0002$). This difference resulted in a 2.56-fold increase in the risk of relapse for children receiving 6-MP and MTX in the morning [29, 30]. This was the most successful chronotherapy trial and, consequently, evening 6-MP dosing is now the accepted standard of care for children with ALL.

Chronochemotherapy has also improved anti-tumor effect in the treatment of metastatic colon cancer. The anti-metabolite 5-fluorouracil (5-FU) is commonly delivered by flat rate infusion. Despite the constant infusion rate, the mean plasma 5-FU concentration fluctuated over time [31]. Studies have identified rhythmic activity of the enzymatic target of 5-FU, thymidylate synthase [32], and an anti-phase rhythm in dihydropyrimidine dehydrogenase (DPD), an enzyme involved in catabolism of 5-FU [33]. Before applying this knowledge to the treatment of patients, a mouse study demonstrated daily rhythms in toxicity to the maximal 5-FU dose, correlating with DPD activity [34]. Metastatic colorectal cancer patients received constant infusions of 5-fluorouracil (5-FU), leucovorin and oxaliplatin, or a chronomodulated delivery of those three drugs for 5 consecutive days per cycle. Chronomodulated delivery consisted of oxaliplatin administration for 11.5 hours (1015 to 2145) with peak delivery at 1600 hours, followed by

delivery of 5-FU and leucovorin from 2215 to 0945 hours, with peak delivery at 0400 hours. The chronomodulated delivery schedule increased the rates of grades 3 and 4 nausea and vomiting and caused a 4-fold increase in peripheral neuropathy compared to constant infusion. However, chronomodulated therapy caused lower rates of grades 3 or 4 mucositis, which is a major dose-limiting toxicity for this treatment protocol. The median overall survival of all patients was 4.1 months longer for chronomodulated vs constant infusion schedule patients (19 vs 14.9 months, $p = 0.03$;[35]). Despite the success of this trial, as well as the 329 citations of this article, chronomodulated therapy is not common practice in the treatment of colorectal cancer patients.

Chronotherapy with other chemotherapeutics has been successful in the treatment of ovarian cancer patients. Delivery of doxorubicin in the morning (0600 h) and cisplatin in the evening (1800 h) was able to improve clinical outcomes in the treatment of advanced ovarian cancer. A clinical trial of 37 patients with stage III or IV ovarian cancer treated patients with doxorubicin at 0600 h (Schedule A) or 1800 h (Schedule B) followed by cisplatin 12 hours later. Patients receiving doxorubicin in the evening and cisplatin in the morning (Schedule B) experienced greater bone marrow toxicity, leading to more dose reductions and/or treatment delays compared to patients on Schedule A. Patients on Schedule A had a 4-fold increase in 5-year survival compared to Schedule B (44% vs 11%; [36]). This approach makes it more difficult to examine the chronotherapeutic benefits of each individual drug. However, this application of chronotherapy is more realistic and applicable to other cancers in the future because most cancers are treated with multiple agents simultaneously.

Chronomodulation in the delivery of a variety of chemotherapeutic medications which act by many different mechanisms. And yet, all have been put to better use by delivering these drugs at a particular time of day. The mechanisms of action of these drugs may influence the outcomes

of chronotherapy, but it is also likely that rhythms within the patient's body are influencing the activity and efficacy and toxicities of these medications. Blood flow changes with time of day [37] which may influence delivery of the drug to the tumor. Drug metabolism by liver enzymes, like cytochrome P450, changes across the day [37]. Elimination of the chemotherapy from the tumor and the body can also change with time of day. All of these rhythms outside of the tumor, but inside the body may influence how tumors respond to chemotherapy and how healthy tissues respond, as well. Some of the chronotherapy examples given above demonstrated reduced toxicity at a particular time of day because the biological rhythms of the patient were "out of sync" with the rhythms of the tumor. Additionally, great improvements in chemotherapeutic outcomes can be made by reducing toxicity alone; if patients have reduced toxicity at a high dose, patients can stay on that higher dose longer and have fewer treatment delays. In some cases, the anti-tumor effect of the chemotherapy may not change during the day, but chronotherapy still provides an advantage in these situations. In this thesis, the focus is on cell-intrinsic anti-tumor efficacy of TMZ. We have demonstrated changes in tumor sensitivity to TMZ using our model of glioblastoma *in vitro*. Future studies may optimize this treatment response further by taking into account the daily rhythms in toxicity.

Rhythms within the tumor and within the patient can influence chemotherapy treatment outcomes. These rhythms exist at the levels of individual cells all the way up to human behavior. In order to achieve the greatest improvement in outcomes following treatment with chemotherapy, we must understand the daily rhythms within the human body.

Links between Circadian Disruption and Cancer in Humans

The literature supporting the connection between shift work and the risk of developing cancer has provided some strong correlations, but none have definitively demonstrated that performing shift work causes cancer.

Breast cancer risk is greater in nurses who worked the night shift for at least 20 years, using data from the Nurses' Health Study [38]. A study conducted in Norway also demonstrated an increased risk of the development of breast cancer in nurses working the night shift for at least 30 years [39]. A recent study demonstrated an increased risk of breast cancer development in female mice subjected to a chronically shift light schedule [40], lending further support to this shift work-breast cancer connection. Studies demonstrating changes in hormone regulation in correlation with light-at-night and disrupted sleep patterns are thought to underlie the increased incidence of hormone-related cancer, like breast cancer [41]. Additional epidemiological studies support the claim of a correlation between night shift work and an increase in the risk of breast cancer [42, 43]. As a result, the WHO lists shift work as a potential carcinogen.

The correlation between disrupted circadian rhythms due to night shift work and cancer are not limited to breast cancer. Risk of developing and dying from lung cancer was increased among nurses working rotating night shift work for greater than 15 years [44-46]. The risk of developing skin cancer was also higher in night shift workers [47]. The risk of developing prostate cancer was higher in long-term (>28 years) night shift workers in Spain [48].

Researchers in Washington state interviewed 1101 ovarian cancer patients about their work schedules and found a higher rate of the development of invasive or borderline ovarian cancer for women doing shift work (24% and 48% increased risk, respectively; [49]). These epidemiological studies demonstrate that the correlation between shift work and cancer goes beyond sex, hormone regulation and breast cancer biology. Chronodisruption may increase the

risk of cancer development through basic biological principles that are common among a variety of cancers.

Inconsistencies in the definition of shift work have led to some controversy over the validity of these epidemiological studies. A major problem contributing to the inconsistency among studies is the loose definition of shift work. Some studies focus on people who have worked the night shift. One caveat to this type of study is the assumption that night shift workers are awake during daytime hours on non-work days, experiencing extreme social jet lag on a regular basis. These studies rarely acknowledge the possibility that long term (>15 years) night shift workers change their entire schedules to accommodate their night shift work schedule, spending every night awake and every day asleep. Other studies look at employees working rotating shift schedules, which provides documented evidence of chronically changing rest-activity schedules. In both cases, workers are exposed to light at night. Several studies were able to demonstrate a specific link between exposure to light-at-night and breast cancer by demonstrating lower rates of breast cancer in blind women [50, 51]. Another possible cause of increased cancer risk is the higher risk of sleep disruption among night shift workers, but little evidence exists to support this hypothesis. Although many studies have been conducted across a variety of types of employment, the specific exposure(s) of shift work that could potentially increase the rate of tumorigenesis remain unknown.

The link between shift work and cancer was further called into question by epidemiological studies that have demonstrated no evidence for increased cancer risk among long-term night shift workers. For example, male chemical workers in Germany and female textile rotating shift workers in China did not have higher rates of developing prostate or breast cancer, respectively. Despite the doubts raised by inconsistencies in analytical methods, shift

work definitions and differences in outcomes between studies, the World Health Organization recognizes night shift work as a potential carcinogen (class IARC 2A carcinogen) [52].

All of the examples listed above draw a link between disrupted circadian rest-activity rhythms and tumorigenesis. Additionally, a link between disruption of daily patterns of activity and response to therapy exists. Colorectal cancer patients with significantly disrupted circadian rhythms had a substantial reduction in median overall survival (11.9 months) compared to patients with intact circadian rest-activity rhythms (21.6 months; [53]). These data suggest that the circadian clock is involved in cancer progression, and possibly response to therapy, in addition to its contribution to development of cancer.

Circadian Rhythms in Mammals

We experience many rhythmic biological processes during an ordinary day. We are aware of some, like the sleep-wake cycle, but other rhythms are happening inside our bodies, unbeknownst to us. Oscillations in physiology and behavior that repeat approximately once per 24 hour cycle are known as circadian rhythms. These oscillations occur in a large variety of organisms with obvious behavioral rhythms in humans, mice and many other species. These rhythms exist at the level of most individual cells within the human body. The molecular clock that drives cell-autonomous rhythms will be described in greater detail in a later section. These rhythms exist in the absence of external cues, but are influenced by environmental stimuli.

The suprachiasmatic nucleus (SCN), the master pacemaker, is located in the hypothalamus. It responds to external cues from the environment and coordinates peripheral clocks within the body [54]. Mammals are able to entrain to external light cues via signals sent to the SCN. In the context of chronobiology, entrainment can be defined as the alignment of the

period and phase of a circadian system to the period and phase of an external rhythm (e.g. light cycles). Any external cue capable of entraining the clock is known as a zeitgeber (“time-giver”) [54]. In chronobiology, the abbreviation ZT is used, accompanied by a number which indicates the length of time that has passed since the organism has been exposed to the zeitgeber, or external cue. In many cases, the onset of light is a zeitgeber used to entrain organisms. In this thesis, the abbreviation ZT0 will indicate the time lights turn on and ZT12 will indicate the time lights turn off. Entrainment to an external signal can change the period or phase of the oscillation, but is not responsible for creating the oscillation. A true circadian rhythm is driven from within the organism, completely independent of external stimuli. The circadian clock exists and exerts its regulation of daily processes at many levels, including individual cells.

Circadian rhythms exist at many levels and in a variety of physiological processes, but they all have a few common characteristics. Every circadian oscillation has a peak (maximum level reached in the oscillation) and a nadir (lowest point within the oscillation). The length of time it takes to complete one cycle, also known as the period of oscillation, is usually close to 24 hours. The phase of the oscillation is the instantaneous state within a period. In the studies described in this thesis, the circadian oscillation of clock gene expression is divided into 4 phases: peak, falling, trough and rising (see **Figure 1.1**).

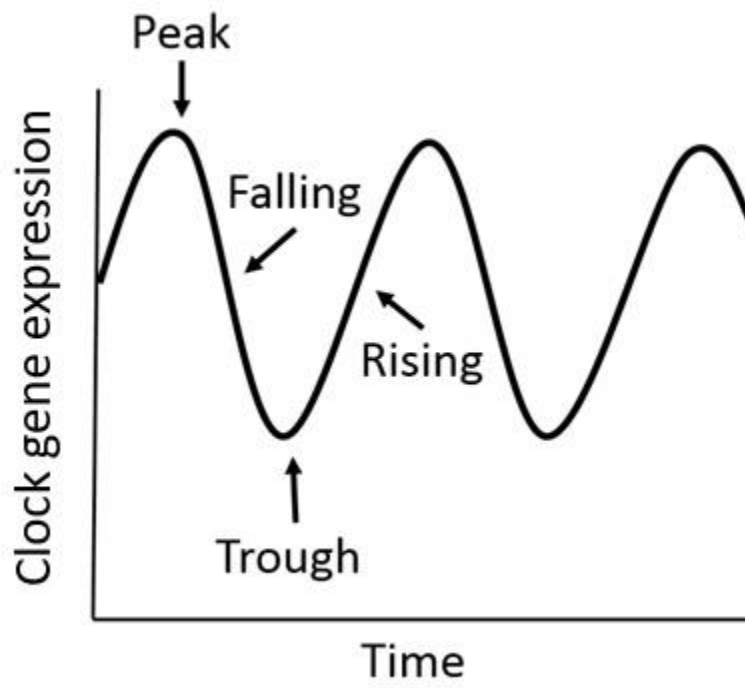


Figure 1.1. Four phases of circadian oscillation in gene expression.

Conservation of the molecular clock across organisms

At all levels of the Tree of Life, survival is achieved by the organisms that are able to adapt to their environment. There is a common understanding that environments change over long periods of time. However, what is often overlooked is the fact that environmental changes can occur quite rapidly and often do so in a cyclical manner. If you have ever endured the blistering heat of a summer day in Phoenix, Arizona, and bundled up in a coat the following night, you understand that within a single day, your environment can change dramatically. You can also anticipate the need for a tank top to prepare for the heat of the following day. The development and conservation of a circadian clock is a way for organisms to anticipate and adapt to cyclical changes in their environment.

Although environmental rhythms exist on many time scales (lunar, tidal, seasonal), we will focus on daily rhythms for the purpose of informing this introduction. The word “circadian” comes from two latin words: “circa”, meaning about, and “dies”, meaning day. Thus, circadian rhythms are oscillations that complete a single cycle in approximately 24 hours. The most obvious example of a daily rhythm, at least at our current latitude, is the day-night cycle. These oscillations in availability and intensity of sunlight generate rhythms in temperature, both of which are external cues that organisms can entrain to. Entrainment means that the internal clock within the organism aligns itself with the daily cycles of the environment. For a variety of organisms, daily rhythms in availability of resources, like food, or the activity of predators require that organisms align themselves to these rhythms to ensure survival.

The leaves of plants change position on a daily basis to accommodate exposure to sunlight for photosynthesis. The scientific literature describing daily leaf movements dates back to 1729, when a French astronomer, de Mairan, described daily rhythms in leaf movements that continued, even in constant darkness [55]. A variety of other organisms also have daily rhythms in response to daily oscillations in resources, like sunlight.

The cyanobacterium *Synechococcus* has an internal clock that drives circadian rhythms in cell division, amino acid uptake, nitrogen fixation, photosynthesis, carbohydrate synthesis and respiration [56, 57]. Temporal separation of mutually exclusive intracellular processes, like nitrogen fixation and photosynthesis, is required to prevent the oxygen used for photosynthesis from blocking the activity of the nitrogenase enzyme [56].

The ways in which different organisms utilize circadian rhythms may vary, but they share common elements in the internal clocks that drive their anticipatory rhythms to adapt to the local environment. Regulation of gene transcription exists at the core of the internal clocks of organisms spread across phyla. Positive elements induce gene expression of clock-controlled genes (CCGs), creating a rhythmic expression of gene products, thus creating rhythms in cellular processes. Among the CCGs produced, some subset of proteins will provide negative feedback on the positive element to reduce transcription of CCGs and create a rhythm [56]. The structures and specific regulation of these common clock elements are not similar across bacteria, fungi, plants, invertebrates and mammals. However, the general structure of the molecular clocks is similar. Among mammals, there are highly conserved circadian genes. These will be described in the next section.

The Mammalian Molecular Clock

Within most mammalian cells, there is a molecular clock regulating daily intracellular activities. The core of this molecular clock is a transcription-translation feedback loop. Transcription factors BMAL1 and CLOCK form a heterodimer and bind E-box sequences within gene promoters. This heterodimer activates expression of the downstream gene, which is known as a clock-controlled gene (CCG). The protein products of CCGs play important roles in a variety of cellular processes, including but not limited to metabolism, cell cycle regulation and DNA repair. Among the CCGs, the Period (PER1/2/3) and Cryptochrome (CRY1/2) proteins exit the nucleus and dimerize in the cytoplasm. Period proteins undergo casein kinase I (epsilon or delta)-mediated phosphorylation and re-enter the nucleus to inhibit further transcriptional activation of the BMAL1-CLOCK heterodimer. After providing negative feedback on the BMAL1-CLOCK dimer, the PER/CRY protein complex gets degraded, allowing the BMAL1-CLOCK dimer to start activating transcription of CCGs again. This constitutes the core transcription-translation feedback loop. This loop is reinforced by a stabilizing loop, consisting of an activator, ROR-alpha, and a repressor, REV-ERB alpha, which act on the R-response element within the *Bmal1* promoter. Transcriptional activation of *Rora* and *Rev-Erb alpha* are regulated by the BMAL1-CLOCK dimer. Together, RORA and REV-ERB alpha regulate expression of *Bmal1*, creating a circadian oscillation in *Bmal1* expression that is anti-phase to the expression of clock-controlled genes ([58]; **Figure 1.2**). To track daily oscillations in the core clock, scientists have developed luciferase reporters of transcriptional activation of core clock genes. In this thesis, we have made use of the luciferase reporters *Bmal1::dLuc* and *Per2::dLuc* [59] to track daily oscillations in circadian clock gene expression in our model of mesenchymal GBM.

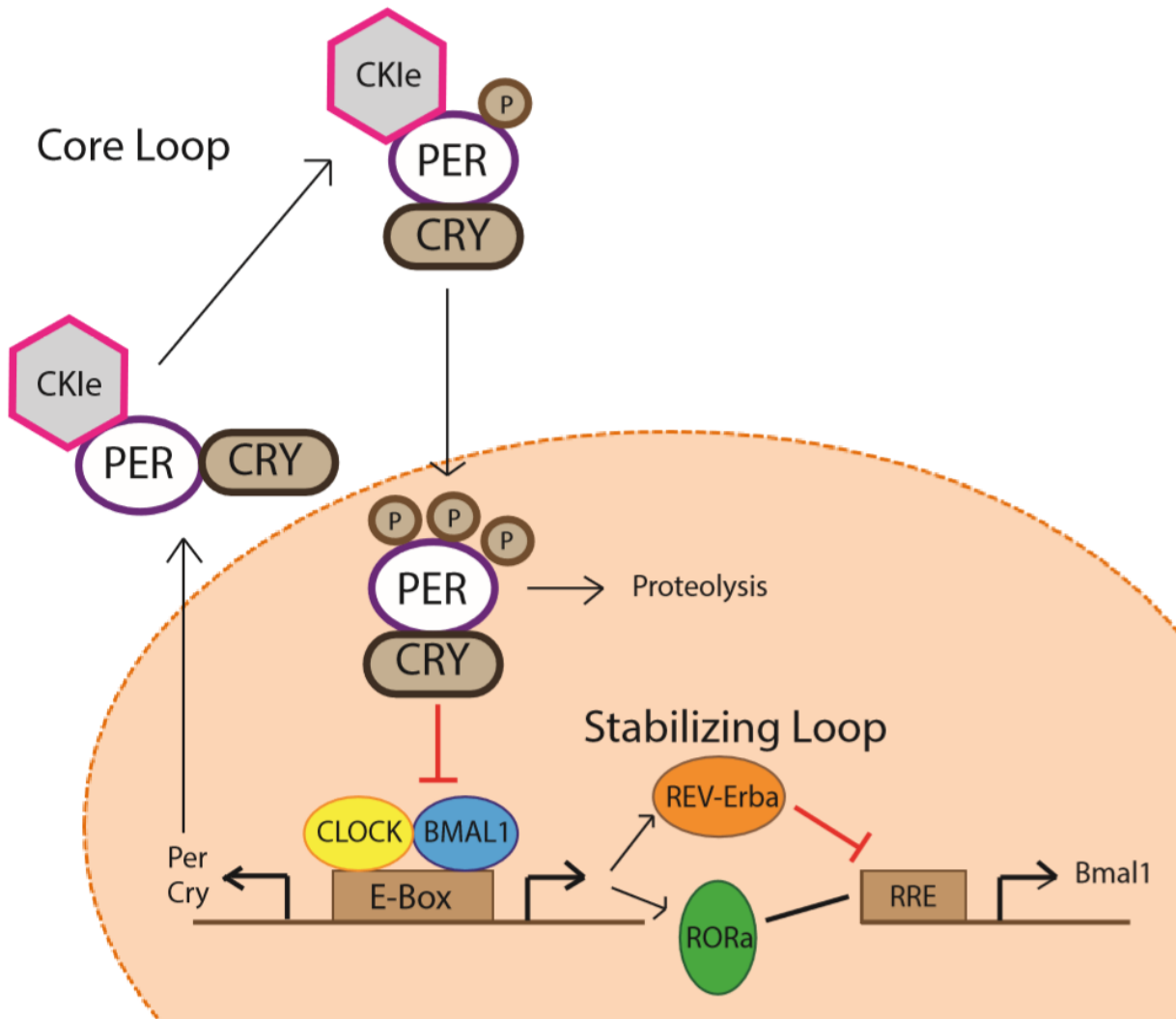


Figure 1.2: Mammalian molecular clock (adapted from Gallego and Virshup, 2007).

Bmal1 disruption abolishes circadian rhythms

Bmal1 is a unique component of the core molecular clock because it is the only gene within the core clock whose deletion leads to loss of cellular rhythms in clock gene expression and loss of locomotor rhythmicity in constant darkness [60]. Deletion of any other component of the core clock is insufficient to disrupt circadian oscillations because there are redundant paralogs that can compensate for their role in the molecular clock in their absence. In many studies, deletion of both *Clock* and *Npas2*, or *Cry1* and *Cry2*, or *Per1* and *Per2* are necessary for disruption of circadian rhythms [61-63]. Many studies have demonstrated loss of daily rhythms in clock gene expression in *Bmal1* knockout cells or tissues [60, 64, 65]. Only one study demonstrates the rescue of behavioral rhythmicity in *Bmal1* knockout mice by constitutive expression of *Bmal2* [66]. However, in this same study, constitutive *Bmal2* expression was not sufficient to restore rhythmic clock gene expression in SCN or lung tissue ex vivo [66]. In our study, we take advantage of the unique lack of molecular redundancy of *Bmal1*. We take advantage of CRISPR-mediated disruption of *Bmal1* expression to efficiently disrupt the molecular clock.

Molecular connections between circadian clock and cancer

Many studies in mammalian cells have described a connection between the core circadian clock and cancer. Several proteins of the core clock have been characterized as tumor suppressors, many of them interacting with key players in the cellular response to DNA damage and regulation of cell cycle progression. The circadian clock also exerts its influence on cell

cycle regulation, and DNA damage response by creating daily oscillations in the expression of clock-controlled genes.

Characterization of core clock genes as tumor suppressors

Several core clock proteins have been characterized as tumor suppressors through genetic manipulations in mouse models and cell culture. Mice expressing a mutant form of PER2 were at increased risk of developing radiation-induced lymphoma than wild type mice [67]. Mouse colon carcinoma C26 cells expressing *Bmal1*-targeted shRNA had a proliferation rate 36.4% higher than control cells 5 days after plating [68]. Overexpression of *Bmal1* in the human colon cancer cell line HCT116 led to enhanced sensitivity to oxaliplatin treatment and greater apoptosis *in vitro*. RNAi-mediated knockdown of *Bmal1* in human colon carcinoma cell line HCT116 led to increased growth rates of subcutaneously implanted tumors in nude mice [69], demonstrating a cell-intrinsic role for *Bmal1* in regulating tumor growth *in vivo*. Overexpression of *Per1* or *Per3* led to reduced growth rates and increased rates of apoptosis *in vitro* [70, 71]. *Cry1/2* double knockout increased UV-induced apoptosis in P53 knockout mouse embryonic fibroblasts by inducing expression of the pro-apoptotic tumor suppressor P73 [72]. Together, these data demonstrate a role for the molecular clock in regulating proliferation and apoptosis in a manner consistent with tumor suppressor function.

Direct interactions of core clock proteins with other proteins, influencing DDR and cell cycle regulation

In response to DNA double strand breaks, ATM kinase phosphorylates downstream targets to signal DNA repair and activation of a cell cycle checkpoint. By phosphorylating Chk2, ATM is able to activate the checkpoint pathway, leading to cell cycle arrest in response to DNA

damage. Direct interactions of PER1 and PER3 with ATM and Chk2 have been demonstrated. Overexpression of PER1 leads to increased phosphorylation of Chk2, causing increased activation of the cell cycle checkpoint. PER1 knockdown leads to reduced phosphorylation of Chk2 after DNA damage [70]. This is the result of an artificial overexpression of exogenous *Per1*, but it suggests an important role for PER1 in modulating the level of ATM-Chk2 signaling following DNA damage. *Per1* mRNA and protein levels oscillate in most tissues. PER1 may mediate daily variations in response to DNA damage.

Following single strand DNA breaks, the ATR-CHK1 pathway is activated. Activated ATR phosphorylates and thus activates Chk1, which leads to cell cycle arrest at the G2-M transition [73]. Following overexpression of Timeless in HEK293T cells, immunoprecipitation assays demonstrate interaction of Timeless with Chk1 and the ATR-ATRIP complex. Knockdown of Timeless causes a reduction in Chk1 phosphorylation, demonstrating a role for Timeless in regulating the degree of Chk1 phosphorylation following activation of the replication checkpoint pathway [74]. Timeless forms a complex with timeless interacting protein (Tipin) to protect cells from DNA damaging agents, like ionizing radiation and inducers of replication stress [75]. The Timeless-Tipin complex stabilizes replication forks and aids in homologous recombination by maintaining cohesion of the sister chromatid [76]. The role of Timeless in the mammalian circadian clock is unknown, but it is expressed in a variety of tissues and interacts with proteins involved in cell cycle regulation and DNA damage response.

Core clock protein cryptochrome1 has been shown to interact with ATR to regulate the ATR-CHK1 checkpoint pathway, creating circadian oscillations in repair following UV-induced DNA damage. CHK1 and P53 phosphorylation are highest one hour after UV-induced DNA damage at ZT12 and at their nadir at ZT24 in NIH3T3 cells, corresponding to the peak and nadir [25]

if CRY1 expression, respectively [77]. Similar rhythms in CRY1 expression and oscillations in ATR activity were observed in wild type mouse embryonic fibroblasts (MEFs). CRY1 knockdown and *Cry1/2* double knockout (DKO), but not CRY2 knockdown, abolished rhythms in ATR-mediated phosphorylation of Chk1, but continue to activate the ATR-mediated DNA damage checkpoint [77]. Thus, CRY1, but not CRY2, regulates the rhythmic DNA damage response through interactions with the ATR-Chk1 pathway.

Circadian regulation of molecular processes via clock-controlled genes

Clock-controlled genes are the outputs of the molecular clock. Several of these genes, whose transcription is regulated by the core transcription-translation feedback loop (TTFL), play important roles in cancer-related molecular pathways. The nucleotide excision repair protein, XPA, is the rate-limiting step in repair of UV-induced DNA damage. XPA protein levels oscillate throughout the day, reaching their peak levels at night. Base excision repair activity reaches its peak near the time of peak XPA expression [78]. Sancar and colleagues have demonstrated a link between DNA repair and skin cancer based on these findings [79].

Cell cycle regulation is also under the influence of the molecular clock, due to daily oscillations in the expression of clock controlled genes Wee1 [80], CyclinD1, and c-Myc [67]. Nuclear kinase Wee1 phosphorylates Cdk1, thus inhibiting cell cycle progression into mitosis. Rhythmic mRNA expression is observed during murine liver regeneration following partial hepatectomy. *Cry1/2* double knockout mice experienced impairment in liver regeneration due to a reduced rate of progression from S phase to mitosis. In the *Cry1/2* DKO livers, *wee1* expression was elevated, while mRNA levels were reduced for cell cycle regulators that would promote entry into mitosis (e.g. Cdc2, CyclinB1). In Clock mutant mice, *wee1* expression is

reduced, demonstrating circadian regulation of *wee1* [80]. Transcription factor c-Myc has multiple E boxes within its promoter and its mRNA levels oscillate in wild type mouse livers. In homozygous *Per2* mutant mouse livers, c-myc mRNA expression is expressed at much higher levels compared to wild type mouse liver. CyclinD1 mRNA expression oscillated in a circadian pattern in wild type mouse livers reaching its peak in the early night (ZT 14). This circadian oscillation was not present in *mPer2* mutant mouse livers, suggesting circadian regulation of CyclinD1 expression [67].

Links between the molecular clock and apoptosis

Through genetic manipulation of clock genes, the molecular clock has been linked to the apoptotic pathway. *Bmal1* knockdown in the C26 colon cancer cell line reduced etoposide-induced apoptosis from 29.4% to 11.2% [68]. Similarly, *Per1* knockdown in the HCT116 colon cancer cell line reduced IR-induced apoptosis rates from 37% to 13% [70]. Gery and colleagues also increased IR-induced apoptosis by overexpressing *Per1* in HCT116 cells [70].

Overexpression of *Per2* in lung and breast cancer cell lines increased the proportions of apoptotic cells without inducing DNA damage. These *Per2* overexpressing-cells had downregulated expression of anti-apoptotic genes *Bcl-XL* and *Bcl2*, in addition to upregulation of pro-apoptotic gene *Bax* [81]. Overexpression of *Per3* in HeLa cells increased caspase-3 and PARP cleavage, indicating increased activation of apoptosis, in the absence of DNA damaging agents[71]. Together, these data indicate that multiple core clock proteins promote apoptosis.

This body of literature demonstrates important roles for core clock proteins in regulating cell proliferation, response to DNA damage and apoptosis. In some cases, these roles are carried out indirectly through BMAL1-CLOCK-mediated transcriptional activation of key regulators of

these cellular pathways. Some studies have demonstrated direct protein-protein interactions of core clock proteins with regulators of cell cycle progression and DNA damage response.

Increasing our understanding of the regulation of all of these processes directly or indirectly by the molecular clock will provide many opportunities for enhancing treatment outcomes using drugs, especially chemotherapies, targeting these cellular pathways.

Conclusions and objectives of the dissertation

Through regulation of transcription and direct protein interactions, the molecular clock is capable of influencing a variety of cellular processes related to tumorigenesis and tumor response to chemotherapies. This thesis seeks to harness the power of the circadian clock to target the tumor with chemotherapy at the time of day when the tumor is least able to defend itself. As discussed in the introduction, TMZ has already provided a significant advancement in clinical outcomes for glioblastoma patients. Its short half-life in the tumor makes TMZ an excellent candidate for further optimization of anti-tumor efficacy through chronotherapy. We use circadian research tools to learn more about the relationship between the circadian molecular clock and the response of glioblastoma to TMZ therapy. By correlating the phase of circadian clock gene expression with daily rhythms in DNA repair and activation of apoptosis, we can predict the timing of optimal sensitivity in future cultures or tumors. By disrupting the molecular clock through deletion of *Bmal1* (*Arntl*) we are able to identify the contributions of the molecular clock to DNA damage response. This thesis is the first application of chronotherapy to brain tumors, which demonstrates the versatility of this technique. This will hopefully encourage other researchers to consider chronotherapy in the future. Although many other cancers are not treated with TMZ, many anti-cancer drugs induce DNA damage. By focusing this thesis on the tumor's

response to TMZ-induced DNA damage, we are providing valuable information that can be applied to other anti-cancer therapies, including ionizing radiation.

References

1. Agnihotri, S., et al., *Glioblastoma, a brief review of history, molecular genetics, animal models and novel therapeutic strategies*. Arch Immunol Ther Exp (Warsz), 2013. **61**(1): p. 25-41.
2. Ferguson, S. and M.S. Lesniak, *Percival Bailey and the classification of brain tumors*. Neurosurg Focus, 2005. **18**(4): p. e7.
3. Louis, D.N., et al., *The 2007 WHO classification of tumours of the central nervous system*. Acta Neuropathol, 2007. **114**(2): p. 97-109.
4. Karsy, M., et al., *Established and emerging variants of glioblastoma multiforme: review of morphological and molecular features*. Folia Neuropathol, 2012. **50**(4): p. 301-21.
5. Ostrom, Q.T., et al., *CBTRUS statistical report: Primary brain and central nervous system tumors diagnosed in the United States in 2006-2010*. Neuro Oncol, 2013. **15 Suppl 2**: p. ii1-56.
6. Ostrom, Q.T., et al., *CBTRUS statistical report: primary brain and central nervous system tumors diagnosed in the United States in 2007-2011*. Neuro Oncol, 2014. **16 Suppl 4**: p. iv1-63.
7. Sturm, D., et al., *Paediatric and adult glioblastoma: multiform (epi)genomic culprits emerge*. Nat Rev Cancer, 2014. **14**(2): p. 92-107.
8. Qaddoumi, I., I. Sultan, and A. Gajjar, *Outcome and prognostic features in pediatric gliomas: a review of 6212 cases from the Surveillance, Epidemiology, and End Results database*. Cancer, 2009. **115**(24): p. 5761-70.
9. Sanders, R.P., et al., *High-grade astrocytoma in very young children*. Pediatr Blood Cancer, 2007. **49**(7): p. 888-93.
10. Huse, J.T. and M.K. Rosenblum, *The Emerging Molecular Foundations of Pediatric Brain Tumors*. J Child Neurol, 2015.
11. Morokoff, A., et al., *Molecular subtypes, stem cells and heterogeneity: Implications for personalised therapy in glioma*. J Clin Neurosci, 2015. **22**(8): p. 1219-26.
12. Ohgaki, H. and P. Kleihues, *Population-based studies on incidence, survival rates, and genetic alterations in astrocytic and oligodendroglial gliomas*. J Neuropathol Exp Neurol, 2005. **64**(6): p. 479-89.
13. Dunn, G.P., et al., *Emerging insights into the molecular and cellular basis of glioblastoma*. Genes Dev, 2012. **26**(8): p. 756-84.
14. Sun, T., N.M. Warrington, and J.B. Rubin, *Why does Jack, and not Jill, break his crown? Sex disparity in brain tumors*. Biol Sex Differ, 2012. **3**: p. 3.
15. Phillips, H.S., et al., *Molecular subclasses of high-grade glioma predict prognosis, delineate a pattern of disease progression, and resemble stages in neurogenesis*. Cancer Cell, 2006. **9**(3): p. 157-73.
16. Verhaak, R.G., et al., *Integrated genomic analysis identifies clinically relevant subtypes of glioblastoma characterized by abnormalities in PDGFRA, IDH1, EGFR, and NF1*. Cancer Cell, 2010. **17**(1): p. 98-110.
17. Huse, J.T., E. Holland, and L.M. DeAngelis, *Glioblastoma: molecular analysis and clinical implications*. Annu Rev Med, 2013. **64**: p. 59-70.

18. Frankel, S.A. and W.J. German, *Glioblastoma multiforme; review of 219 cases with regard to natural history, pathology, diagnostic methods, and treatment*. J Neurosurg, 1958. **15**(5): p. 489-503.
19. Maher, E.A., et al., *Malignant glioma: genetics and biology of a grave matter*. Genes Dev, 2001. **15**(11): p. 1311-33.
20. Shapiro, W.R., et al., *Randomized trial of three chemotherapy regimens and two radiotherapy regimens in postoperative treatment of malignant glioma*. Brain Tumor Cooperative Group Trial 8001. J Neurosurg, 1989. **71**(1): p. 1-9.
21. Stupp, R., et al., *Radiotherapy plus concomitant and adjuvant temozolomide for glioblastoma*. N Engl J Med, 2005. **352**(10): p. 987-96.
22. Hirose, Y., et al., *Delayed depletion of O6-methylguanine-DNA methyltransferase resulting in failure to protect the human glioblastoma cell line SF767 from temozolomide-induced cytotoxicity*. J Neurosurg, 2003. **98**(3): p. 591-8.
23. Hegi, M.E., et al., *MGMT gene silencing and benefit from temozolomide in glioblastoma*. N Engl J Med, 2005. **352**(10): p. 997-1003.
24. Wick, W., et al., *MGMT testing--the challenges for biomarker-based glioma treatment*. Nat Rev Neurol, 2014. **10**(7): p. 372-85.
25. Kitange, G.J., et al., *Induction of MGMT expression is associated with temozolomide resistance in glioblastoma xenografts*. Neuro Oncol, 2009. **11**(3): p. 281-91.
26. Ohka, F., A. Natsume, and T. Wakabayashi, *Current trends in targeted therapies for glioblastoma multiforme*. Neurol Res Int, 2012. **2012**: p. 878425.
27. Levi, F. and A. Okyar, *Circadian clocks and drug delivery systems: impact and opportunities in chronotherapeutics*. Expert Opin Drug Deliv, 2011. **8**(12): p. 1535-41.
28. Rivard, G.E., et al., *Maintenance chemotherapy for childhood acute lymphoblastic leukaemia: better in the evening*. Lancet, 1985. **2**(8467): p. 1264-6.
29. Rivard, G.E., et al., *Circadian time-dependent response of childhood lymphoblastic leukemia to chemotherapy: a long-term follow-up study of survival*. Chronobiol Int, 1993. **10**(3): p. 201-4.
30. Schmiegelow, K., et al., *Impact of morning versus evening schedule for oral methotrexate and 6-mercaptopurine on relapse risk for children with acute lymphoblastic leukemia*. Nordic Society for Pediatric Hematology and Oncology (NOPHO). J Pediatr Hematol Oncol, 1997. **19**(2): p. 102-9.
31. Petit, E., et al., *Circadian rhythm-varying plasma concentration of 5-fluorouracil during a five-day continuous venous infusion at a constant rate in cancer patients*. Cancer Res, 1988. **48**(6): p. 1676-9.
32. Lincoln, D.W., 2nd, W.J. Hrushesky, and P.A. Wood, *Circadian organization of thymidylate synthase activity in normal tissues: a possible basis for 5-fluorouracil chronotherapeutic advantage*. Int J Cancer, 2000. **88**(3): p. 479-85.
33. Harris, B.E., et al., *Relationship between dihydropyrimidine dehydrogenase activity and plasma 5-fluorouracil levels with evidence for circadian variation of enzyme activity and plasma drug levels in cancer patients receiving 5-fluorouracil by protracted continuous infusion*. Cancer Res, 1990. **50**(1): p. 197-201.
34. Zhang, R., et al., *Relationship between circadian-dependent toxicity of 5-fluorodeoxyuridine and circadian rhythms of pyrimidine enzymes: possible relevance to fluoropyrimidine chemotherapy*. Cancer Res, 1993. **53**(12): p. 2816-22.
35. Levi, F., et al., *Chronomodulation of chemotherapy against metastatic colorectal cancer*. International Organization for Cancer Chronotherapy. Eur J Cancer, 1995. **31A**(7-8): p. 1264-70.

36. Kobayashi, M., P.A. Wood, and W.J. Hrushesky, *Circadian chemotherapy for gynecological and genitourinary cancers*. *Chronobiol Int*, 2002. **19**(1): p. 237-51.
37. Paschos, G.K., et al., *The role of clock genes in pharmacology*. *Annu Rev Pharmacol Toxicol*, 2010. **50**: p. 187-214.
38. Schernhammer, E.S., et al., *Night work and risk of breast cancer*. *Epidemiology*, 2006. **17**(1): p. 108-11.
39. Lie, J.A., J. Roessink, and K. Kjaerheim, *Breast cancer and night work among Norwegian nurses*. *Cancer Causes Control*, 2006. **17**(1): p. 39-44.
40. Van Dycke, K.C., et al., *Chronically Alternating Light Cycles Increase Breast Cancer Risk in Mice*. *Curr Biol*, 2015. **25**(14): p. 1932-7.
41. Davis, S. and D.K. Mirick, *Circadian disruption, shift work and the risk of cancer: a summary of the evidence and studies in Seattle*. *Cancer Causes Control*, 2006. **17**(4): p. 539-45.
42. Davis, S., D.K. Mirick, and R.G. Stevens, *Night shift work, light at night, and risk of breast cancer*. *J Natl Cancer Inst*, 2001. **93**(20): p. 1557-62.
43. Hansen, J., *Increased breast cancer risk among women who work predominantly at night*. *Epidemiology*, 2001. **12**(1): p. 74-7.
44. Schernhammer, E.S., et al., *Rotating night-shift work and lung cancer risk among female nurses in the United States*. *Am J Epidemiol*, 2013. **178**(9): p. 1434-41.
45. Gu, F., et al., *Total and cause-specific mortality of U.S. nurses working rotating night shifts*. *Am J Prev Med*, 2015. **48**(3): p. 241-52.
46. Schernhammer, E.S., et al., *Rotating night shifts and risk of skin cancer in the nurses' health study*. *J Natl Cancer Inst*, 2011. **103**(7): p. 602-6.
47. Schernhammer, E.S., et al., *Rotating night shifts and risk of breast cancer in women participating in the nurses' health study*. *J Natl Cancer Inst*, 2001. **93**(20): p. 1563-8.
48. Papantoniou, K., et al., *Night shift work, chronotype and prostate cancer risk in the MCC-Spain case-control study*. *Int J Cancer*, 2014.
49. Bhatti, P., et al., *Nightshift work and risk of ovarian cancer*. *Occup Environ Med*, 2013. **70**(4): p. 231-7.
50. Hahn, R.A., *Profound bilateral blindness and the incidence of breast cancer*. *Epidemiology*, 1991. **2**(3): p. 208-10.
51. Feychting, M., B. Osterlund, and A. Ahlbom, *Reduced cancer incidence among the blind*. *Epidemiology*, 1998. **9**(5): p. 490-4.
52. Straif, K., et al., *Carcinogenicity of shift-work, painting, and fire-fighting*. *Lancet Oncol*, 2007. **8**(12): p. 1065-6.
53. Levi, F., et al., *Wrist actimetry circadian rhythm as a robust predictor of colorectal cancer patients survival*. *Chronobiol Int*, 2014. **31**(8): p. 891-900.
54. Vitaterna, M.H., J.S. Takahashi, and F.W. Turek, *Overview of circadian rhythms*. *Alcohol Res Health*, 2001. **25**(2): p. 85-93.
55. McClung, C.R., *Plant circadian rhythms*. *Plant Cell*, 2006. **18**(4): p. 792-803.
56. Dunlap, J.C., *Molecular bases for circadian clocks*. *Cell*, 1999. **96**(2): p. 271-90.
57. Golden, S.S., et al., *Cyanobacterial Circadian Rhythms*. *Annu Rev Plant Physiol Plant Mol Biol*, 1997. **48**: p. 327-354.
58. Gallego, M. and D.M. Virshup, *Post-translational modifications regulate the ticking of the circadian clock*. *Nat Rev Mol Cell Biol*, 2007. **8**(2): p. 139-48.
59. Ramanathan, C., et al., *Monitoring cell-autonomous circadian clock rhythms of gene expression using luciferase bioluminescence reporters*. *J Vis Exp*, 2012(67).

60. Bunger, M.K., et al., *Mop3 is an essential component of the master circadian pacemaker in mammals*. Cell, 2000. **103**(7): p. 1009-17.
61. DeBruyne, J.P., D.R. Weaver, and S.M. Reppert, *CLOCK and NPAS2 have overlapping roles in the suprachiasmatic circadian clock*. Nat Neurosci, 2007. **10**(5): p. 543-5.
62. Vitaterna, M.H., et al., *Differential regulation of mammalian period genes and circadian rhythmicity by cryptochromes 1 and 2*. Proc Natl Acad Sci U S A, 1999. **96**(21): p. 12114-9.
63. Zheng, B., et al., *Nonredundant roles of the mPer1 and mPer2 genes in the mammalian circadian clock*. Cell, 2001. **105**(5): p. 683-94.
64. Marpegan, L., et al., *Circadian regulation of ATP release in astrocytes*. J Neurosci, 2011. **31**(23): p. 8342-50.
65. Vollmers, C., S. Panda, and L. DiTacchio, *A high-throughput assay for siRNA-based circadian screens in human U2OS cells*. PLoS One, 2008. **3**(10): p. e3457.
66. Shi, S., et al., *Circadian clock gene Bmal1 is not essential; functional replacement with its paralog, Bmal2*. Curr Biol, 2010. **20**(4): p. 316-21.
67. Fu, L., et al., *The circadian gene Period2 plays an important role in tumor suppression and DNA damage response in vivo*. Cell, 2002. **111**(1): p. 41-50.
68. Zeng, Z.L., et al., *Effects of the biological clock gene Bmal1 on tumour growth and anti-cancer drug activity*. J Biochem, 2010. **148**(3): p. 319-26.
69. Zeng, Z.L., et al., *Overexpression of the circadian clock gene Bmal1 increases sensitivity to oxaliplatin in colorectal cancer*. Clin Cancer Res, 2014. **20**(4): p. 1042-52.
70. Gery, S., et al., *The circadian gene per1 plays an important role in cell growth and DNA damage control in human cancer cells*. Mol Cell, 2006. **22**(3): p. 375-82.
71. Im, J.S., et al., *Per3, a circadian gene, is required for Chk2 activation in human cells*. FEBS Lett, 2010. **584**(23): p. 4731-4.
72. Lee, J.H. and A. Sancar, *Circadian clock disruption improves the efficacy of chemotherapy through p73-mediated apoptosis*. Proc Natl Acad Sci U S A, 2011. **108**(26): p. 10668-72.
73. Brown, E.J. and D. Baltimore, *Essential and dispensable roles of ATR in cell cycle arrest and genome maintenance*. Genes Dev, 2003. **17**(5): p. 615-28.
74. Unsal-Kacmaz, K., et al., *Coupling of human circadian and cell cycles by the timeless protein*. Mol Cell Biol, 2005. **25**(8): p. 3109-16.
75. Chou, D.M. and S.J. Elledge, *Tipin and Timeless form a mutually protective complex required for genotoxic stress resistance and checkpoint function*. Proc Natl Acad Sci U S A, 2006. **103**(48): p. 18143-7.
76. Leman, A.R., et al., *Human Timeless and Tipin stabilize replication forks and facilitate sister-chromatid cohesion*. J Cell Sci, 2010. **123**(Pt 5): p. 660-70.
77. Kang, T.H. and S.H. Leem, *Modulation of ATR-mediated DNA damage checkpoint response by cryptochrome 1*. Nucleic Acids Res, 2014. **42**(7): p. 4427-34.
78. Kang, T.H., et al., *Circadian oscillation of nucleotide excision repair in mammalian brain*. Proc Natl Acad Sci U S A, 2009. **106**(8): p. 2864-7.
79. Gaddameedhi, S., et al., *Control of skin cancer by the circadian rhythm*. Proc Natl Acad Sci U S A, 2011. **108**(46): p. 18790-5.
80. Matsuo, T., et al., *Control mechanism of the circadian clock for timing of cell division in vivo*. Science, 2003. **302**(5643): p. 255-9.
81. Hua, H., et al., *Circadian gene mPer2 overexpression induces cancer cell apoptosis*. Cancer Sci, 2006. **97**(7): p. 589-96.

**Chapter 2: Characterization of circadian rhythms in gene expression and
TMZ sensitivity in U87 glioma cell line *in vitro***

Abstract

Glioblastoma (GBM) is the most common and aggressive malignant primary brain tumor in adults. Current therapy involves surgical resection, radiotherapy with concomitant temozolomide (TMZ) chemotherapy, and 6 cycles of adjuvant TMZ chemotherapy. Despite initial response to these treatments, GBM very frequently recurs. Our goal is to improve upon the efficacy of TMZ treatments. Previous studies have demonstrated improved clinical outcomes in cancer patients by timing the delivery of chemotherapy to biological rhythms, a method known as chronotherapy. To investigate the role of cell-intrinsic circadian rhythms in modulating the response to TMZ, we developed an *in vitro* system to track rhythms in gene expression with luciferase reporters and measure TMZ response throughout the day. Using an established GBM cell line, we were able to observe circadian rhythms in clock gene expression and rhythmic sensitivity to TMZ *in vitro*. TMZ sensitivity, as measured by a cell survival assay, showed rhythms with peak survival consistently correlating with the peak of *Per2* expression across two independent experiments. In a single preliminary experiment, we have also demonstrated a rhythm in phosphorylation of H2AX, reaching the highest percent of phospho-H2AX positive cells at the time of peak *Bmal1* expression. We used single cell gel electrophoresis to measure dose-dependent changes in TMZ-induced DNA damage. We also observed shifts in clock gene expression following TMZ treatment, suggesting that TMZ-induced damage resets the molecular clock. These preliminary data are the first to demonstrate circadian rhythms in TMZ sensitivity in a human glioblastoma cell line. The knowledge gained from the results of these preliminary experiments was applied to the design of future *in vitro* experiments to measure circadian rhythms in TMZ response in a murine astrocyte model of glioblastoma.

Introduction

Glioblastoma is the most common and aggressive malignant primary brain tumor in adults. Surgical resection, radiation and chemotherapy are able to lengthen survival, but tumors ultimately recur in most patients [82]. Temozolomide, a DNA alkylator, was the first chemotherapy to significantly lengthen survival in GBM patients [21]. Despite this advancement, median survival is still only approximately 15 months [83]. Development of new treatments is crucial for improving survival of future GBM patients, but the development of new therapeutics takes many years. Therefore, patients who are currently suffering from GBM cannot afford to wait for new treatments; we need to make sure we are providing optimal care with the therapies that are currently available.

One method of optimizing treatment outcomes is chronomodulation of chemotherapy. The delivery of chemotherapy according to biological rhythms, known as chronochemotherapy, has successfully increased survival and reduced toxicity for a variety of chemotherapies [30, 35, 36, 84]. Chronochemotherapy has been applied to many cancer types, but our study is the first to apply it to brain tumors.

Before we tried chronotherapy in a mouse model of GBM, we wanted to learn about the cell intrinsic circadian properties of GBM cells. We used a human glioblastoma cell line, U87, to characterize circadian rhythms in gene expression and TMZ sensitivity *in vitro*. U87 cells are sensitive to TMZ treatment because they have hypermethylation of the MGMT promoter, which prevents expression of an enzyme known to provide resistance to TMZ-induced DNA damage [85]. Starting with a TMZ sensitive cell line, we were interested in testing whether the time of day of treatment would alter the sensitivity. The studies presented in this chapter are preliminary; many experiments were performed only one or two times. Even though the observations made

from these studies will not be published, they provided an early indication that circadian biology would impact TMZ responses and represent a critical stage in the development of the knowledge and skills that were required to perform the publishable studies in this thesis.

Materials and Methods

Cell Culture: The U87MG human glioblastoma cell line was purchased from American Type Cell Culture (ATCC). U87 cells were maintained at 37°C at 5% CO₂ in CO₂-buffered Dulbecco's Modified Eagle Medium (DMEM) supplemented with 10% Fetal Bovine Serum (FBS) (Gibco/Life Technologies, Carlsbad, CA) and 1% penicillin/streptomycin (Gibco/Life Technologies, Carlsbad, CA). During bioluminescence recordings, lids were sealed with vacuum grease and cell cultures were maintained in HEPES-buffered DMEM supplemented with 10% FBS, B27 (1X; Gibco/Life Technologies, Carlsbad, CA), as previously reported [86]. All bioluminescent cultures were maintained at 34°C. U87 cells were used up to passage 8 for experiments.

Temozolomide treatment of cultures: Temozolomide from Temodar capsules was dissolved in DMSO at a stock concentration of 100 mM and used at a concentration of 0.5 mM for experiments.

Bioluminescence recordings in vitro: Light from clock-gene reporters (*Bmal1::dLuc* or *Per2::dLuc*) was detected in customized light-tight incubators (34°C) equipped with photomultiplier tubes (PMT) (HC135--11; Hamamatsu Corp.) [86-88] or with an ultra-sensitive Charge-coupled device (CCD) camera in a light tight box (Stanford Photonics; bin factor, 2; 1/f stop; open filter; Stanford Photonics, Palo Alto, CA). Bioluminescence was integrated every 6 min over 4 –7 days in HEPES-buffered DMEM supplemented with 10% FBS, B27 (Life Technologies, Carlsbad, CA) and 0.1 mM D-luciferin (Xenogen, Alameda, CA). U87 cells plated

[36]

in the 96-well plate were cultured in 1% FBS instead of 10% FBS to prevent overgrowth in the dish during the 7 day experiment.

Expression of Per2::dLuc and Bmal1::dLuc reporters: We performed lentiviral infections of pure astrocyte cultures using lentiviral reporter constructs expressing firefly luciferase driven by the mouse *Bmal1* or (*Bmal1::dLuc*) [89, 90] or *Period2* (*Per2::dLuc*) [59] promoters. Astrocytes were incubated with the viral particles for 48 h. Infected cultures were split and re-plated twice before the start of an experiment.

Phospho-H2AX immunofluorescence staining and quantification: U87 cells plated on poly-d-lysine-coated glass coverslips were fixed with 4% paraformaldehyde, washed, permeabilized with Triton-X-100, incubated with phospho-S139 H2AX primary antibody (Molecular Probes) for 3 hours at 37C, washed with 1x PBS, incubated with Alexa fluor 568 Donkey α mouse IgG (Gibco/Life Technologies, Carlsbad, CA) for 1 hour at RT. Then, stained with DAPI (4',6'-diamino-2-phenylindole) (Gibco/Life Technologies, Carlsbad, CA) and mounted on glass slides with Immu-mount (Thermo Scientific, Pittsburgh, PA). Nuclear staining intensity was quantified by two individuals blinded to treatment conditions using an ImageJ plugin. Staining was quantified across 5 fields of view per coverslip and averaged across two coverslips per treatment condition. The threshold for positive staining was set after the completion of staining quantification using a histogram of a TMZ-treated versus DMSO-treated.

Counting DAPI-stained nuclei for cell survival assay: After fixation, U87 cells were permeabilized with Triton-X-100, then stained with DAPI for 10 minutes, then stoeed in 1xPBS (Gibco/Life Technologies, Carlsbad, CA). Nuclei were counted using an ImageJ plugin. Two

independent counters counted 5 representative images and achieved similar results, counting the same number of cells within 10% per field of view.

Single Cell Gel Electrophoresis (Comet assay): U87 cell cultures were treated with vehicle or TMZ for 6 hours, then trypsinized and counted. Cells were added to Comet Assay Low-Melt Agarose (Trevigen, Gaithersburg, MD), and spread on Comet Assay slides (Trevigen, Gaithersburg, MD). Agarose gel-suspended cells were lysed in ice cold lysis buffer (Trevigen, Gaithersburg, MD) for 30 min. Slides were exposed to 35V in a gel electrophoresis apparatus. Slides were washed in water and ethanol, then stained with ethidium bromide (Sigma, St. Louis, MO). Images were acquired on a fluorescence microscope. Images were quantified by CometScore software, measuring a minimum of 50 cells per treatment group.

Results

Circadian rhythms in clock gene expression in U87 glioblastoma cells *in vitro*

The human U87MG glioblastoma cell line (U87) had daily oscillations in clock gene luciferase reporters (**Figure 2.1A**). The time it takes to complete one oscillation, known as the period, was measured using 3-7 days of photomultiplier tube (PMT) recordings of either *Per-Luc* or *Bmal1-Luc* expression for each dish. The mean periods for *Per2-luc* and *Bmal1-luc* U87 recordings were 23.6 h and 25.7 h, respectively (**Table 2.1**). As seen in other cell types, the *Per2-luc* and *Bmal1-luc* bioluminescence oscillate in anti-phase (**Figure 2.1A**), with an average phase difference of 12.1 h between *Per2-luc* peak and *Bmal1-luc* peak on Day 2 of each recording. For the purposes of our studies, we consider the differential effects of treatments at four times (trough, rising, peak, or falling phases) in the daily *Bmal1-luc* expression rhythm (**Figure 2.1B**).

Table 2.1. Characterization of circadian rhythms in clock gene expression in U87 cells *in vitro*.

Circadian characterization of bioluminescence recordings	Mean \pm SEM	N
Period of Clock Gene Expression (<i>Per2</i> and <i>Bmal1</i> reporters)	24.5 \pm 0.8 h	5
Period of <i>Per2-luc</i> Expression	23.6 \pm 0.5 h	2
Period of <i>Bmal1-luc</i> Expression	25.7 \pm 1.7 h	3
Time between <i>Per2</i> and <i>Bmal1</i> peaks on Day 2 of recording	12.1 \pm 1.6 h	2 (Pairs)

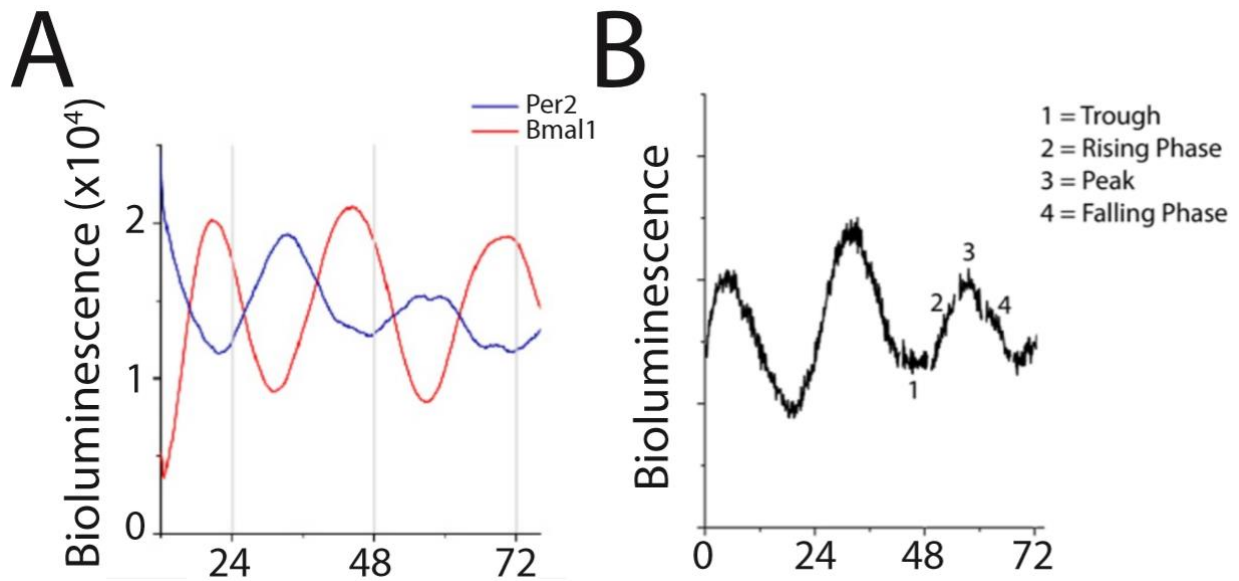


Figure 2.1. Circadian oscillations in clock gene expression in U87 cells *in vitro*. **A)** Representative traces from *Per2-luc* and *Bmal1-luc* bioluminescence reporters. **B)** Representative trace with circadian phases labeled: trough, rising, peak and falling.

Circadian rhythms in TMZ sensitivity in U87 glioblastoma cells *in vitro*

Per2-luc-expressing U87 cells were plated in a 96-well plate and immediately placed in a light tight box for bioluminescent recording with a Charge-coupled device camera.

Bioluminescence images were captured over time. Wells were treated in triplicate with 0.5 mM TMZ or vehicle (DMSO) for 6 hours, with each set of wells treated at different phases of *Per2-luc* expression: trough, rising, peak or falling phase. After 5 days of recording, the cells were fixed and stained with DAPI. In order to measure TMZ cytotoxicity, DAPI-stained nuclei were counted in three high powered fields per well. The survival of the TMZ-treated cells was expressed as a fraction of the number of cells counted in the DMSO-treated wells. In two independently plated experiments, there was a rhythm in the survival fraction (**Figure 2.2C&D**). Across the two experiments, there was a consistent correlation between lowest survival fraction and TMZ treatment at the trough of *Per2-luc* expression.

To determine whether these rhythms in cell survival could be attributed to rhythms in the DNA damage response, we measured phosphorylation of H2AX, an early step in sensing DNA damage [91]. U87 cells were plated on coverslips and treated with 0.5 mM TMZ or vehicle at different phases of *Bmal1-luc* expression: trough, rising, peak or falling phase. Eighteen hours after treatment, cells were fixed and stained for phospho-H2AX and DAPI. The number of phospho-H2AX positive nuclei was counted and divided by the total number of nuclei per field of view. Percent of phospho-H2AX positive staining was measured across 5 fields of view and two replicate coverslips per treatment group. The *Per2-luc* reporter corresponded closely with the rhythm we identified in cell survival, but we wanted to assess the utility of both *Per2-luc* and *Bmal1-luc* reporters in these studies. Based on the consistent anti-phase relationship established by early characterization of *Per2-luc* and *Bmal1-luc* expression in U87 cells, we chose to use the

Bmal1-luc reporter in this experiment to address the basis for the rhythm in TMZ response. A rhythm in phospho-H2AX positivity was evident with a peak response in those cells treated at the peak of *Bmal1-luc* expression (**Figure 2.2E&F**), which coincides with the trough of *Per2*. These data demonstrate a rhythm in sensing of TMZ-induced DNA damage in U87 cells that is in phase with the rhythm we have observed in cell survival. Moreover these data indicated that both of our reporters behaved as expected and provided reliable readouts of circadian time.

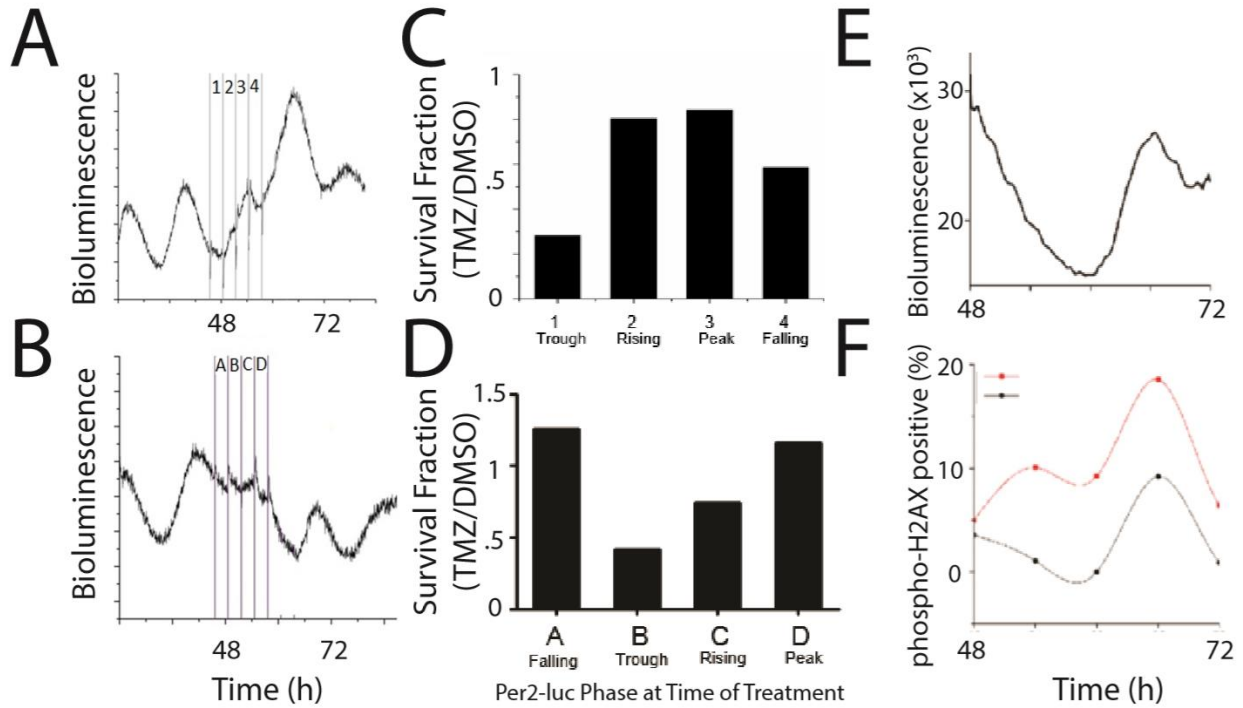


Figure 2.2. Rhythms in cell survival and DNA damage response to TMZ. Representative traces of *Per2-luc* recordings of U87 cell cultures treated at different phases of *Per2-luc* expression for two independent experiments (A & B). Surviving fraction of cells for each independent experiment were calculated by dividing the number of cells in TMZ-treated wells to vehicle-treated wells at each treatment time point (C&D). **E)** *Bmal1-luc* expression from reporter dish plated in parallel with wells treated with TMZ and stained for phospho-H2AX. **F)** Results of chronotherapy of U87 cell cultures fixed and stained for H2AX phosphorylation in TMZ-treated (red) and DMSO-treated (black) wells (n= 1).

Temozolomide-induced DNA damage measured by comet assay

The rhythm we observed in TMZ-induced H2AX phosphorylation could be due to rhythms in the number of double strand breaks (DSBs) created after TMZ treatment or a rhythm in the DNA damage response to an equal number of TMZ-induced breaks created at all times of day. We aimed to test whether DNA damage by TMZ varies with time of day using single cell gel electrophoresis (comet assay)[92]. In the absence of DNA damage, ethidium bromide-stained nuclei travel through the gel as a discrete circle (**Figure 2.3A**, vehicle). However, a “comet tail” is formed after DNA damage by the faster movement of ethidium bromide stained DNA fragments (**Figure 2.3B**, 1000 μ M TMZ). The extent of DNA damage can be quantified from fluorescence images of these comets using CometScore software and reported as the olive tail moment [93]. We measured the extent of DNA damage after 6 hours of treatment with vehicle, 100, 500 or 1000 μ M of TMZ (**Figure 2.3C**). Unfortunately, large standard deviations for the olive tail moments measured for each dose along the dose-response curve did not allow us to reliably distinguish between the amounts of damage induced by different doses of TMZ. Therefore, we were unable to use the comet assay to quantify DNA damage induced by a single dose of TMZ at different times of day.

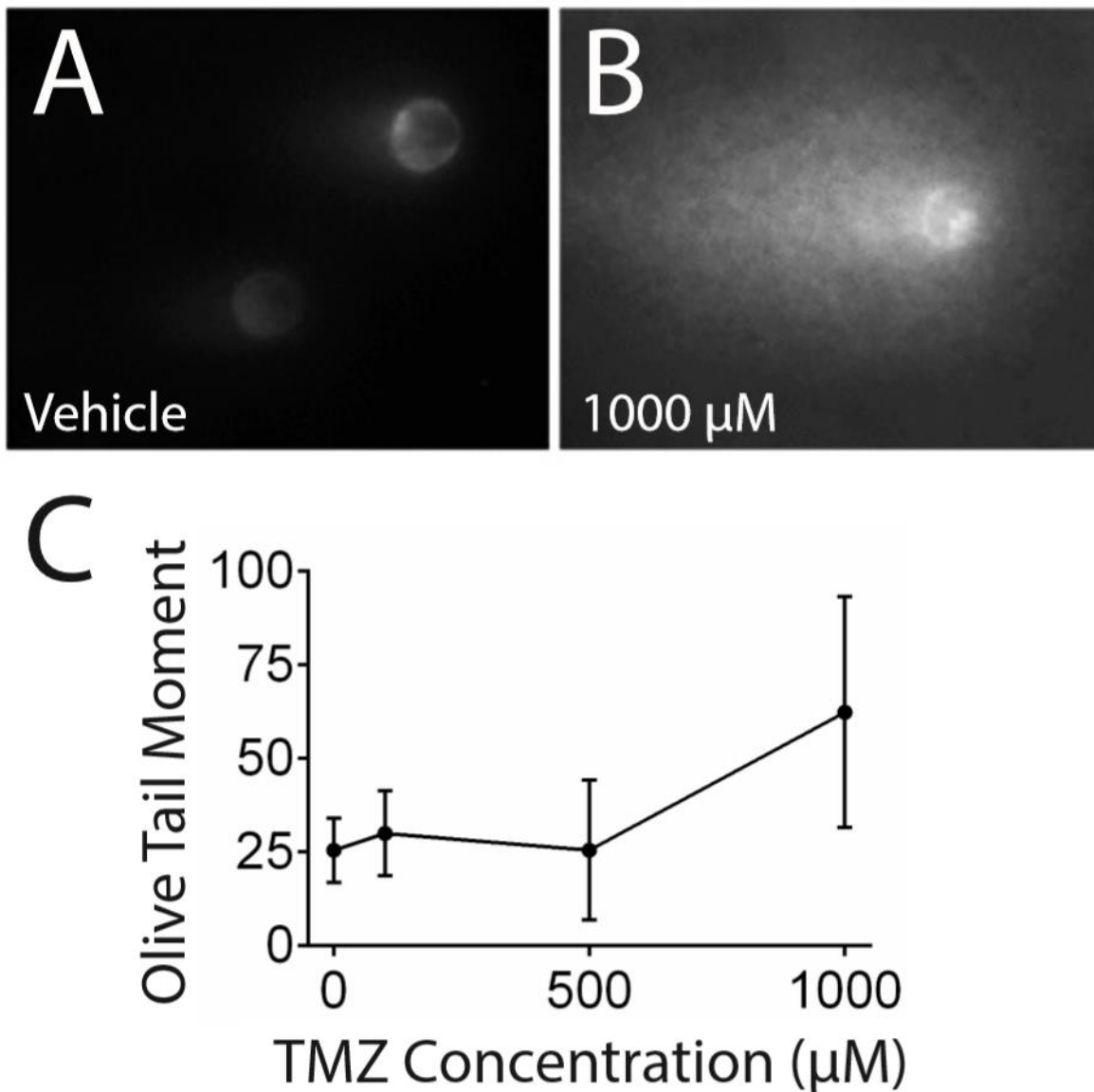


Figure 2.3. Comet Assay reveals highly variable TMZ-induced DNA damage in U87 cells *in vitro*. **A)** Representative image of ethidium-bromide stained nuclei from DMSO-treated U87 cells 6 hours after treatment. **B)** Representative image of an ethidium-bromide stained nucleus 6 hours after TMZ-induced DNA damage. **C)** Quantification of a TMZ dose-response curve (0, 100, 500, 1000 μM TMZ). Olive Tail Moment quantifies the extent of DNA damage induced at each dose of TMZ (Mean ± SD).

Treatment-induced phase shifts in *Per2-luc* rhythms *in vitro*

We observed shifts in the phase of *Per2-luc* expression after treating wells at different times of day in the cell survival assay described above (Figure 2). We chose to measure rhythms on Day 4 because all treatments included in this analysis were completed by the start of Day 4. We did not measure the timing of peaks on Day 5 because some *Per2-luc* traces damped out considerably by Day 5, making it difficult to identify peaks for all treated cultures. This dampening of *Per2-luc* amplitude on Day 5 is consistent with what we have previously seen in bioluminescence recordings in the absence of TMZ or vehicle treatments. Figure 4A shows TMZ-treated wells reached the *Per2* peak earlier than the wells treated with DMSO during the same 6 hour time frame (yellow bar). The average timing of *Per2* peak expression is expressed as hours after the start of Day 4, the day after treatment (Figure 4B). DMSO-treated dishes reached their *Per2* peaks (black circle) at different times of day depending upon the timing of treatment on the previous day. TMZ-treated wells did not reach peak of *Per2* expression at the same time on Day 4 as the DMSO-treated wells (Figure 4B). Relative to vehicle controls, we observed delayed *Per2* peaks in wells treated with TMZ at the peak or falling phases of *Per2* expression. In contrast, wells treated at the trough or rising phases of *Per2* expression had TMZ-treated wells reaching the peak of *Per2* earlier than vehicle controls. These data demonstrated treatment-induced shifts in the phase of *Per2-luc* expression. The direction of the TMZ-induced shifts was dependent on the *Per2* phase at the time of treatment: treatments at peak and falling phases caused phase delays and treatments at the trough and rising phases caused phase advances in *Per2* rhythms. This observation is important because repeated it shows that treatments delivered at the same time of day on two consecutive days could be delivered to cells at two different phases of clock gene expression. Therefore, these data represent an important

complicating factor to keep in mind in future experiments: DNA damage-induced phase shifts in circadian clock gene expression may alter the way cells respond to treatment on subsequent days.

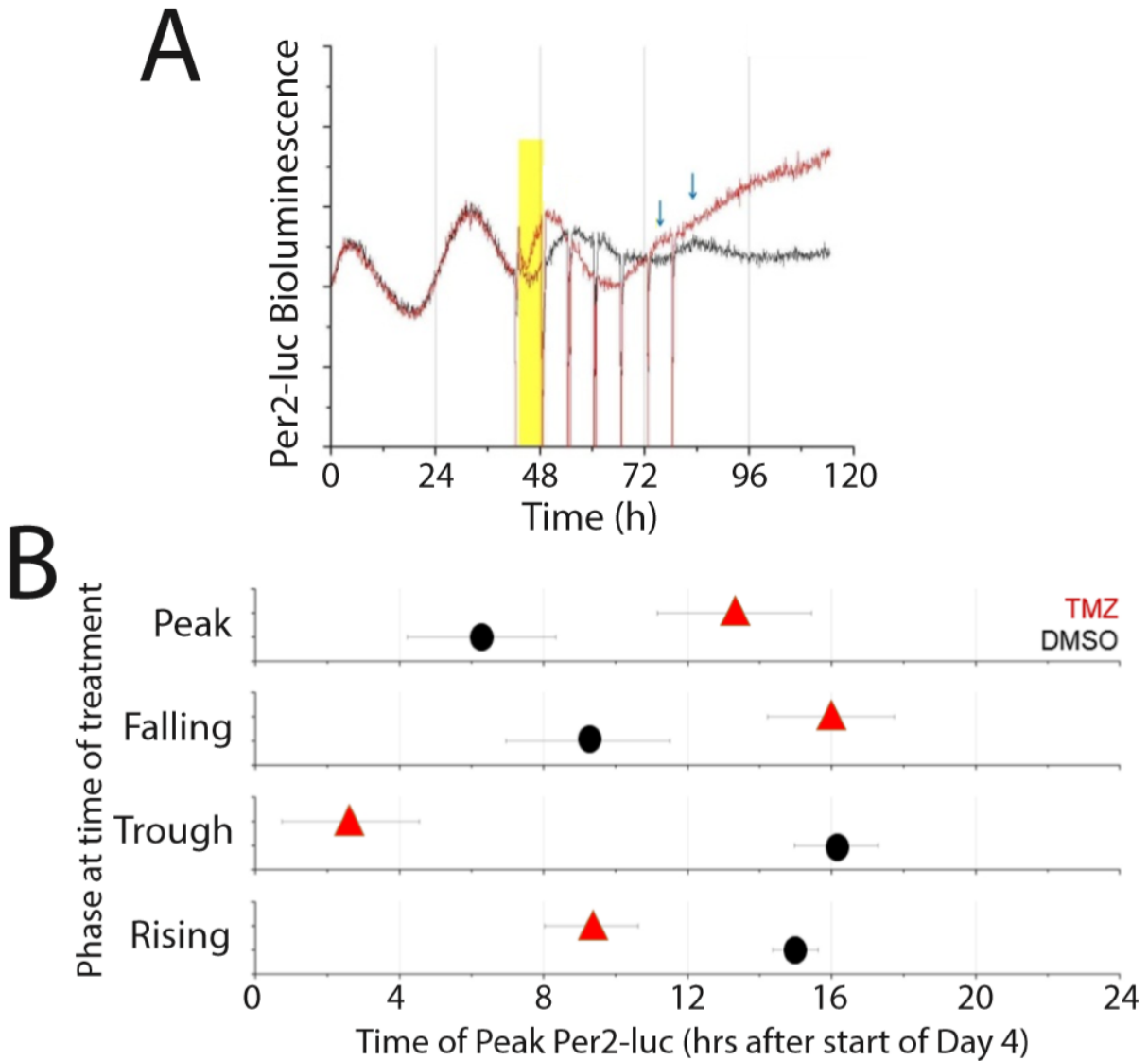


Figure 2.4. Direction of TMZ-induced phase shifts is circadian phase-dependent. A)

Representative trace of TMZ-treated (red) and DMSO-treated (black) *Per2-luc* traces from U87 cell cultures. Yellow bar represents 6 h exposure time to TMZ or vehicle. The timing of peak *Per2-luc* expression on Day 4 (one day after treatment; blue arrows) is earlier for TMZ-treated cultures than DMSO-treated cultures.

B) The average timing of peak *Per2-luc* expression on Day

4 is reported for TMZ-treated (red rectangle) and DMSO-treated (black circle). Each graph represents wells treated at the same phase of *Per2-luc* expression on Day 3 (n = 1).

Discussion

Daily oscillations in expression of *Per2-luc* and *Bmal1-luc* reporters demonstrated that U87 cells have an intact molecular clock and that we can reliably measure its activity. Many human cancer cell lines that have been tested have failed to demonstrate rhythmic clock gene expression (Robert Dallman and John Hogenesch, personal communication). The anti-phase oscillations of *Per2-luc* and *Bmal1-luc* demonstrate canonical regulation of the molecular clock within the U87 cells. Therefore, these data demonstrate a functional clock within U87 cells, providing a cell-intrinsic mechanism by which TMZ sensitivity could change with time of day.

Preliminary data demonstrate circadian oscillations in TMZ sensitivity in U87 cells *in vitro*. The fraction of cells that survive TMZ treatment varies in a time of day-dependent manner. Across two independent experiments, we demonstrated that U87 cells have the lowest survival fraction, and therefore are the most sensitive to TMZ at the trough of *Per2-luc* expression. In a single preliminary experiment, we have demonstrated a circadian rhythm in phosphorylation of histone H2AX, with the greatest phosphorylation occurring at the peak of *Bmal1* expression. This correlation with circadian clock gene expression is consistent with the results of our survival assay. As demonstrated in Figure 1A, *Bmal1* reaches its peak at the time that *Per2* reaches its trough. Therefore, TMZ treatment at the peak of *Bmal1*/trough of *Per2* results in the greatest amount of DNA damage sensing and the lowest survival. These data are consistent with data from Dulong and colleagues demonstrating greatest irinotecan sensitivity at *Bmal1* peak in colon cancer cells [94]. Taken together, these preliminary data demonstrate greatest TMZ sensitivity of U87 cells at the peak of *Bmal1* expression *in vitro*. Future studies should repeat these assays to assess reproducibility of these findings. Reproducing these findings in a different cell line would further strengthen the biological link between *Bmal1* expression and TMZ

sensitivity. Furthermore, these studies demonstrate a cell-intrinsic rhythm governing response to TMZ, not simply a rhythm in drug metabolism or delivery to the tumor via rhythms of the host. The tumor cell-intrinsic nature of this rhythm creates an opportunity to manipulate the rhythms of the tumor to specifically enhance TMZ anti-tumor efficacy, without altering the sensitivity of the host.

The rhythms observed in phosphorylation of H2AX could be due to rhythms in the amount of TMZ-induced DNA damage or the cellular response to DNA damage. The comet assay is the most direct way to assess DNA damage. We have demonstrated that TMZ-induced DNA damage is greater than baseline DNA damage in vehicle-treated U87 cells using this assay. However, the high degree of variability within each sample limits the sensitivity of the comet assay. Since we are looking at low-amplitude changes, we need to use highly sensitive methods to detect and measure changes in the response of U87 cells to TMZ treatment. For these reasons, we chose not to use this method to determine whether there was a circadian rhythm in the amount of TMZ-induced DNA damage in future experiments. We were unable to determine whether the amount of TMZ-induced DNA damage oscillated in a circadian manner because we did not have a sensitive enough assay to quantify DNA damage. Future studies might examine the early induction of H2AX phosphorylation as a proxy for DNA damage prior to the initiation of DNA repair.

We observed treatment-induced shifts in the phase of *Per2-luc* expression. If the DMSO treatments had not caused any phase shifts in *Per2* rhythms, we would have seen the *Per2* peaks occurring at the same time on Day 4 in all DMSO-treated wells. However, we saw the DMSO-treated wells reaching peak of *Per2* at different times on Day 4 due to treatment at different phases of *Per2-luc* expression. These shifts in the DMSO-treated wells could be explained by the

media change which occurred at the end of the 6 hour treatment window. In our lab, we have seen media changes, shifts in temperature and physical movement of dishes reset the rhythms of clock gene expression in other *in vitro* experiments (data not shown). What is more interesting is the timing of peak *Per2* in the TMZ-treated wells relative to the vehicle-treated wells. If the media change, temperature change or movement of the 96-well plate were the only mechanisms underlying these phase shifts in *Per2* rhythms, we would have seen shifts in the same direction in TMZ- and DMSO-treated wells. However, we saw TMZ-induced shifts away from vehicle control rhythms. The directionality of the phase shift was dependent upon the *Per2* phase at the time of treatment. TMZ induces phase delays in *Per2* rhythms when treating at *Per2* peak or falling phases. In contrast, TMZ induces phase advances in wells treated at the *Per2* trough or rising phases. These data are consistent with a study showing ionizing radiation-induced phase advances in *Per2-luc* rhythms in Rat-1 cells [95]. Following up on those findings, another paper presented a mathematical model where IR-induced activation of Chk2 led to premature degradation of PER proteins, thus advancing the phase of the clock [96]. A recent publication presented Hausp-dependent stabilization of Cry1 as the mechanism underlying ionizing radiation-induced phase advances in circadian rhythms in fibroblasts [97]. In the context of the literature, it seems likely that the phase shifts created in the TMZ-treated wells are due to TMZ-induced DNA damage. In all of these papers, DNA damage only induces phase advances. In contrast, our preliminary study shows phase advances and delays relative to vehicle-treated controls. The published studies used ionizing radiation to induce immediate DNA double strand breaks (DSBs). However, our studies utilize a DNA alkylator, which indirectly leads to DSBs during failed mismatch repair [98]. Also, our study requires media change at the end of the 6 h TMZ treatment window, which could also induce phase shifts. We can be confident that the

phase shifts we see in the TMZ-treated dishes are not due solely to media change because the TMZ- and DMSO-treated dishes do not shift together in equal magnitude, or in the same direction. The added complication of media change-induced phase shifts may provide an opportunity for phase delays that are not possible in the published IR-induced phase advance studies. Alternatively, there may be unique aspects of the molecular clock in U87 cells that allow for phase delays. Also, it is important to recognize that our studies are preliminary. We would need to perform this experiment several more times to make sure these results are repeatable. Future studies would require treatments at shorter intervals to create a full phase response curve with TMZ and DMSO to identify the differences in phase shifts caused by each treatment condition. Extending these studies to other cell lines and other DNA damaging agents will help us understand which principles of DNA damage-induced phase shifts are universal across all DNA damaging agents and all cell lines possessing circadian rhythms.

The knowledge gained from these preliminary U87 *in vitro* studies guided the design of the studies that follow. We were able to optimize our protocol for luciferase reporter expression and bioluminescence recordings using U87 cell cultures. We established a relationship between the peak of *Per2-luc* expression and the greatest cell survival. This relationship was consistent with the rhythm we observed in phosphorylation of H2AX, showing a correlation between the phase of clock gene expression and TMZ sensitivity by two independent methods. Our observations of DNA damage-induced shifts in circadian rhythms made us keenly aware of the complexity of our model system. Therefore, in all future studies we chose to limit our *in vitro* experiments to single doses of TMZ per dish due to the DNA damage-induced rhythms we observed in these preliminary studies. The information we learned from these *in vitro* studies set the stage for the experiments we performed in our mouse model of mesenchymal GBM. The

results of these *in vitro* studies indicate cell-intrinsic circadian rhythms in gene expression and DNA damage response, which provides a strong rationale for further investigation into the cell-intrinsic properties contributing to circadian rhythms in TMZ sensitivity.

Acknowledgements: Thanks to Jasmin Sponagel, Julia Button and Manar Il-ur Al Swaby for technical assistance. Thanks to Dr. Andrew Liu for providing the *Per2::dLuc* and *Bmal1::dLuc* lentiviruses. Special thanks to Drs. Susana Gonzalo and Ignacio Gonzalez-Suarez for teaching me the single-cell gel electrophoresis technique.

References

1. Ogura, K., et al., *Initial and cumulative recurrence patterns of glioblastoma after temozolomide-based chemoradiotherapy and salvage treatment: a retrospective cohort study in a single institution*. *Radiat Oncol*, 2013. **8**: p. 97.
2. Stupp, R., et al., *Radiotherapy plus concomitant and adjuvant temozolomide for glioblastoma*. *N Engl J Med*, 2005. **352**(10): p. 987-96.
3. Stupp, R., et al., *Effects of radiotherapy with concomitant and adjuvant temozolomide versus radiotherapy alone on survival in glioblastoma in a randomised phase III study: 5-year analysis of the EORTC-NCIC trial*. *Lancet Oncol*, 2009. **10**(5): p. 459-66.
4. Levi, F., et al., *Implications of circadian clocks for the rhythmic delivery of cancer therapeutics*. *Adv Drug Deliv Rev*, 2007. **59**(9-10): p. 1015-35.
5. Schmiegelow, K., et al., *Impact of morning versus evening schedule for oral methotrexate and 6-mercaptopurine on relapse risk for children with acute lymphoblastic leukemia*. *Nordic Society for Pediatric Hematology and Oncology (NOPHO)*. *J Pediatr Hematol Oncol*, 1997. **19**(2): p. 102-9.
6. Levi, F., et al., *Chronomodulation of chemotherapy against metastatic colorectal cancer*. *International Organization for Cancer Chronotherapy*. *Eur J Cancer*, 1995. **31A**(7-8): p. 1264-70.
7. Kobayashi, M., P.A. Wood, and W.J. Hrushesky, *Circadian chemotherapy for gynecological and genitourinary cancers*. *Chronobiol Int*, 2002. **19**(1): p. 237-51.
8. Jiang, G., et al., *Strategies to improve the killing of tumors using temozolomide: targeting the DNA repair protein MGMT*. *Curr Med Chem*, 2012. **19**(23): p. 3886-92.
9. Marpegan, L., T.J. Krall, and E.D. Herzog, *Vasoactive intestinal polypeptide entrains circadian rhythms in astrocytes*. *J Biol Rhythms*, 2009. **24**(2): p. 135-43.

10. Prolo, L.M., J.S. Takahashi, and E.D. Herzog, *Circadian rhythm generation and entrainment in astrocytes*. J Neurosci, 2005. **25**(2): p. 404-8.
11. Beaulé, C., et al., *In vitro circadian rhythms: imaging and electrophysiology*. Essays Biochem, 2011. **49**(1): p. 103-17.
12. Liu, A.C., et al., *Redundant function of REV-ERB α and β and non-essential role for Bmal1 cycling in transcriptional regulation of intracellular circadian rhythms*. PLoS Genet, 2008. **4**(2): p. e1000023.
13. Zhang, E.E., et al., *A genome-wide RNAi screen for modifiers of the circadian clock in human cells*. Cell, 2009. **139**(1): p. 199-210.
14. Ramanathan, C., et al., *Monitoring cell-autonomous circadian clock rhythms of gene expression using luciferase bioluminescence reporters*. J Vis Exp, 2012(67).
15. Bonner, W.M., et al., *GammaH2AX and cancer*. Nat Rev Cancer, 2008. **8**(12): p. 957-67.
16. Collins, A.R., *The comet assay for DNA damage and repair: principles, applications, and limitations*. Mol Biotechnol, 2004. **26**(3): p. 249-61.
17. Mozaffarieh, M., et al., *Comet assay analysis of single-stranded DNA breaks in circulating leukocytes of glaucoma patients*. Mol Vis, 2008. **14**: p. 1584-8.
18. Dulong, S., et al., *Identification of circadian determinants of cancer chronotherapy through in vitro chronopharmacology and mathematical modeling*. Mol Cancer Ther, 2015.
19. Oklejewicz, M., et al., *Phase resetting of the mammalian circadian clock by DNA damage*. Curr Biol, 2008. **18**(4): p. 286-91.

20. Hong, C.I., J. Zamborszky, and A. Csikasz-Nagy, *Minimum criteria for DNA damage-induced phase advances in circadian rhythms*. PLoS Comput Biol, 2009. **5**(5): p. e1000384.
21. Papp, S.J., et al., *DNA damage shifts circadian clock time via Hausp-dependent Cry1 stabilization*. Elife, 2015. **4**.
22. Friedman, H.S., et al., *Methylator resistance mediated by mismatch repair deficiency in a glioblastoma multiforme xenograft*. Cancer Res, 1997. **57**(14): p. 2933-6.

Chapter 3: *Bmal1*-dependent rhythms in temozolomide sensitivity in Mes-GBM astrocytes *in vitro*

Abstract

The safety and efficacy of multiple cancer chemotherapeutics can vary as a function of when during the day they are delivered. This study aimed to improve the treatment of glioblastoma multiforme (GBM), the most common brain cancer, by testing the efficacy of the DNA alkylator Temozolomide (TMZ) on GBM *in vitro* and *in vivo* as a function of time of day. We found cell-intrinsic, daily rhythms in susceptibility of GBM tumor cells (mouse astrocytes deficient in NF1 and p53 signaling) to TMZ *in vitro*. The greatest TMZ-induced DNA damage response, activation of apoptosis and growth inhibition, occurred near the peak expression of the core clock gene *Bmal1* in cultured GBM cells. Deletion of *Bmal1* abolished rhythmic circadian clock gene expression and circadian rhythms in TMZ-induced activation of apoptosis and growth inhibition in GBM tumor cells *in vitro*. Taken together, these data suggest an important role for the core molecular clock in regulating the tumor cell-intrinsic response to TMZ-induced DNA damage. These results may be important broadly for how we design TMZ and other DNA damaging approaches to GBM treatment.

Introduction

Glioblastoma, a WHO grade IV astrocytoma, is the most common and aggressive malignant primary brain tumor in adults. Despite decades of research and many clinical trials, median survival is still only approximately 15 months [83]. Therefore, all opportunities to improve upon the current treatment outcomes should be pursued.

For many years, surgical resection and radiation therapy were the standard of care. In 2005, a landmark paper published in the New England Journal of Medicine demonstrated an increase in progression-free and overall survival with the addition of temozolomide (TMZ) chemotherapy [21]. Clinicians have tried a variety of TMZ treatment schedules to optimize

treatment, eventually settling on a 5-day course every 28 days to minimize toxicity [99, 100]. However, none of these studies took into account the time of day of TMZ administration. As an oral medication, it is easy to regulate the timing of treatment. TMZ has a blood plasma half-life of 1.8 h [101], in addition to a short half-life (1.7-2.6 h) within tumors in animal models of GBM [102, 103], making it an ideal candidate for chronotherapy.

Oncologists have tested the efficacy and tolerability of chemotherapeutic agents at different times of day in a variety of cancer types. The administration of medications based on daily rhythms in biological processes is known as chronotherapy. Chronotherapy has increased 5-year survival rates in acute lymphoblastic leukemia and ovarian cancer patients, and increased the objective response rate in colorectal cancer while simultaneously reducing toxicities [30, 35, 36]. Despite successful therapeutic outcomes, chronotherapy has never been applied to the treatment of brain tumors.

Our daily rhythms in sleep, hormone release, and many other physiological processes are driven by an internal circadian clock [54]. Molecular clocks exist within most cells to keep daily time at the cellular level. The core molecular clock includes two transcription factors, BMAL1 and CLOCK, which activate transcription of downstream genes. Genes activated at different times of day by the BMAL1-CLOCK transcription dimer are known as clock-controlled genes (CCGs). Among those CCGs, the gene products of the *Period* family (*Per1*, *Per2*, *Per3*), and the *Cryptochrome* family (*Cry1* and *Cry2*) provide negative feedback to block further transcriptional activation by the BMAL1-CLOCK dimer [104]. This feedback loop creates circadian oscillations in clock-controlled gene expression. A stabilizing feedback loop regulates transcription of the *Bmal1* gene (*Arntl*), creating an oscillation in *Arntl* expression that is anti-phase to the clock-controlled genes [105-107]. Loss of *Arntl* leads to loss of rhythms in individual cells, and rest-

activity rhythms demonstrating the crucial role *Bmal1* plays in regulating circadian function [60]. Our studies take advantage of the importance of *Bmal1* to explore the contributions of the circadian clock to the response of glioblastoma to TMZ.

Many links have been made between circadian clocks and cancer. Epidemiological studies have demonstrated that shift workers have a higher risk of developing cancer [47, 108], creating a correlation between disrupted clocks and tumorigenesis in humans. To build on this shift work-cancer link, scientists have recently demonstrated an increased risk of breast cancer development in female mice exposed to a chronically shifting light schedule [40]. Circadian rhythms in human physiology have also been linked to survival for colorectal and breast cancer patients [84]. Expression of circadian clock genes has been deregulated in a variety of cancer types, including gliomas [109-113]. At the molecular level, circadian clock proteins have been directly linked to DNA damage response. The circadian role of mammalian TIMELESS (Tim) remains unknown, but requirement of Tim for DNA damage checkpoint responses has been demonstrated through interactions with the ATR-Chk1, and ATM-Chk2 pathways [74, 77, 114-116]. PER1 protein interacts directly with ATM and Chk2, enhancing activation of the checkpoint pathway [70]. PER3 also interacts with and enhances ATM-mediated phosphorylation of Chk2 [71]. Rhythmic expression of the base excision repair protein, XPA, creates daily rhythms in UV-induced DNA damage [78]. Circadian rhythms in transcription have been demonstrated for cell cycle regulators Wee1, c-Myc and CyclinD1 [67, 80]. We know circadian regulation of expression of these cell cycle regulators is relevant to cancer biology because their expression has been dysregulated in chronic lymphocytic leukemia [111]. Coupling of the circadian cycle and cell cycle has been tested experimentally and with mathematical modeling [117]. A recently published study demonstrates that colon cancer cells have *Bmal1*-

dependent circadian oscillations in sensitivity to irinotecan, based on *in vitro* experiments and mathematical modeling [94]. The molecular clockwork seems to play an important role in the regulation of pathways relevant to cancer biology.

Our studies demonstrate that glioblastoma susceptibility to TMZ is regulated by the circadian clock in a murine model of glioblastoma. We demonstrate a rhythm in TMZ sensitivity based on the timing of treatment *in vitro*. Greatest sensitivity to TMZ occurs at the peak of *Bmal1* expression. Through CRISPR-Cas9-mediated disruption of *Arntl*, we have demonstrated an important role for *Bmal1* in maintaining rhythmic expression of circadian clock genes and rhythmic response to TMZ *in vitro*.

Materials and Methods

Animals: All animals were used in accordance with established Animal Studies Protocols (no. 20140098 and 20120174) approved by the Washington University Animal Studies Committee and followed National Institutes of Health guidelines. Male NCR nude mice used for flank implantations were purchased from Taconic Farms, Inc (NY, USA). Founder *Nf1flox/flox;GFAP-Cre* mice were provided by Dr. David Gutmann (Washington University, St. Louis, MO) and were housed in the Animal Facilities at Washington University's School of Medicine and Danforth Campus.

Male Astrocyte Cultures: Primary cultures of astrocytes were prepared from individual postnatal day 1 *Nf1flox/flox;GFAP-Cre* mice as previously described [118]. Sex of each mouse was determined from tail DNA by PCR for *JARID 1C* as previously described [119]. All cells from a single litter with the same *Neurofibromin 1 (Nf1)* genotype were pooled based on sex and cultured in Dulbecco's Modified Eagle's Medium (DMEM) supplemented with F12 and 10%

fetal bovine serum (FBS). Replicate experiments were performed using astrocytes isolated from at least three independent litters. Only male astrocytes were used for these experiments.

Expression of DNp53: A dominant negative P53-encoding retrovirus (DNp53-IRES-eGFP) [120] was generated by transfecting Plat-E cells with a pMIG-DNp53-eGFP construct. Media containing retrovirus was harvested 48-72 hours post-transfection and stored at -80°C until use. The resultant viral media was used to infect male *Nf1*^{-/-} astrocytes with polybrene (5µg/ml, Millipore, Billerica, MA). *Nf1*^{-/-};*DNp53-eGFP* positive cells were sorted to purity using a MoFlo high speed flow cytometer (Beckman Coulter, Fort Collins), as previously described [119]. Results are reported from Mes-GBM astrocytes that were used for up to 8 passages following GFP-positive selection by flow cytometry.

Expression of CRISPR-Cas9 expression vectors: Six guide RNAs targeting the *Bmal1* (*Arntl*) locus were designed and cloned by the Genome Engineering Center at Washington University in St. Louis. Lentiviruses were generated by transfecting 293T HEK cells with the LentiCRISPRv2-Cas9, delta8.9 and VSV-G plasmids. Media containing CRISPR-Cas9 lentivirus was harvested 48 hours after transfection and stored at -80°C until use. The resultant viral media was used to infect Mes-GBM astrocytes with polybrene (5µg/ml, Millipore, Billerica, MA). Mes-GBM astrocytes were infected with 6 pooled CRISPR-Cas9 lentiviruses, each containing a unique *Arntl*-targeting guide RNA (*Bmal1* CRISPR) or an equivalent titer of CRISPR-Cas9 lacking a guide RNA sequence (Control CRISPR). After infection, *Nf1*^{-/-};*DNp53-Cas9* astrocytes were selected with puromycin (2µg/ml, Fisher Scientific, Pittsburgh, PA) for 3 weeks. Clonal lines were derived by serial dilution and expansion of single clones. *Bmal1* deletion was confirmed by

Western Blot (1:500, Novus Biologicals, Littleton, CO). Results are reported from CRISPR-Cas9 clonal lines used up to 17 passages.

Expression of Per2::dLuc and Bmal1::dLuc reporters: We performed lentiviral infections of pure astrocyte cultures using lentiviral reporter constructs expressing firefly luciferase driven by the mouse *Bmal1* or (*Bmal1::dLuc*) [89, 90] or *Period2* (*Per2::dLuc*) [59] promoters. Astrocytes were incubated with the viral particles for 48 h and then reporter-expressing cells were selected based on blasticidin resistance. Media was supplemented with Blasticidin S HCl for 7 days (4 ug/mL, TOKU-E, Bellingham, WA).

Expression of Caspase-luc reporter: We transfected Mes-GBM astrocyte cultures with the Caspase-3/7-luciferase plasmid (*Casp-luc*; generous gift of Dr. Alnawaz Rehemtulla (University of Michigan, Ann Arbor, MI) [121] using Fugene 6 (Promega, Madison, WI). Stable lines were selected with 400 ug/ml geneticin (G418; Santa Cruz Biotechnology, Dallas ,TX) and maintained in CO₂-buffered *DMEM* supplemented with 10% FBS, 1% penicillin/streptomycin for up to 17 passages.

Cell Culture: The primary Mes-GBM mouse astrocyte cultures (*Nf1^{-/-};DNp53-eGFP*) were maintained at 37°C at 5% CO₂ in CO₂-buffered *DMEM* supplemented with 10% FBS (Gibco/Life Technologies, Carlsbad, CA) and 1% penicillin/streptomycin (Gibco/Life Technologies, Carlsbad, CA). During bioluminescence recordings, lids were sealed with vacuum grease and cell cultures were maintained in HEPES-buffered *DMEM* supplemented with 10% FBS, B27 (1X; Gibco/Life Technologies, Carlsbad, CA), as previously reported [86]. All bioluminescent

cultures were maintained at 34°C, with the exception of temperature shifts used to entrain cultures. Temperature shifts between 30C and 34C occurred every 12 hours across 48 hours prior to the start of treatment of the caspase-luciferase reporter dishes. In separate incubators, temperatures were shifted in opposite directions to entrain cultures to different phases of circadian clock gene expression.

Subcutaneous implantations: *Nf1*^{-/-};*DNp53* astrocytes were treated with human epidermal growth factor (EGF) (Sigma, St. Louis, MO) for 48 hours prior to implantation into the flanks of nude mice. To mobilize and support cell growth in flank implantations, matrigel (100 µL/side flank, BD Bioscience) was added to the cells prior to injection. Flank tumors were measured weekly with a digital caliper.

Temozolomide treatment of mice: Mice bearing Mes-GBM flank tumors expressing Cas9-only (*Bmal1* WT) or *Bmal1/Arntl*-targeting gRNA-Cas9 (*Bmal1* KO) were treated with 21 mg/kg/day temozolomide (TMZ, Sigma, St. Louis, MO) by oral gavage at 12pm or 12am for 5 consecutive days. Vehicle control mice received oral gavage of DMSO diluted in water at 12 am or 12 pm.

Real-time qPCR: All real-time qPCR assays were performed with iTaq™ Universal SYBR® Green Supermix (Biorad, Hercules, CA). cDNA was generated from total RNA with Superscript III reverse transcriptase (Invitrogen, Carlsbad, CA) per manufacturer's instructions. PCR and data collection were done using the BioRad CFX Connect Real-Time PCR machine and Opticon Monitor 3 Software (Biorad, Hercules, CA). Relative transcript copy number for each gene and corresponding GAPDH sample were calculated using the delta-delta-C(q) method [122].

Nuclear and histone extractions: Cells in culture were scraped off dishes in PBS and pelleted at 12,000xg for 15 minutes. The pellet was resuspended in Triton extraction buffer (TEB) (PBS, 0.5% Triton X-100, 0.02% Sodium Azide, protease (Complete, 1:50, Roche, Basel, Switzerland) & phosphatase inhibitor cocktails (II, 1:100; IV, 1:50, Calbiochem, Billerica, MA) and incubated for ten minutes at 4C. Lysates from cells or tissue homogenate was pelleted at 2,000 x g for 10 minutes and pellets were resuspended in hydrochloric acid (HCl) (0.2M), rotating overnight at 4C. Precipitate was pelleted at 2,000 x g for 10 minutes and supernatant containing histones was used for Westerns. Histone protein concentration was assessed by Bradford protein assay prior to loading SDS-PAGE gels with histone extracts.

Western blot: Western blots were performed and imaged using the Odyssey Infrared Imaging system (LI-COR, Lincoln, NE) as previously described (45). Total protein (30~50 µg per lane) was loaded onto a 4% to 12% Nu-Page gradient gel (Invitrogen). Primary antibodies were incubated at 4°C overnight. Secondary antibody incubation was at room temperature for 1 hour. Primary antibodies used in this study were phospho-S139 H2AX (Molecular Probes, 1:1000), H2AX (CST, Danvers, MA, 1:1000), Caspase 3 (CST, Danvers, MA, 1:1000), Cleaved Caspase 3 (Asp175) (CST, Danvers, MA, 1:800), Mouse anti- β-actin (1:30,000, Sigma); IRdye680 or 800 conjugated donkey anti-mouse or rabbit IgG (1: 40,000), LI-COR).

Phospho-H2AX immunofluorescence staining and quantification: Mes-GBM astrocytes plated on poly-d-lysine-coated glass coverslips were fixed with 4% paraformaldehyde, washed, permeabilized with Triton-X-100, incubated with phospho-S139 H2AX primary antibody

(Molecular Probes) for 3 hours at 37°C, washed with 1x PBS, incubated with Alexa fluor 568 Donkey α mouse IgG (Life Technologies, Carlsbad, CA) for 1 hour at RT. Then, stained with DAPI (Life Technologies, Carlsbad, CA) and mounted on glass slides with Immu-mount (Thermo Scientific, Pittsburgh, PA). Nuclear staining intensity was quantified by two individuals blinded to treatment conditions using an ImageJ plugin. Staining was quantified across 5 high powered fields of view per coverslip and averaged across two coverslips per treatment condition. The threshold for positive staining was set after the completion of staining quantification using a histogram of a TMZ-treated versus DMSO-treated.

Bioluminescence recordings in vitro: Light from clock-gene reporters (*Bmal1::dLuc* or *Per2::dLuc*) was detected in customized light-tight incubators (34°C) equipped with photomultiplier tubes (HC135--11; Hamamatsu Corp.) [86-88]. Bioluminescence was integrated every 6 min over 4–7 d after culture medium was exchanged with HEPES-buffered DMEM supplemented with B27 (Life Technologies, Carlsbad, CA) and 0.1 mM D-luciferin (Xenogen, Alameda, CA).

Bioluminescence recordings in vivo: Adult NCR nude male mice bearing subcutaneous flank mes-GBM xenografts were synchronized to a 12-h light/12-h dark cycle for at least 2 weeks (lights on from 7:00 A.M. to 7:00 P.M. (LD)). On the first day of imaging, each mouse was anesthetized with isoflurane (2% vaporized in O₂) at 10:00 A.M., injected i.p. with d-luciferin (150 μ g/g body weight; Biosynth, Itasca, IL) One minute exposures were captured 10 minutes after injection. Every 4 h, the mice were reanesthetized with isoflurane and imaged with an ultra-sensitive CCD camera in a light tight box (Stanford Photonics; bin factor, 2; 1/f stop; open filter; Stanford Photonics, Palo Alto, CA). Mice received subcutaneous saline for hydration (0.5 cc

every 8 hours), were returned to their cages, and awoke within 3 min after removal of the anesthetic. This procedure was repeated every 4 h for 48 h, during which time the mice showed no adverse effects of repeated 20-min anesthesia.

Statistical Analysis: Standard statistical analyses were completed with GraphPad Prism version 6.0 (GraphPad, San Diego, CA). Circadian period of bioluminescence recordings were analyzed with Chronostar V2.0 software.

Results

Clock genes are genetically altered in human gliomas

The epidemiologic evidence supporting a link between the circadian clock and cancer is strengthened by the deregulation of expression of core circadian clock genes in a variety of cancer types [108, 109]. To compare the frequency of genetic alterations in core clock genes across cancers, we queried The Cancer Genome Atlas (TCGA) database and identified the frequency of amplifications, deletions and mutations in 16 core circadian clock genes (**Table 3.1**) across 9 cancer types (**Figure 3.1A**). Uterine cancer had the highest rate of genetic alteration in core clock genes, while acute myeloid leukemia had the lowest rate of the cancers surveyed in this analysis. GBM ranked in between these two, with core clock genes are altered in 14.6% of GBM patients in a TCGA dataset of 281 GBM patient specimens [123]. The most frequently altered genes are listed in Figure 3.1B with the types of genetic alterations listed for each gene (**Figure 3.1B**). Less frequently altered core clock genes are listed in the figure legend. A full list of frequency of genetic alteration for each core clock gene can be found in Table 3.1. This analysis indicates the presence of copy number alterations and mutations in a variety of cancers that alter the molecular clock.

Table 3.1. List of Core Circadian Clock Genes

Clock Gene Symbol	Clock Gene Product Name	Role in the Molecular Clock	Frequency of Genetic Alteration In GBM
<i>Arntl</i>	BMAL1	Transcription factor; Activate transcription of CCGs	1%
<i>Clock</i>	CLOCK	Transcription factor; Activate transcription of CCGs	5%
<i>Arntl2</i>	BMAL2	Transcription factor; Activate transcription of CCGs	1%
<i>NPAS2</i>	NPAS2	Transcription factor; Activate transcription of CCGs	0.4%
<i>Per1</i>	PERIOD1	CCG; negative feedback on Clock-Bmal1 dimer	0.7%
<i>Per2</i>	PERIOD2	CCG; negative feedback on Clock-Bmal1 dimer	0.7%
<i>Per3</i>	PERIOD3	CCG; negative feedback on Clock-Bmal1 dimer	2%
<i>Cry1</i>	CRYPTOCHROME1	CCG; negative feedback on Clock-Bmal1 dimer	0.7%

<i>Cry2</i>	CRYPTOCHROME2	CCG; negative feedback on Clock-Bmal1 dimer	0.4%
<i>CSNK1D</i>	CASEIN KINASE 1 delta	Phosphorylate Period proteins	0.4%
<i>CSNK1E</i>	CASEIN KINASE 1 epsilon	Phosphorylate Period proteins	0.4%
<i>RORA</i>	Retinoid-related orphan receptor alpha	Activate Bmal1 transcription	0.7%
<i>RORB</i>	Retinoid-related orphan receptor beta	Activate <i>Bmal1</i> transcription	2%
<i>RORC</i>	Retinoid-related orphan receptor gamma	Activate <i>Bmal1</i> transcription	0.4%
<i>Nr1d1</i>	REV-ERB alpha	Repress <i>Bmal1</i> transcription	0.4%
<i>Nr1d2</i>	REV-ERB beta	Repress <i>Bmal1</i> transcription	0%

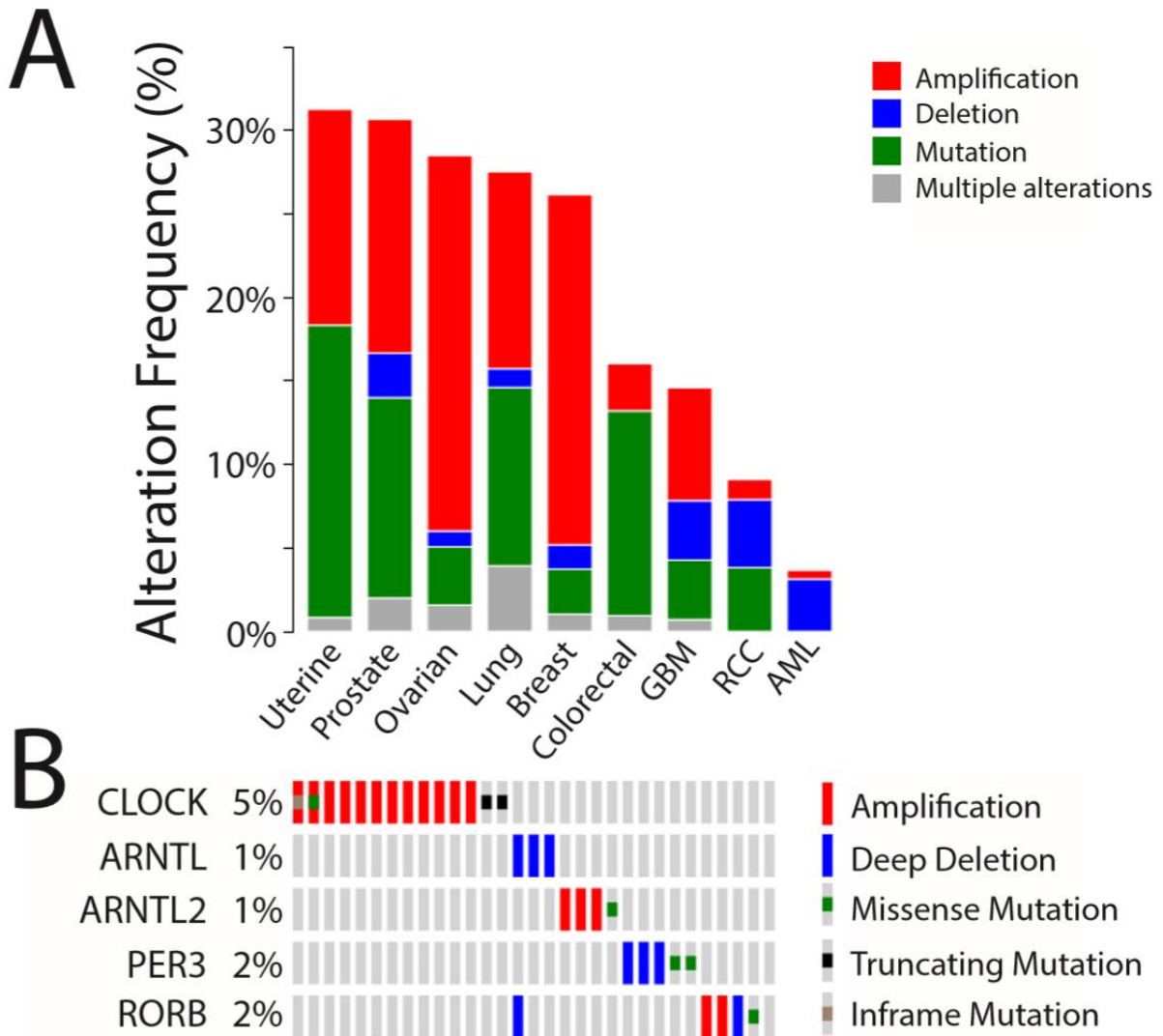


Figure 3.1. Frequency of genetic alterations in core clock genes in cancer. A) Comparison of frequency of genetic alterations in core clock genes (full list of genes in Table 3.1) in different types of cancer using data from The Cancer Genome Atlas (TCGA). Types of genetic alterations are color coded: amplifications (red), deletions (blue), mutations (green) or tumors with multiple alterations (gray). Cancer type (Total % Frequency, [Ref]): Uterine corpus endometroid carcinoma (31.3%, [124]), Metastatic prostate cancer (30.7%, [125]), Ovarian serous

cystadenocarcinoma (28.5%, [126]), Lung squamous cell carcinoma (27.5%, [127]), breast invasive carcinoma (26.1%, [128]), colorectal adenocarcinoma (16%, [129]), glioblastoma (14.6%, [123]), renal clear cell carcinoma (9.1%, [130]), acute myeloid leukemia (3.7%, [131]).

B) Frequency and identity of genetic alterations in clock genes in a dataset from 281 GBM patients [123]. Core clock genes with greatest alteration frequency are listed in the figure. The following core clock genes had low rates of genetic alteration: NPAS2 (0.4%), CRY1 (0.7%), CRY2 (0.4%), PER1 (0.7%), PER2 (0.7%), CSNK1D (0.4%), CSNK1E (0.4%), RORA (0.7%), RORC (0.4%), NR1D1 (0.4%).

Circadian oscillations in clock gene expression in Mes-GBM astrocytes

In order to investigate the circadian biology of GBM, we utilize a mesenchymal GBM murine astrocyte model (Mes-GBM) that has been previously used and characterized by our lab [119]. The Mes-GBM mouse astrocytes have lost *Neurofibromin 1 (Nf1)* expression and express a dominant-negative *p53* construct [120] to mimic deletion/mutation of *Nf1* and *p53*, two genetic alterations commonly found in mesenchymal GBM [16]. Due to the known sexual dimorphism in mesenchymal GBM and previous research demonstrating greater benefit of chronotherapy in male patients with metastatic colorectal cancer [132], we limited our studies to male mes-GBM astrocytes. To characterize gene expression rhythms in the male mes-GBM astrocytes, we transduced the cells to express a luciferase reporters of gene expression for *Period2 (Per2-luc)* or *Bmal1 (Bmal1-luc)* [59, 89, 90]. To characterize these rhythms as circadian, we calculated the period of circadian oscillation across 4-7 days of recording. Male mes-GBM astrocytes showed oscillations in *Per2-luc* and *Bmal1-luc* expression (**Figure 3.2A**) with periods of 22.2 h and 25.3 h, respectively, in these examples. On average, the periods of *Per2-luc* and *Bmal1-luc* oscillations are 23.0 h and 23.6 h, respectively (please see Table 3.2 for details). Previous studies have shown that *Bmal1* transcription oscillates in anti-phase to clock-controlled genes (CCGs), reaching peak expression levels at the nadir of CCG expression levels [104]. To examine the phase relationship between *Per2* and *Bmal1* expression in the Mes-GBM astrocytes, we calculated the average length of time between *Bmal1* peak and *Per2* peak across paired cultures plated and recorded simultaneously. This analysis revealed an average gap of 8.8 h between the peaks of *Per2* and *Bmal1* expression on Day 2 of recording (see **Table 3.2**). This demonstrates that most, but not all, paired *Bmal1-luc* and *Per2-luc* cultures reach their peaks at opposite times of day. This fairly reliable anti-phase oscillation of *Bmal1* and *Per2* reporters demonstrates that

the transcription-translation feedback loop, and the stabilizing loop of *Bmal1* expression are intact in the Mes-GBM astrocytes with slight variations between platings. Due to this minor variability, TMZ chronotherapy experiments was performed with a reporter dish recording bioluminescent rhythms of *Per2-luc* and/or *Bmal1-luc* to measure the exact phase of gene expression for the plating of each individual experiment. Based on these data, we conclude that Mes-GBM astrocytes have an intact molecular clock with a period of oscillation near 24 h.

Table 3.2. Summary of *Per2-luc* and *Bmal1-luc* traces in Mes-GBM astrocytes *in vitro*.

Circadian characterization of clock gene reporters	Mean \pm SEM	N
Period of <i>Per2-luc</i> bioluminescence	23.0 \pm 0.7 h	16
Period of <i>Bmal1-luc</i> bioluminescence	23.6 \pm 0.4 h	22
Period of clock gene expression (<i>Per2-luc</i> and <i>Bmal1-luc</i>)	23.3 \pm 0.4 h	38
Time between peaks in <i>Per2-luc</i> and <i>Bmal1-luc</i> expression on Day 2	8.8 \pm 2.1 h	4 (Pairs)

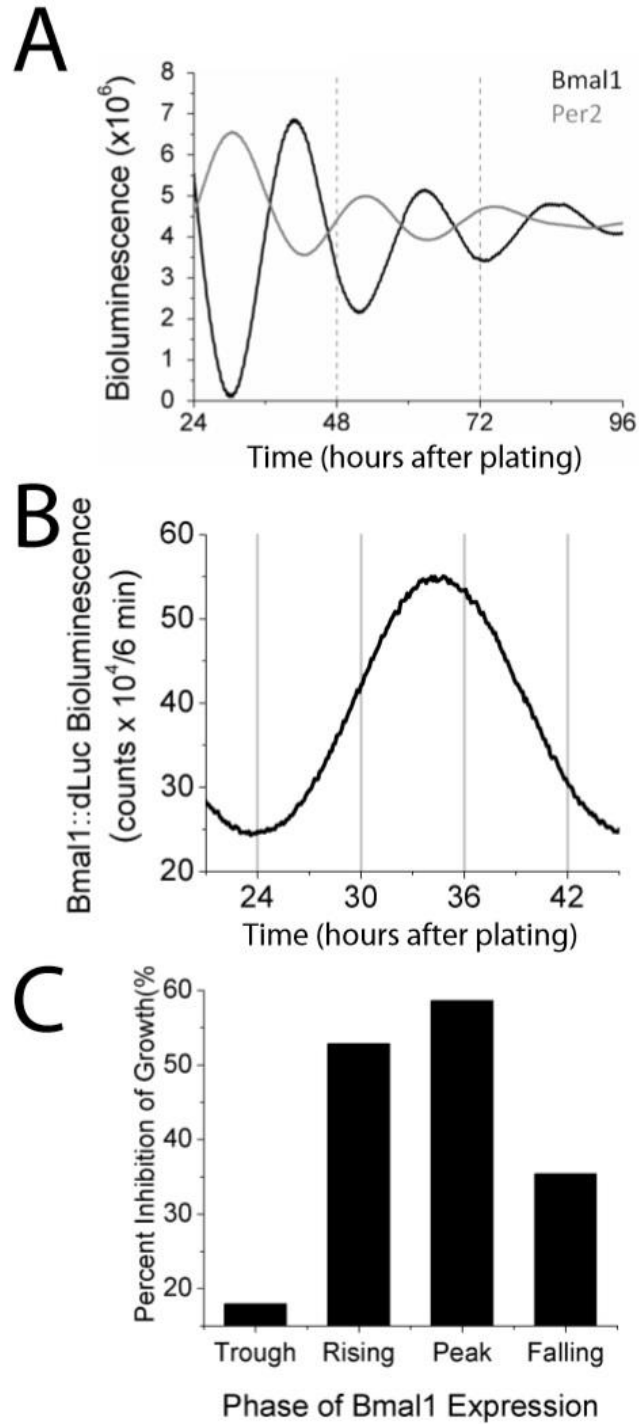


Figure 3.2. Mes-GBM astrocytes have rhythmic sensitivity to temozolomide *in vitro*. **A)**

Mes-GBM astrocytes express luciferase reporters of *Bmal1* (black) and *Per2* (gray) in anti-phase, with rhythmic periods of 25.3 h and 22.2 h, respectively, in these representative traces. **B)**

Bmal1::dLuciferase reporter dish showed oscillation of bioluminescence over time (one representative trace, N=3). Arrows indicate times of TMZ or DMSO treatment (hours after plating). C) TMZ-induced growth inhibition varies with time of treatment (one representative experiment, N =3).

Circadian rhythms in Temozolomide-induced growth inhibition *in vitro*

To determine whether the circadian oscillations in clock gene expression rendered the Mes-GBM astrocytes differentially sensitive to TMZ when treated at different phases of *Bmal1-luc* expression, we treated cells with 1 mM TMZ or vehicle (DMSO) at 1 of 4 time points for 6 hours from 24 to 42 hours post-plating (**Figure 3.2B, arrows**). Trypan blue-stained cells were counted 72 hours after the addition of TMZ or vehicle. Growth inhibition for each time point was calculated as the number of TMZ-treated living cells divided by the number of DMSO-treated living cells. This fraction was expressed as a percentage, with 100% growth inhibition equivalent to the death of all TMZ-treated cells. The greatest TMZ-induced inhibition of growth occurred near the peak of *Bmal1-luc* expression (**Figure 3.2C**). The results shown in Figure 2 are from one representative experiment. The correlation between greatest growth inhibition and *Bmal1* peak occurred in two additional experiments, using two independently derived lots of Mes-GBM astrocytes (data not shown). Thus, TMZ sensitivity of Mes-GBM astrocytes varies with the phase of *Bmal1* expression.

Circadian rhythms in DNA damage response

To assess whether the time-dependent oscillations in growth inhibition are due to rhythms in response to TMZ-induced DNA damage, we treated mes-GBM astrocytes with 1mM TMZ or vehicle (DMSO) at 4 different times of day and stained for phosphorylation of histone H2AX, a commonly used marker for DNA double strand breaks [91] and an early step in the DNA damage response pathway [133]. Each dish was exposed to TMZ or vehicle for 6 hours, media was changed and cells were fixed 18 hours after the addition of TMZ or vehicle. Nuclear staining for phospho-H2AX (p-Ser139) was quantified by ImageJ analysis of integrated density of

fluorescent images. We set a threshold for positive staining and counted the number of phospho-H2AX positive cells per sample. Representative images of fluorescence staining for each treatment group are shown in Figure 3A. Phospho-H2AX-positive cells were quantified as a percentage of total DAPI-stained nuclei per field of view (**Figure 3.3C**). Greatest phosphorylation of H2AX occurred near the peak of *Bmal1-luc* expression in the reporter dish (**Figure 3.3B**). We quantified the increase in the percent of phospho-H2AX-positive staining by normalizing to Mes-GBM astrocytes treated with DMSO at the trough of *Bmal1-luc* expression (**Figure 3.3D**). The mean difference between TMZ- and DMSO-induced phosphorylation of H2AX was statistically significant at the peak of *Bmal1-luc* expression, not the trough (Two-way ANOVA, Tukey's multiple comparisons, $p < 0.05$, $n = 3$). There was a 2.8-fold difference in the average TMZ response at the peak versus trough of *Bmal1-luc* expression. These results demonstrate a time of day-dependent rhythm in the response of Mes-GBM astrocytes to TMZ-induced DNA double strand breaks.

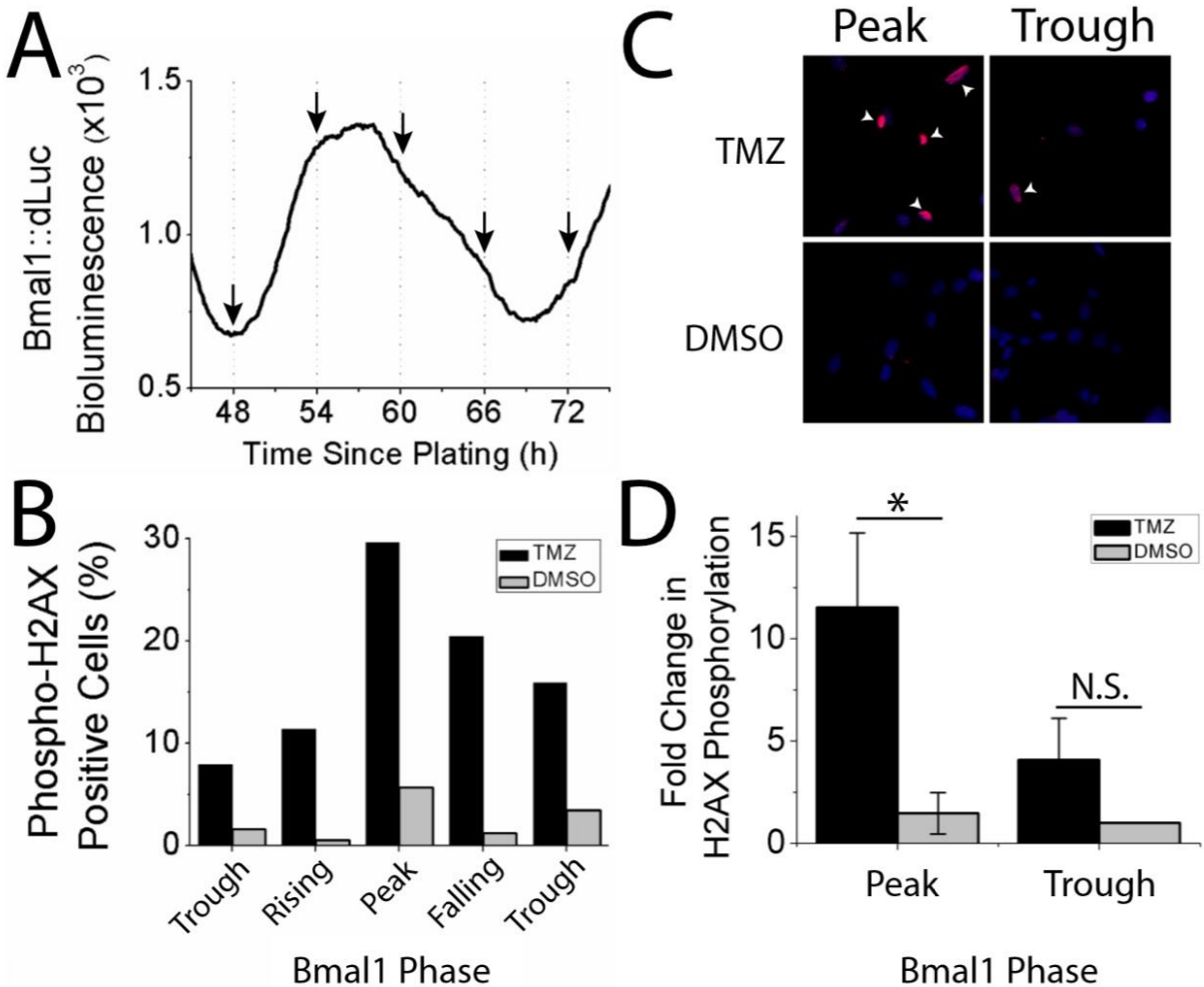


Figure 3.3. Phosphorylation of histone H2AX varies with time of treatment *in vitro*. **A)** Representative nuclear staining of DNA (blue, DAPI) and phospho-H2AX (red) near the peak and trough of *Bmal1::dLuc* bioluminescence. **B)** Percent of cells positive for nuclear phospho-H2AX staining varies with time of TMZ or DMSO treatment (one representative experiment, N =3). **C)** *Bmal1::dLuc* reporter dish showed oscillation of bioluminescence over time (one representative experiment, N =3). **D)** Fold change in percent phospho-H2AX staining relative to DMSO-treated Mes-GBM astrocytes treated at the trough of *Bmal1* expression.

Circadian rhythms in TMZ-induced activation of apoptosis

The growth inhibition studies demonstrated a rhythm in TMZ sensitivity based on cell counting. The number of cells in a culture after treatment is the sum of cell proliferation and cell death. This rhythm in cell number combined with the rhythm we have identified in H2AX phosphorylation led us to test whether there was a time of day-dependent rhythm in TMZ-induced apoptosis. To test whether TMZ-induced apoptosis changes with time of day of treatment, we quantified the activation of apoptosis with a luciferase reporter of caspase 3 and 7 activity [121]. We treated Mes-GBM astrocytes stably expressing the caspase reporter with TMZ or DMSO for 6 hours at four different phases of *Per2-luc* expression (**Figure 3.4A**) and tracked bioluminescence after treatment. To quantify the TMZ-induced activation of the caspase reporter, the DMSO-induced bioluminescence was subtracted from the TMZ-induced bioluminescence at each time point. We quantified the bioluminescence in each culture 48 hours after the addition of TMZ and expressed the caspase reporter activation as fold change relative to treatment at the falling phase of *Per2-luc* in the *Bmal1* WT reporter dish (**Figure 3.4B**). There was a statistically significant increase in caspase-luc bioluminescence when Mes-GBM astrocytes were treated at the trough of *Per2* (Dunn's multiple comparisons test, $p < 0.05$). Thus, the Mes-GBM astrocytes have a circadian rhythm in TMZ-induced activation of apoptosis.

CRISPR-Cas9-mediated disruption of *Bmal1* led to loss of rhythmic *Per2* expression

The correlation between high *Bmal1* expression and high TMZ sensitivity led us to hypothesize that increased TMZ sensitivity is *Bmal1*-dependent. We used the CRISPR-Cas9 system to target and disrupt *Arntl*, the gene encoding BMAL1. This disruption led to loss of BMAL1 protein expression (data not shown). Loss of *Bmal1* disrupted circadian rhythms in

Per2-luc expression (**Figure 3.4C**). These data demonstrate disrupted regulation of the molecular clock in *Bmal1* KO Mes-GBM astrocytes.

Circadian rhythms in activation of apoptosis are *Bmal1*-dependent

To determine the necessity of *Bmal1* expression to generate rhythms in TMZ-induced apoptosis, *Bmal1* knockout Mes-GBM astrocytes stably expressing the caspase reporter were treated at four different times according to the *Per2-luc* rhythm of a *Bmal1* WT culture (**Figure 3.4A**). CRISPR-mediated loss of *Bmal1* expression abolished the rhythm in TMZ-induced caspase activity (**Figure 3.4D**). There is no statistically significant difference in caspase reporter induction across treatment times (One-way ANOVA, Dunn's multiple comparisons test, $p > 0.05$). The loss of rhythmic activation of TMZ-induced apoptosis in the *Bmal1* KO Mes-GBM astrocytes demonstrates a disruption of the circadian regulation of sensitivity to TMZ.

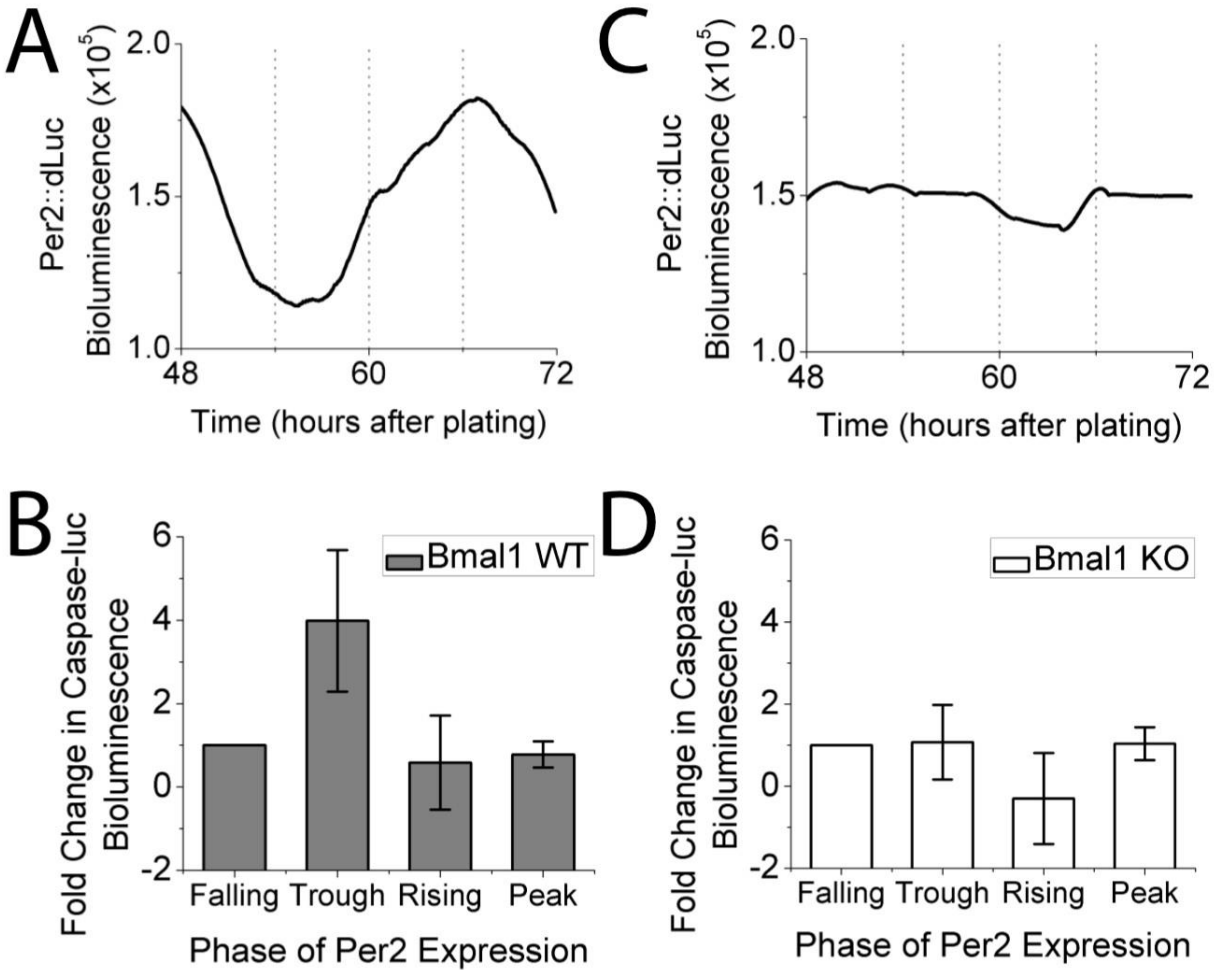


Figure 3.4. Rhythmic *Per2::dLuc* expression and activation of apoptosis are *Bmal1*-dependent *in vitro*. **A)** Mes-GBM astrocytes expressed *Per2::dLuc* rhythmically, with a period of 22.2 h. **B)** CRISPR-mediated loss of *Bmal1* was associated with arrhythmic expression of *Per2::dLuc*. **C)** Temozolomide-induced activation of the bioluminescent caspase reporter created a time of day –dependent change in bioluminescence in *Bmal1* WT, with the highest caspase activation at the trough of *Per2* (peak of *Bmal1*) (One-way ANOVA, Dunn’s multiple comparisons test, $p < 0.05$). **D)** There was no statistically significant change in caspase reporter activation in *Bmal1* KO Mes-GBM astrocytes over time. (One-way ANOVA, Dunn’s multiple comparisons test, $p > 0.05$)

Discussion

Our study uniquely demonstrates a tumor cell-intrinsic time of day-dependent variation in response to TMZ-induced DNA damage in glioblastoma. We employed a variety of methods to assess tumor response to TMZ treatment: measurements of DNA repair, apoptosis and overall growth inhibition. We demonstrated a daily rhythm in DNA repair by demonstrating a rhythm in histone H2AX phosphorylation. We have also demonstrated a circadian rhythm in the activation of apoptosis using a bioluminescent reporter of effector caspase activity. These rhythms in DNA repair and apoptosis correlate well with the rhythm we observed in growth inhibition following treatment with TMZ at different times of day. Taken together, these data support a rhythm in tumor response to TMZ that exists at the level of DNA repair and leads to a rhythm in programmed cell death.

These experiments build upon research that has previously demonstrated regulation of the DNA damage response by the circadian clock. Direct protein-protein interactions of PER1 and PER3 with ATM and Chk2 enhanced Chk2 phosphorylation and activation of cell cycle arrest in response to DNA double strand breaks [70, 71]. CRY1 and TIMELESS modulate Chk1 phosphorylation in a similar manner [74-76]. All of these studies utilized overexpression vectors or RNAi-mediated knockdown to study their influence on DNA damage response. In contrast, our studies assess circadian modulation of the cellular response to DNA damage without knocking down or overexpressing any components of the clock, providing insight into the daily fold-change in sensitivity we see based on endogenous rhythms. Future studies should characterize endogenous rhythms in sensitivity to chemotherapy in a variety of cancer cell types to determine whether our studies demonstrate cell-intrinsic rhythms in chemotherapy sensitivity that are unique to GBM.

Timing of chemotherapy administration to biological rhythms like DNA damage response can alter the clinical outcomes of chemotherapy treatments in cancer patients. Cancer treatments with several DNA damaging agents have been improved through chronotherapy. Chronomodulated delivery of oxaliplatin with peak delivery at 0400 h combined with 5-fluorouracil and leucovorin delivered overnight reduced mucositis to allow patients to stay on higher chemotherapy doses for a longer time. Thus, improving tumor response to treatment (Levi 1994). Treatment of advanced ovarian cancer with doxorubicin in the morning and cisplatin in the evening reduced bone marrow toxicity, thereby causing fewer dose reductions and treatment delays [36]. In both of these applications of chronotherapy effectively reduced toxicity.

There was a consistent correlation between the peak of *Bmal1* expression and the greatest sensitivity to TMZ. Growth inhibition was maximal at the peak of *Bmal1* expression. The greatest number of TMZ-treated cells were phospho-H2AX positive 18 hours after treatment near the peak of *Bmal1*. This level of phosphorylation is the net result of DNA damage (phosphorylation of H2AX by ATM) and resolution of DNA damage (dephosphorylation as DNA is repaired). Eighteen hours after exposure to TMZ, the phosphorylation state of H2AX likely corresponds to the kinetics of DNA repair more than sensing of DNA damage. Therefore, the high phosphorylation state of H2AX at the peak of *Bmal1* expression corresponds to slower kinetics of repair. The activation of apoptosis, as reported by the caspase-3/7 bioluminescent reporter, was greatest at the trough of *Per2-luc* expression. Consistent with canonical regulation of the molecular clock, Mes-GBM astrocytes have antiphase oscillations of *Bmal1-luc* and *Per2-luc in vitro*. Therefore, we can conclude that greatest activation of apoptosis occurs at the peak of *Bmal1*. At every level of response to TMZ that has been tested in the Mes-GBM astrocytes, there has been a correlation between high *Bmal1* expression and reduced ability for the tumor cell to

survive TMZ-induced DNA damage. These findings are consistent with daily variations in colon cancer cell sensitivity to irinotecan. Dulong and colleagues have described a correlation between peak *Bmal1* expression and greatest irinotecan-induced cytotoxicity *in vitro* [94]. Irinotecan and TMZ both cause DNA damage and induce the greatest cytotoxicity at the peak of *Bmal1*, suggesting circadian regulation of a common DNA repair pathway in response to both of these chemotherapies.

The correlation between the peak of *Bmal1* expression and the greatest sensitivity to TMZ combined with the loss of circadian rhythm in TMZ-induced apoptosis in *Bmal1* KO Mes-GBM astrocytes suggests an important role for BMAL1 in regulating response to DNA damage. Overexpression of *Bmal1* increases sensitivity of colon cancer cells to oxaliplatin [69]. *Bmal1* knockdown reduced etoposide-induced apoptosis of colon cancer cells [68]. These data are consistent with our findings that loss of *Bmal1* leads to ablation of the high level of caspase activation correlated to the trough of *Per2-luc* expression in rhythmic tumor cells. There are no data showing a direct interaction of BMAL1 with proteins involved in apoptosis, but there are reports of *Per2* overexpression altering expression of apoptotic genes [81]. These findings suggest that one or more clock-controlled gene products mediate the daily oscillations in activation of apoptosis following DNA damage.

Based on *Bmal1* knockout studies performed in other cell types [60, 64], we predicted that loss of *Bmal1* would lead to loss of daily oscillations in *Per2-luc* expression *in vitro*. We have demonstrated rhythmic expression of the *Per2-luc* bioluminescent reporter in cultured cells. Loss of *Bmal1* leads to arrhythmic expression of *Per2-luc* *in vitro*. We use the *Per2-luc* reporter as a way to detect and measure oscillations in clock-controlled genes (CCGs). The loss of rhythm in TMZ sensitivity in the *Bmal1* KO Mes-GBM astrocytes provides a functional output

supporting the hypothesis that rhythmic clock gene expression is required for regulation of response to TMZ. Currently, the mechanism underlying circadian regulation of TMZ sensitivity is unknown. However, future studies of CCGs related to DNA damage response and apoptosis may help identify the key regulators of this rhythmic sensitivity. Identifying rhythmic transcripts of DDR- and apoptosis-related genes that lose rhythmicity in *Bmal1* KO cells would provide a list of candidate regulators. At present, the *Bmal1-luc* and *Per2-luc* reporters serve as useful tools to help us understand the regulation of the circadian clock within tumor cells and to guide the search for the mechanism of circadian regulation of the tumor cell-intrinsic response to TMZ.

Acknowledgements

Special thanks for technical assistance from Tatiana Simon, Najla Kfoury, Nicole Warrington, Stacey Ward, Jasmin Sponagel and Andrea Binz. Constructive critiques and helpful scientific discussions were provided by many members of the Rubin and Herzog labs. Thanks to Daniel Granados-Fuentes, Tao Sun, Stacey Ward and Nicole Warrington for expert advice. Thanks to Cell-Cell Communication in Cancer, Clocksclub and Bioforum Seminars for providing scientific feedback on my project. Shondra Miller and the Genome Engineering Center for consultation and gRNA Cas9-CRISPR design and production. Andrew Liu provided the *Bmal1::dLuc* and *Per2::dLuc* lentiviruses. The caspase-3 bioluminescence reporter was provided by Dr. Alnawaz Rehemtulla (University of Michigan, Michigan, MI). Chronostar V2.0 was generously provided by B. Meier and A. Kramer.

References

1. Stupp, R., et al., *Effects of radiotherapy with concomitant and adjuvant temozolomide versus radiotherapy alone on survival in glioblastoma in a randomised phase III study: 5-year analysis of the EORTC-NCIC trial*. *Lancet Oncol*, 2009. **10**(5): p. 459-66.
2. Stupp, R., et al., *Radiotherapy plus concomitant and adjuvant temozolomide for glioblastoma*. *N Engl J Med*, 2005. **352**(10): p. 987-96.
3. Stevens, M.F., et al., *Antitumor activity and pharmacokinetics in mice of 8-carbamoyl-3-methyl-imidazo[5,1-d]-1,2,3,5-tetrazin-4(3H)-one (CCRG 81045; M & B 39831), a novel drug with potential as an alternative to dacarbazine*. *Cancer Res*, 1987. **47**(22): p. 5846-52.
4. Newlands, E.S., et al., *Phase I trial of temozolomide (CCRG 81045; M&B 39831; NSC 362856)*. *Br J Cancer*, 1992. **65**(2): p. 287-91.
5. Beale, P., et al., *Effect of gastric pH on the relative oral bioavailability and pharmacokinetics of temozolomide*. *Cancer Chemother Pharmacol*, 1999. **44**(5): p. 389-94.
6. Grossman, R., et al., *Microdialysis measurement of intratumoral temozolomide concentration after cediranib, a pan-VEGF receptor tyrosine kinase inhibitor, in a U87 glioma model*. *Cancer Chemother Pharmacol*, 2013. **72**(1): p. 93-100.
7. Gupta, S.K., et al., *Discordant in vitro and in vivo chemopotentiating effects of the PARP inhibitor veliparib in temozolomide-sensitive versus -resistant glioblastoma multiforme xenografts*. *Clin Cancer Res*, 2014. **20**(14): p. 3730-41.
8. Kobayashi, M., P.A. Wood, and W.J. Hrushesky, *Circadian chemotherapy for gynecological and genitourinary cancers*. *Chronobiol Int*, 2002. **19**(1): p. 237-51.

9. Schmiegelow, K., et al., *Impact of morning versus evening schedule for oral methotrexate and 6-mercaptopurine on relapse risk for children with acute lymphoblastic leukemia. Nordic Society for Pediatric Hematology and Oncology (NOPHO). J Pediatr Hematol Oncol*, 1997. **19**(2): p. 102-9.
10. Levi, F., et al., *Chronomodulation of chemotherapy against metastatic colorectal cancer. International Organization for Cancer Chronotherapy. Eur J Cancer*, 1995. **31A**(7-8): p. 1264-70.
11. Vitaterna, M.H., J.S. Takahashi, and F.W. Turek, *Overview of circadian rhythms. Alcohol Res Health*, 2001. **25**(2): p. 85-93.
12. Reppert, S.M. and D.R. Weaver, *Coordination of circadian timing in mammals. Nature*, 2002. **418**(6901): p. 935-41.
13. Preitner, N., et al., *The orphan nuclear receptor REV-ERB α controls circadian transcription within the positive limb of the mammalian circadian oscillator. Cell*, 2002. **110**(2): p. 251-60.
14. Nakajima, Y., et al., *Bidirectional role of orphan nuclear receptor ROR α in clock gene transcriptions demonstrated by a novel reporter assay system. FEBS Lett*, 2004. **565**(1-3): p. 122-6.
15. Sato, T.K., et al., *A functional genomics strategy reveals Rora as a component of the mammalian circadian clock. Neuron*, 2004. **43**(4): p. 527-37.
16. Bunger, M.K., et al., *Mop3 is an essential component of the master circadian pacemaker in mammals. Cell*, 2000. **103**(7): p. 1009-17.
17. Stevens, R.G., *Circadian disruption and breast cancer: from melatonin to clock genes. Epidemiology*, 2005. **16**(2): p. 254-8.

18. Schernhammer, E.S., et al., *Rotating night shifts and risk of breast cancer in women participating in the nurses' health study*. J Natl Cancer Inst, 2001. **93**(20): p. 1563-8.
19. Van Dycke, K.C., et al., *Chronically Alternating Light Cycles Increase Breast Cancer Risk in Mice*. Curr Biol, 2015. **25**(14): p. 1932-7.
20. Levi, F., et al., *Implications of circadian clocks for the rhythmic delivery of cancer therapeutics*. Adv Drug Deliv Rev, 2007. **59**(9-10): p. 1015-35.
21. Wang, F., et al., *Correlation between deregulated expression of PER2 gene and degree of glioma malignancy*. Tumori, 2014. **100**(6): p. e266-72.
22. Yu, C., et al., *Hypoxia disrupts the expression levels of circadian rhythm genes in hepatocellular carcinoma*. Mol Med Rep, 2015. **11**(5): p. 4002-8.
23. Rana, S., et al., *Deregulated expression of circadian clock and clock-controlled cell cycle genes in chronic lymphocytic leukemia*. Mol Biol Rep, 2014. **41**(1): p. 95-103.
24. Sahar, S. and P. Sassone-Corsi, *Circadian clock and breast cancer: a molecular link*. Cell Cycle, 2007. **6**(11): p. 1329-31.
25. Lin, Y.M., et al., *Disturbance of circadian gene expression in hepatocellular carcinoma*. Mol Carcinog, 2008. **47**(12): p. 925-33.
26. Kang, T.H. and S.H. Leem, *Modulation of ATR-mediated DNA damage checkpoint response by cryptochrome 1*. Nucleic Acids Res, 2014. **42**(7): p. 4427-34.
27. Unsal-Kacmaz, K., et al., *Coupling of human circadian and cell cycles by the timeless protein*. Mol Cell Biol, 2005. **25**(8): p. 3109-16.
28. Yang, X., P.A. Wood, and W.J. Hrushesky, *Mammalian TIMELESS is required for ATM-dependent CHK2 activation and G2/M checkpoint control*. J Biol Chem, 2010. **285**(5): p. 3030-4.

29. Kemp, M.G., et al., *Tipin-replication protein A interaction mediates Chk1 phosphorylation by ATR in response to genotoxic stress*. J Biol Chem, 2010. **285**(22): p. 16562-71.
30. Smith, K.D., M.A. Fu, and E.J. Brown, *Tim-Tipin dysfunction creates an indispensable reliance on the ATR-Chk1 pathway for continued DNA synthesis*. J Cell Biol, 2009. **187**(1): p. 15-23.
31. Gery, S., et al., *The circadian gene per1 plays an important role in cell growth and DNA damage control in human cancer cells*. Mol Cell, 2006. **22**(3): p. 375-82.
32. Im, J.S., et al., *Per3, a circadian gene, is required for Chk2 activation in human cells*. FEBS Lett, 2010. **584**(23): p. 4731-4.
33. Kang, T.H., et al., *Circadian oscillation of nucleotide excision repair in mammalian brain*. Proc Natl Acad Sci U S A, 2009. **106**(8): p. 2864-7.
34. Fu, L., et al., *The circadian gene Period2 plays an important role in tumor suppression and DNA damage response in vivo*. Cell, 2002. **111**(1): p. 41-50.
35. Matsuo, T., et al., *Control mechanism of the circadian clock for timing of cell division in vivo*. Science, 2003. **302**(5643): p. 255-9.
36. Feillet, C., et al., *Coupling between the Circadian Clock and Cell Cycle Oscillators: Implication for Healthy Cells and Malignant Growth*. Front Neurol, 2015. **6**: p. 96.
37. Dulong, S., et al., *Identification of circadian determinants of cancer chronotherapy through in vitro chronopharmacology and mathematical modeling*. Mol Cancer Ther, 2015.

38. Warrington, N.M., et al., *Spatiotemporal differences in CXCL12 expression and cyclic AMP underlie the unique pattern of optic glioma growth in neurofibromatosis type 1*. *Cancer Res*, 2007. **67**(18): p. 8588-95.
39. Sun, T., et al., *Sexually dimorphic RB inactivation underlies mesenchymal glioblastoma prevalence in males*. *J Clin Invest*, 2014. **124**(9): p. 4123-33.
40. Tu, H.C., et al., *The p53-cathepsin axis cooperates with ROS to activate programmed necrotic death upon DNA damage*. *Proc Natl Acad Sci U S A*, 2009. **106**(4): p. 1093-8.
41. Liu, A.C., et al., *Redundant function of REV-ERBalpha and beta and non-essential role for Bmal1 cycling in transcriptional regulation of intracellular circadian rhythms*. *PLoS Genet*, 2008. **4**(2): p. e1000023.
42. Zhang, E.E., et al., *A genome-wide RNAi screen for modifiers of the circadian clock in human cells*. *Cell*, 2009. **139**(1): p. 199-210.
43. Ramanathan, C., et al., *Monitoring cell-autonomous circadian clock rhythms of gene expression using luciferase bioluminescence reporters*. *J Vis Exp*, 2012(67).
44. Galban, S., et al., *Imaging proteolytic activity in live cells and animal models*. *PLoS One*, 2013. **8**(6): p. e66248.
45. Marpegan, L., T.J. Krall, and E.D. Herzog, *Vasoactive intestinal polypeptide entrains circadian rhythms in astrocytes*. *J Biol Rhythms*, 2009. **24**(2): p. 135-43.
46. Livak, K.J. and T.D. Schmittgen, *Analysis of relative gene expression data using real-time quantitative PCR and the 2^{-Delta Delta C(T)} Method*. *Methods*, 2001. **25**(4): p. 402-8.
47. Prolo, L.M., J.S. Takahashi, and E.D. Herzog, *Circadian rhythm generation and entrainment in astrocytes*. *J Neurosci*, 2005. **25**(2): p. 404-8.

48. Beaulieu, C., et al., *In vitro circadian rhythms: imaging and electrophysiology*. Essays Biochem, 2011. **49**(1): p. 103-17.
49. Brennan, C.W., et al., *The somatic genomic landscape of glioblastoma*. Cell, 2013. **155**(2): p. 462-77.
50. Cancer Genome Atlas Research, N., et al., *Integrated genomic characterization of endometrial carcinoma*. Nature, 2013. **497**(7447): p. 67-73.
51. Robinson, D., et al., *Integrative clinical genomics of advanced prostate cancer*. Cell, 2015. **161**(5): p. 1215-28.
52. Cancer Genome Atlas Research, N., *Integrated genomic analyses of ovarian carcinoma*. Nature, 2011. **474**(7353): p. 609-15.
53. Cancer Genome Atlas Research, N., *Comprehensive genomic characterization of squamous cell lung cancers*. Nature, 2012. **489**(7417): p. 519-25.
54. Cancer Genome Atlas, N., *Comprehensive molecular portraits of human breast tumours*. Nature, 2012. **490**(7418): p. 61-70.
55. Cancer Genome Atlas, N., *Comprehensive molecular characterization of human colon and rectal cancer*. Nature, 2012. **487**(7407): p. 330-7.
56. Cancer Genome Atlas Research, N., *Comprehensive molecular characterization of clear cell renal cell carcinoma*. Nature, 2013. **499**(7456): p. 43-9.
57. Cancer Genome Atlas Research, N., *Genomic and epigenomic landscapes of adult de novo acute myeloid leukemia*. N Engl J Med, 2013. **368**(22): p. 2059-74.
58. Verhaak, R.G., et al., *Integrated genomic analysis identifies clinically relevant subtypes of glioblastoma characterized by abnormalities in PDGFRA, IDH1, EGFR, and NF1*. Cancer Cell, 2010. **17**(1): p. 98-110.

59. Giacchetti, S., et al., *Sex moderates circadian chemotherapy effects on survival of patients with metastatic colorectal cancer: a meta-analysis*. Ann Oncol, 2012.
60. Bonner, W.M., et al., *GammaH2AX and cancer*. Nat Rev Cancer, 2008. **8**(12): p. 957-67.
61. Rogakou, E.P., et al., *Megabase chromatin domains involved in DNA double-strand breaks in vivo*. J Cell Biol, 1999. **146**(5): p. 905-16.
62. Chou, D.M. and S.J. Elledge, *Tipin and Timeless form a mutually protective complex required for genotoxic stress resistance and checkpoint function*. Proc Natl Acad Sci U S A, 2006. **103**(48): p. 18143-7.
63. Leman, A.R., et al., *Human Timeless and Tipin stabilize replication forks and facilitate sister-chromatid cohesion*. J Cell Sci, 2010. **123**(Pt 5): p. 660-70.
64. Zeng, Z.L., et al., *Overexpression of the circadian clock gene Bmal1 increases sensitivity to oxaliplatin in colorectal cancer*. Clin Cancer Res, 2014. **20**(4): p. 1042-52.
65. Zeng, Z.L., et al., *Effects of the biological clock gene Bmal1 on tumour growth and anti-cancer drug activity*. J Biochem, 2010. **148**(3): p. 319-26.

Chapter 4: Circadian clock gene expression and TMZ chronotherapy of glioblastoma models *in vivo*

Abstract

A series of *in vivo* GBM mouse studies have been performed to test whether the observations we made about circadian regulation of gene expression and TMZ sensitivity *in vitro* will persist *in vivo*. Using a human glioblastoma cell line (U87) and a murine model on the mesenchymal subtype of GBM (*Nf1*^{-/-};*DNp53*), we identified daily rhythms in clock gene and clock-controlled gene expression *in vivo*. We have demonstrated *Bmal1*-dependence of this rhythm in our murine GBM model *in vivo*. In our *in vivo* chronotherapy trials, we timed the delivery of TMZ to the *in vivo* rhythms we measured. The U87 xenograft chronotherapy trials yielded inconsistent tumor growth and TMZ-induced growth inhibition. None of these U87 xenograft chronotherapy trials revealed a time of day-dependent difference in overall survival. *Bmal1* KO Mes-GBM flank tumors showed no difference in acute or long-term TMZ treatment outcomes based on timing of TMZ administration. Together these data are insufficient to support the translation of our *in vitro* data to a pre-clinical model of TMZ chronotherapy for GBM. However, the variable and unexpected outcomes of these *in vivo* chronotherapy trials provide valuable information that will guide the design of future studies.

Introduction

Glioblastoma, a WHO grade IV astrocytoma, is the most common and aggressive malignant primary brain tumor in adults. Despite decades of research and countless clinical trials, median survival is still only approximately 15 months. Therefore, all opportunities to improve upon the current treatment outcomes should be pursued.

For many years, surgical resection and radiation therapy were the standard of care. In 2005, a landmark paper published in the New England Journal of Medicine demonstrated an increase in progression-free and overall survival with the addition of temozolomide (TMZ)

chemotherapy [21]. Since then, clinicians have tried a variety of TMZ treatment schedules, but none of them have taken into account the time of day of TMZ administration. As an oral medication, it is easy to regulate the timing of treatment. TMZ has a blood plasma half-life of 1.8 h [101], in addition to a short half-life (1.7-2.6 h) within tumors in animal models of GBM [102, 103], making it an ideal candidate for chronotherapy.

Oncologists have tested the efficacy and tolerability of chemotherapeutic agents at different times of day in a variety of cancer types. The administration of medications based on daily rhythms in biological processes is known as chronotherapy. Chronotherapy has increased 5-year survival rates in acute lymphoblastic leukemia and ovarian cancer patients, and increased the objective response rate in colorectal cancer while simultaneously reducing toxicities [30, 35, 36]. Despite successful therapeutic outcomes, chronotherapy has never been applied to the treatment of brain tumors.

Our daily rhythms in sleep, hormone release, and many other physiological processes are driven by an internal clock [54]. A molecular clock exists within most cells to keep time at the cellular level. The core molecular clock consists of two transcription factors, *Bmal1* and *Clock*, which activate transcription of downstream genes. The genes activated by the *Bmal1*-*Clock* transcription dimer are known as clock-controlled genes (CCGs). Among those CCGs, the gene products of the *Period* family (*Per1*, *Per2*, *Per3*), and the *Cryptochrome* family (*Cry1* and *Cry2*) provide negative feedback to block further transcriptional activation by the *Bmal1*-*Clock* dimer [104]. This feedback loop creates circadian oscillations in clock-controlled gene expression. A stabilizing feedback loop regulates transcription of the *Bmal1* gene (*Arntl*), creating an oscillation in *Arntl* expression that is anti-phase to the clock-controlled genes [105-107]. Loss of *Arntl* leads to loss of rhythms in individual cells [60, 64], and rest-activity rhythms [60],

demonstrating the crucial role *Bmall* plays in regulating circadian function. Our studies take advantage of that weakness in the clock to explore the contributions of the circadian clock to the response of glioblastoma to TMZ.

Many links have been made between circadian clocks and cancer in humans and mice. Epidemiological studies have demonstrated that shift workers have a higher risk of developing cancer [47, 108], creating a correlation between disrupted clocks and tumorigenesis in humans. To build on this shift work-cancer link, scientists have recently demonstrated an increased risk of breast cancer development in female mice exposed to a chronically shifting light schedule [40]. Circadian rhythms in human physiology have also been linked to survival for colorectal and breast cancer patients [84]. These studies provide correlations between circadian rhythms and cancer, but do not prove that disruption of circadian rhythms cause cancer.

A rapidly growing field of research has demonstrated molecular ties between the circadian clock and cancer-relevant pathways. Expression of circadian clock genes has been deregulated in a variety of cancer types, including gliomas [109, 111, 113]. At the molecular level, circadian clock proteins have been directly linked to DNA damage response. Localization of CLOCK proteins at sites of H2AX phosphorylation demonstrate a recruitment of CLOCK to sites of DNA damage, but do not establish a role for CLOCK at those sites. The circadian role of mammalian Timeless (Tim) remains unknown, but requirement of Tim for DNA damage checkpoint responses has been demonstrated through interactions with the ATR-Chk1, and ATM-Chk2 pathways [74, 77, 114-116]. PER1 protein interacts directly with ATM and Chk2, enhancing activation of the checkpoint pathway [70]. PER3 also interacts with and enhances ATM-mediated phosphorylation of Chk2 [71]. Rhythmic expression of the base excision repair protein, XPA, creates daily rhythms in UV-induced DNA damage [78]. Circadian rhythms in [97]

transcription have been demonstrated for cell cycle regulators Wee1, c-Myc and CyclinD1 [67, 80]. Deregulated expression of circadian and these three cell cycle regulators has been demonstrated in chronic lymphocytic leukemia [111]. Coupling of the circadian cycle and cell cycle has been tested experimentally and with mathematical modeling [117]. This field of study has provided many examples of regulation of DNA damage response, cell cycle and apoptosis by the molecular clock. These studies outline a role for the molecular clock in regulating cellular processes that often become aberrant in the setting of cancer, characterizing clock proteins as tumor suppressors.

Many rodent chronotherapy studies have demonstrated improved outcomes for a variety of tumor models. Mouse models of leukemia and mammary adenocarcinoma had greater survival rates following treatment with doxorubicin during the day time compared to night [134, 135]. Sarcoma-bearing rats had greater tumor growth inhibition when treated with doxorubicin in the middle of the night compared to the early daylight hours [136]. Osteosarcoma-bearing mice had greater tumor growth inhibition and median survival when treated with oxaliplatin during the early night compared to mid-day [135]. However, two cisplatin-based chronotherapy studies in rats with plasmacytoma and mice with pancreatic adenocarcinoma showed no changes in anti-tumor efficacy with timing of chemotherapy administration [135]. Chronotherapy may not always provide improved outcomes, but there are many examples of success using a variety of chemotherapeutics in several different rodent models of cancer.

Our study seeks to understand the circadian regulation of susceptibility to TMZ in a murine model of glioblastoma. We have previously demonstrated rhythms in clock gene expression and TMZ sensitivity based on the timing of treatment *in vitro*. We now test whether

the observations we have made in cell culture are maintained *in vivo*. We have demonstrated an important role for *Bmal1* in maintaining rhythmic expression of circadian clock genes *in vivo*. However, we have not demonstrated a time of day-dependent sensitivity to TMZ in *Bmal1* WT U87 xenografts or *Bmal1* KO Mes-GBM flank tumors. These experiments teach us valuable lessons in experimental design that will help us design future experiments.

Materials and Methods

Animals: All animals were used in accordance with established Animal Studies Protocols (no. 20140098 and 20120174) approved by the Washington University Animal Studies Committee and followed National Institutes of Health guidelines. Male NCR nude mice used for flank implantations were purchased from Taconic Farms, Inc (NY, USA). Founder *Nf1flox/flox;GFAP-Cre* mice were provided by Dr. David Gutmann (Washington University, St. Louis, MO) and were housed in the Animal Facilities at Washington University's School of Medicine and Danforth Campus.

Male Astrocyte Cultures: Primary cultures of astrocytes were prepared from individual postnatal day 1 *Nf1flox/flox;GFAP-Cre* mice as previously described [118]. Sex of each mouse was determined from tail DNA by PCR for *JARID 1C* as previously described [119]. All cells from a single litter with the same *Neurofibromin 1 (Nf1)* genotype were pooled based on sex. Replicate experiments were performed using astrocytes isolated from at least three independent litters. Only male astrocytes were used for these experiments.

Expression of DNp53: A dominant negative P53-encoding retrovirus (DNp53-IRES-eGFP) [120] was generated by transfecting Plat-E cells with a pMIG-DNp53-eGFP construct. Media

containing retrovirus was harvested 48-72 hours post-transfection and stored at -80°C until use. The resultant viral media was used to infect male *Nf1*^{-/-} astrocytes with polybrene (5µg/ml, Millipore, Billerica, MA). *Nf1*^{-/-};*DNp53-eGFP* positive cells were sorted to purity using a MoFlo high speed flow cytometer (Beckman Coulter, Fort Collins), as previously described[119]. Results are reported from Mes-GBM astrocytes that were used for up to 8 passages following GFP-positive selection by flow cytometry.

Expression of CRISPR-Cas9 expression vectors: Six guide RNAs targeting the *Bmal1* (*Arntl*) locus were designed and cloned by the Genome Engineering Center at Washington University in St. Louis. Lentiviruses were generated by transfecting 293T HEK cells with the LentiCRISPRv2-Cas9, delta8.9 and VSV-G plasmids. Media containing CRISPR-Cas9 lentivirus was harvested 48 hours after transfection and stored at -80°C until use. The resultant viral media was used to infect Mes-GBM astrocytes with polybrene (5µg/ml, Millipore, Billerica, MA). Mes-GBM astrocytes were infected with CRISPR-Cas9 lentiviruses containing 6 unique *Arntl*-targeting guide RNAs (*Bmal1* CRISPR) or an equivalent titer of CRISPR-Cas9 lacking a guide RNA sequence (Control CRISPR). After infection, *Nf1*^{-/-};*DNp53-Cas9* astrocytes were selected with puromycin (2µg/ml, Fisher Scientific, Pittsburgh, PA) for 3 weeks. Clonal lines were derived by serial dilution and expansion of single clones. Results are reported from CRISPR-Cas9 clonal lines used up to 16 passages for subcutaneous implantation.

*Expression of Per2::*dLuc* and Bmal1::*dLuc* reporters:* We performed lentiviral infections of pure astrocyte cultures using lentiviral reporter constructs expressing firefly luciferase driven by the mouse *Bmal1* or (*Bmal1*::*dLuc*) [89, 90] or *Period2* (*Per2*::*dLuc*) [59] promoters. Astrocytes

were incubated with the viral particles for 48 h and then reporter-expressing cells were selected based on blasticidin resistance. Media was supplemented with Blasticidin S HCl for 7 days (4 ug/mL, TOKU-E, Bellingham, WA) to select Mes-GBM astrocytes. The U87MG cells were not Blasticidin-selected after infection with the *Bmal1::dLuc* reporter.

Cell Culture: The human U87 glioblastoma cell line was purchased from American Type Culture Collection (ATCC). For the chronotherapy experiment, U87 cells were infected with a CMV-GFP-luciferase (CMV-luc) lentivirus and selected by GFP signal intensity by flow cytometry prior to intracranial implantation, as done previously [137, 138]. The murine mesenchymal GBM astrocyte model was generated in the lab, as described above. Prior to *in vivo* implantation, all cells were maintained at 37°C at 5% CO₂ in CO₂-buffered DMEM supplemented with 10% FBS (Gibco/Life Technologies, Carlsbad, CA) and 1% penicillin/streptomycin (Gibco/Life Technologies, Carlsbad, CA).

Intracranial implantations: Intracranial xenografts were generated as described previously [137, 138]. Homozygous NCR nude mice (Taconic Farms, Germantown, NY) were anesthetized [intraperitoneal ketamine (87 mg/kg)/xylazine (13 mg/kg); Phoenix Pharmaceuticals, Burlingame, CA], the cranium was exposed, and a small hole was made 2mm lateral and posterior to the bregma with a size 34 inverted cone burr (Dremel, Racine, WI). Mice were positioned in a stereotactic frame (Stoelting, Wood Dale, IL) and 50,000 cells in PBS were injected through a 27-gauge needle over 2 min at 2.5 mm below the dura mater. The incision was closed with Vetbond (3M, St. Paul, MN).

Subcutaneous implantations: *Nfl*^{-/-};*DNp53* astrocytes were treated with human EGF (Sigma, St. Louis, MO) for 48 hours prior to implantation into the flanks of nude mice. To mobilize and support cell growth in flank implantations, matrigel (100 μ L/side flank, BD Bioscience) was added to the cells prior to injection. Cohort 1 received 1×10^6 cells per flank injection. Cohort 2 received 2×10^6 cells per flank injection. Flank tumors were measured weekly with a digital caliper.

Temozolomide treatment of mice: Mice bearing intracranial U87 xenografts or Mes-GBM flank tumors expressing Cas9-only (*Bmal1* WT) or *Bmal1/Arntl*-targeting gRNA-Cas9 (*Bmal1* KO) were treated with 21 mg/kg/day temozolomide (TMZ, Sigma, St. Louis, MO) by oral gavage for 5 consecutive days. Vehicle control mice received oral gavage of DMSO diluted in water.

Real-time qPCR: All real-time qPCR assays were performed with iTaq™ Universal SYBR® Green Supermix (Biorad, Hercules, CA). cDNA was generated from total RNA with Superscript III reverse transcriptase (Invitrogen, Carlsbad, CA) per manufacturer's instructions. PCR and data collection were done using the BioRad CFX Connect Real-Time PCR machine and Opticon Monitor 3 Software (Biorad, Hercules, CA). Relative transcript copy number for each gene and corresponding *Gapdh* sample were calculated using the delta-delta-C(q) method [122]. PCR primers used in these studies are listed in Supplemental Table 1.

Nuclear and histone extractions: Extraction from tissue required homogenization in 10mM DTT supplemented with PMSF, protease and phosphatase inhibitor cocktails, 30 min incubation on ice and 10 seconds of sonication. The pellet was resuspended in TEB (PBS, 0.5% Triton X-100,

0.02% Sodium Azide, protease (Complete, 1:50, Roche, Basel, Switzerland) & phosphatase inhibitor cocktails (II, 1:100; IV, 1:50, Calbiochem, Billerica, MA) and incubated for ten minutes at 4C. Lysates from tissue homogenate was pelleted at 2,000xg for 10 minutes and pellets were resuspended in HCl (0.2M for cells, 0.4M for tissue), rotating overnight at 4C. Precipitate was pelleted at 2,000 x g for 10 minutes and supernatant containing histones was used for Westerns. Histone protein concentration was assessed by Bradford protein assay prior to loading SDS-PAGE gels with histone extracts.

Western blot: Western blots were performed and imaged using the Odyssey Infrared Imaging system (LI-COR, Lincoln, NE) as previously described (45). Total protein (30~50 µg per lane) was loaded onto a 4% to 12% Nu-Page gradient gel (Invitrogen). Primary antibodies were incubated at 4°C overnight. Secondary antibody incubation was at room temperature for 1 hour. Primary antibodies used in this study were phospho-S139 H2AX (Molecular Probes, 1:1000), H2AX (CST, Danvers, MA, 1:1000), Caspase 3 (CST, Danvers, MA, 1:1000), Cleaved Caspase 3 (Asp175) (CST, Danvers, MA, 1:800), Mouse anti- β-actin (1:30,000, Sigma); IRdye680 or 800 conjugated donkey anti-mouse or rabbit IgG (1: 40,000), LI-COR, Lincoln, NE).

Bioluminescence recordings of intracranial xenografts in vivo: NCR nude mice bearing intracranial xenografts of CMV-luc-expressing U87 cells were injected with 150 Ag/g D-luciferin (Biosynth, Itasca, IL) as previously described [137]. After anesthesia using 2.5% isoflurane, mice were imaged with a charge-coupled device camera-based bioluminescence imaging system (IVIS 50; Xenogen; exposure time 1-30 s, binning 8, field of view 12, f/stop 1, open filter). Signals were displayed as photons/s/cm² /sr [44]. Regions of interest were defined

manually and images were processed using Living Image and IgorPro Software (Version 2.50) as described [137]. Raw data were expressed as total photon flux (photons/s; [139]).

Bioluminescence is reported in the paper as a normalized value, dividing all bioluminescence values by the bioluminescence measured at 1 week post tumor implantation.

Bioluminescence recordings of flank tumors in vivo: Adult NCR nude male mice bearing subcutaneous flank mes-GBM xenografts were synchronized to a 12-h light/12-h dark cycle for at least 2 weeks (lights on from 7:00 A.M. to 7:00 P.M. (LD)). On the first day of imaging, each mouse was anesthetized with isoflurane (2% vaporized in O₂) at 6:00 A.M., injected i.p. with d-luciferin (150 ug/g body weight; Biosynth, Itasca, IL). One minute exposures were captured 10 minutes after d-luciferin injection. Every 4 h, the mice were reanesthetized with isoflurane and imaged with an ultra-sensitive CCD camera in a light tight box (Stanford Photonics; bin factor, 2; 1/f stop; open filter; Stanford Photonics, Palo Alto, CA). Mice received subcutaneous saline for hydration (0.5 cc every 8 hours), were returned to their cages, and awoke within 3 min after removal of the anesthetic. This procedure was repeated every 4 h for 48 h, during which time the mice showed no adverse effects of repeated 20-min anesthesia.

Statistical Analysis: Statistical analyses were performed using Prism software. Outliers within technical replicates for bioluminescent imaging were excluded using Grubbs' Test. Analysis of rhythmicity of Per2-luc bioluminescence was performed using JTK Cycle, software created by Michael Hughes [140].

Results

Bmal1-luc bioluminescence is higher in the morning *in vivo*

We have already demonstrated circadian rhythms in clock gene expression in U87 cells *in vitro*. Our next step was to determine whether clock gene expression rhythms in U87 cells are maintained *in vivo*. To test the hypothesis that clock gene expression continues to oscillate *in vivo*, we measured bioluminescence from nude mice bearing intracranial U87 *Bmal1-luc*-expressing xenografts. We saw greater *Bmal1-luc* bioluminescence at 9am versus 9pm in two mice. These preliminary data demonstrate higher *Bmal1-luc* expression in the morning compared to night time.

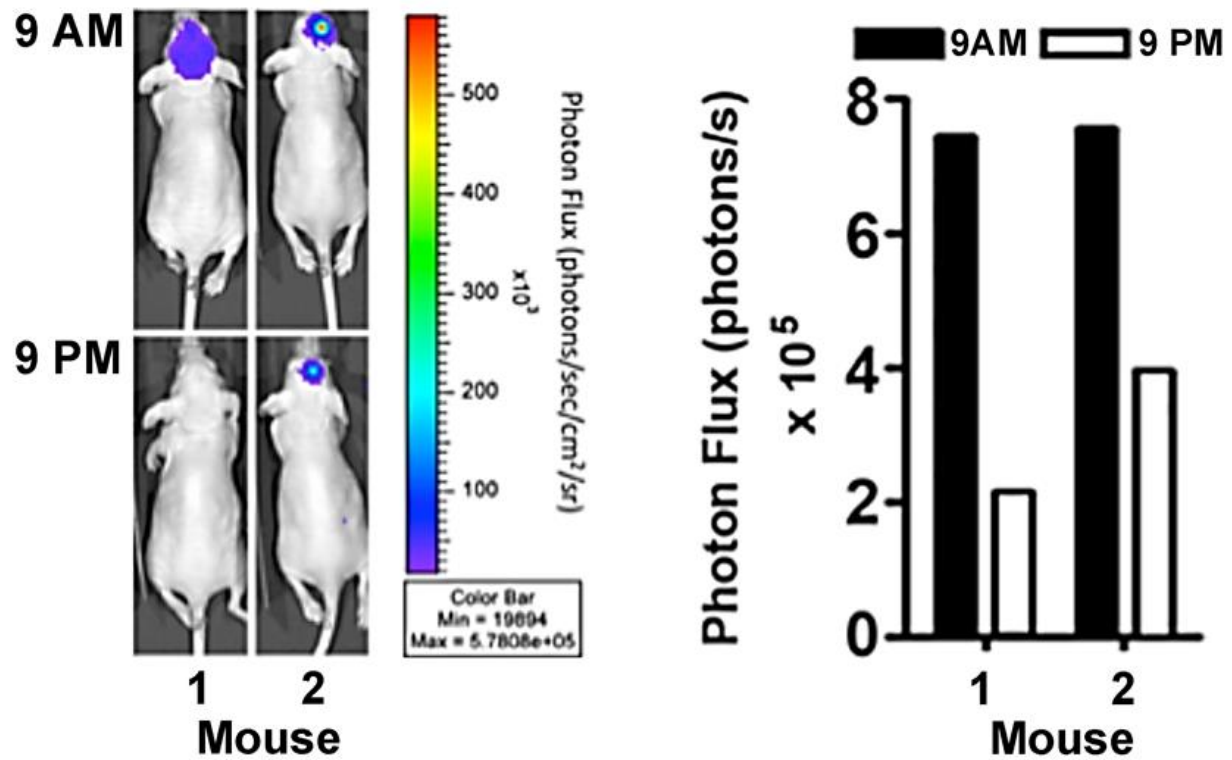


Figure 4.1. *Bmall-luc* expression is higher in the morning. A) Bright field images of mice with bioluminescence overlay shows relative *Bmall-luc* bioluminescence when imaging mice at 9am versus 9pm. B) Bar graph shows bioluminescence from each U87 *Bmall-luc* tumor-bearing mouse at 9am versus 9pm (photons/sec, n=2).

TMZ-induced growth inhibition of U87 xenografts did not vary in a time of day-dependent manner

Our U87 *in vitro* studies have shown a correlation between the peak of *Bmall-luc* expression and highest sensitivity to TMZ. With the knowledge that *Bmall* expression is higher in the morning in intracranial U87 xenografts, we hypothesized that U87 tumors would be more sensitive to TMZ in the morning. To test this hypothesis, we treated U87 CMV-luc tumor-bearing mice with TMZ by oral gavage at 7am or 7pm for 5 consecutive days two weeks and six weeks after tumor implantation. We followed tumor growth over time by weekly imaging of CMV-luc bioluminescence, which correlates very closely with tumor burden, as assessed by MRI [141]. In Cohort 1, we saw very similar growth patterns between the 7AM and 7PM treatment groups (**Figure 4.2A**), but the overall growth of intracranial U87 xenografts over time was not significantly different between the 7AM and 7PM treatment groups (ANOVA, $p > 0.05$). Cohort 2 the tumor burden of the 7PM TMZ-treated group was statistically significantly higher than the 7AM TMZ group (**Figure 4.2B**, ANOVA, $p < 0.05$). In Cohort 3, we treated mice with either TMZ or vehicle (DMSO) at 7AM or 7PM using the same treatment schedule as the first two cohorts. Cohort 3 revealed a significantly greater reduction of tumor burden in the 7AM TMZ group compared to the 7PM TMZ group (**Figure 4.2C**, ANOVA, $p < 0.05$). In Cohorts 1 and 2, there was a brief reduction in tumor burden after TMZ treatment (**Figure 4.2A&B**). In contrast to the first two cohorts, Cohort 3 showed a long-lasting, significant reduction in tumor burden after TMZ treatment. There was a reduction in tumor burden in some mice in the DMSO treatment groups, suggesting that the biology of the Cohort 3 xenografts is different from the biology of the xenografts in the first two cohorts. Two out of 3 cohorts demonstrated a greater reduction in tumor burden in the 7AM TMZ treatment groups compared to 7PM TMZ.

TMZ Chronotherapy does not alter overall survival of U87 xenograft-bearing mice

The overall survival of mice varied among the three cohorts, but never showed a significant difference in survival between 7AM and 7PM treatment groups. Cohort 1 shows almost completely overlapping survival curves for the two treatment groups (**Figure 4.2D**, Log-rank test, $p > 0.05$). Cohort 2 shows a trend toward longer survival for the 7AM treatment group, but the trend is not significant (**Figure 4.2E**, Log-rank test, $p > 0.05$). All TMZ-treated mice survived for the duration of the study (data not shown), unlike the other two cohorts, and the TMZ response we have previously published [138]. When the survival of all three cohorts was combined, there was no difference in overall survival based on time of day of treatment. Taken together, we have seen variability in survival among the three cohorts with no statistically significant difference in survival based on the timing of TMZ administration.

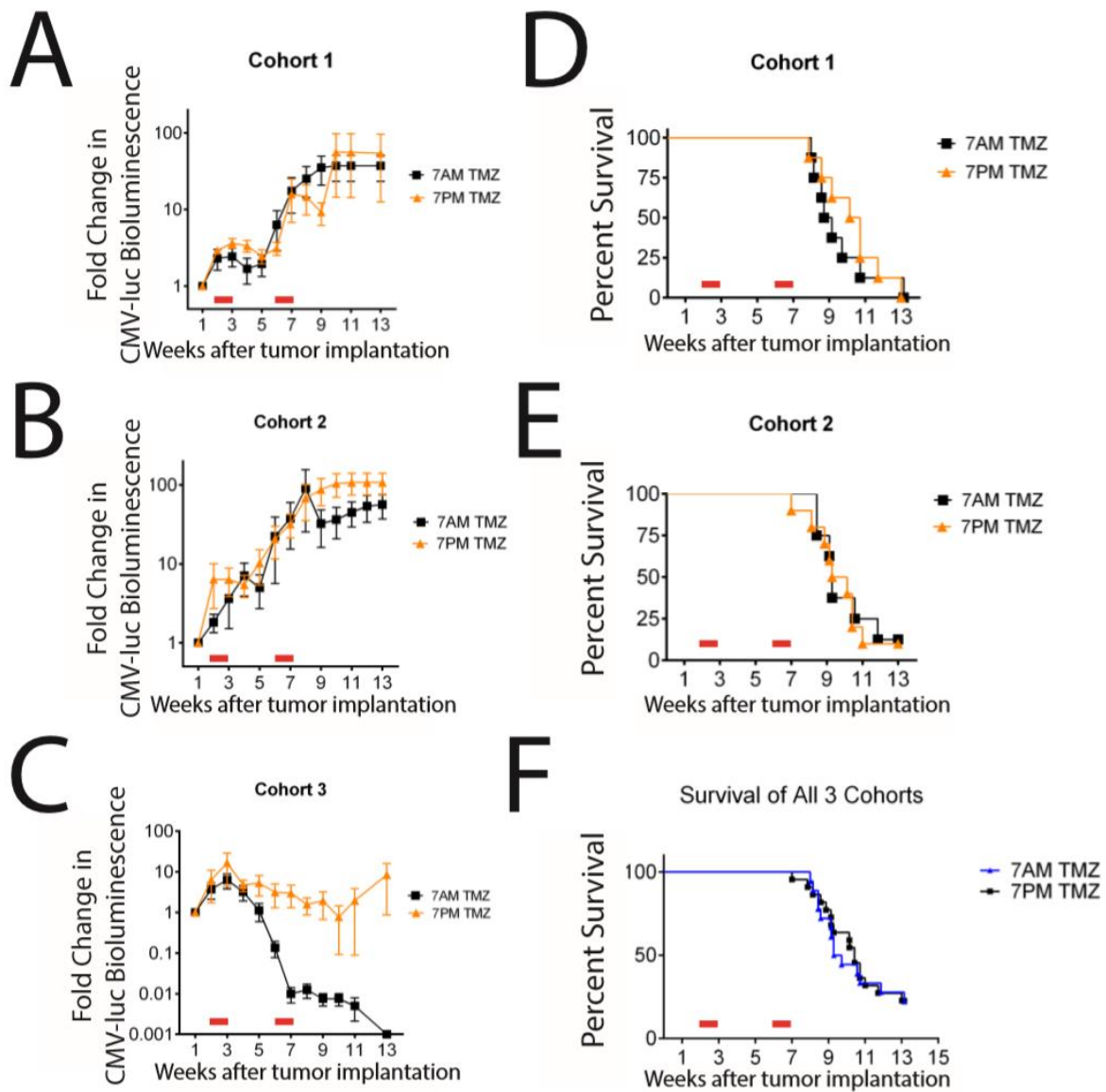


Figure 4.2. Chronotherapy of U87 intracranial xenografts yielded variable tumor growth and no significant difference in overall survival for morning versus evening. Graphs of fold change in CMV-luciferase bioluminescence, a measure of tumor burden, varied among 3 independently treated cohorts of mice (A-C). Survival for individual cohorts 1 (D) and 2 (E) show no significant difference in overall survival (Log-rank test, $p > 0.05$). All TMZ-treated mice in cohort 3 survived (survival curve not shown). F) Combined survival of all cohorts was not

significantly different when comparing 7AM vs 7PM TMZ treatment (Log-rank test, $p > 0.05$). 7AM treatment group (blue) and 7PM treatment group (black) combined all 3 cohorts. Each red bar represents one treatment cycle (5 days). TMZ was delivered 2 and 6 weeks after tumor implantation.

Loss of *Bmal1* enhances tumorigenesis

To determine whether tumor growth rates differed between *Bmal1* WT and *Bmal1* KO flank tumors, we measured tumor volumes over time. The *Bmal1* WT Mes-GBM astrocyte implants did not grow over time (Figure 2A). However, the *Bmal1* KO Mes-GBM astrocytes tumor volumes increased rapidly over time, achieving a 4.5-fold increase in mean tumor volume 9 weeks after implantation (Figure 2A, $p < 0.0001$). These data demonstrate that *Bmal1* KO Mes-GBM astrocytes have a greater ability to form tumors than the *Bmal1* WT Mes-GBM astrocytes.

Circadian regulation of gene expression is *Bmal1*-dependent *in vivo*

After characterizing the cell-intrinsic rhythms of the Mes-GBM astrocytes *in vitro*, we implanted these cells subcutaneously to determine whether our tissue culture results would persist in the more complex *in vivo* environment. We began by characterizing the clock gene expression of the Mes-GBM astrocyte flank tumors using the *Per2-luc* bioluminescent reporter. Every 4 hours across 36 hours, we anesthetized *Bmal1* WT and *Bmal1* KO flank tumor-bearing mice, injected d-luciferin, then measured bioluminescence with a low-light imaging system. We saw a circadian oscillation in *Bmal1* WT Mes-GBM astrocytes with a 2.3-fold change in mean bioluminescence from *Per2-luc* trough to peak. *Per2-luc* peak occurred at ZT 15 (10PM) on two consecutive days for *Bmal1* WT implants. We used JTK Cycle to assess whether the *Per2-luc* was rhythmic over time and determined that *Bmal1* WT, but not *Bmal1* KO, flank tumors were rhythmic (**Figure 4.3B**; JTK p -value < 0.05 ; $n = 10$). In contrast, we saw a lack of circadian rhythmicity in *Per2-luc* bioluminescence in *Bmal1* KO flank tumors over time (Figure 4.5A; JTK p -value > 0.05 , $n = 8$). This demonstrates a cell-intrinsic *Bmal1*-dependent regulation of the molecular clock.

To verify that loss of rhythmic *Per2-luc* bioluminescence reflects a loss of circadian regulation of endogenous clock gene expression, we performed RT-qPCR on *Bmal1* KO flank tumors harvested at 4 different circadian times across the day. To directly test the correlation between endogenous *Per2* transcription and *Per2-luc* expression, we measured *Per2* mRNA levels. As a negative, noncycling control, we measured β -actin mRNA levels. We chose two additional target genes based on their rhythmic expression profiles in the CircaDB database (<http://circadb.hogeneschlab.org/>). *Atm* is rhythmically expressed in mouse kidney in this database (JTK Cycle, $p < 0.05$, period = 26.0 h). *Ppp1r3c*, a gene highly expressed in glia, was also rhythmic in mouse pituitary in this database (JTK Cycle, $p < 0.05$, period = 24.0 h). The change in mean expression levels across time was not statistically significant for any of these genes. These qPCR data demonstrate a lack of rhythmic gene expression in *Bmal1* KO tumors *in vivo*.

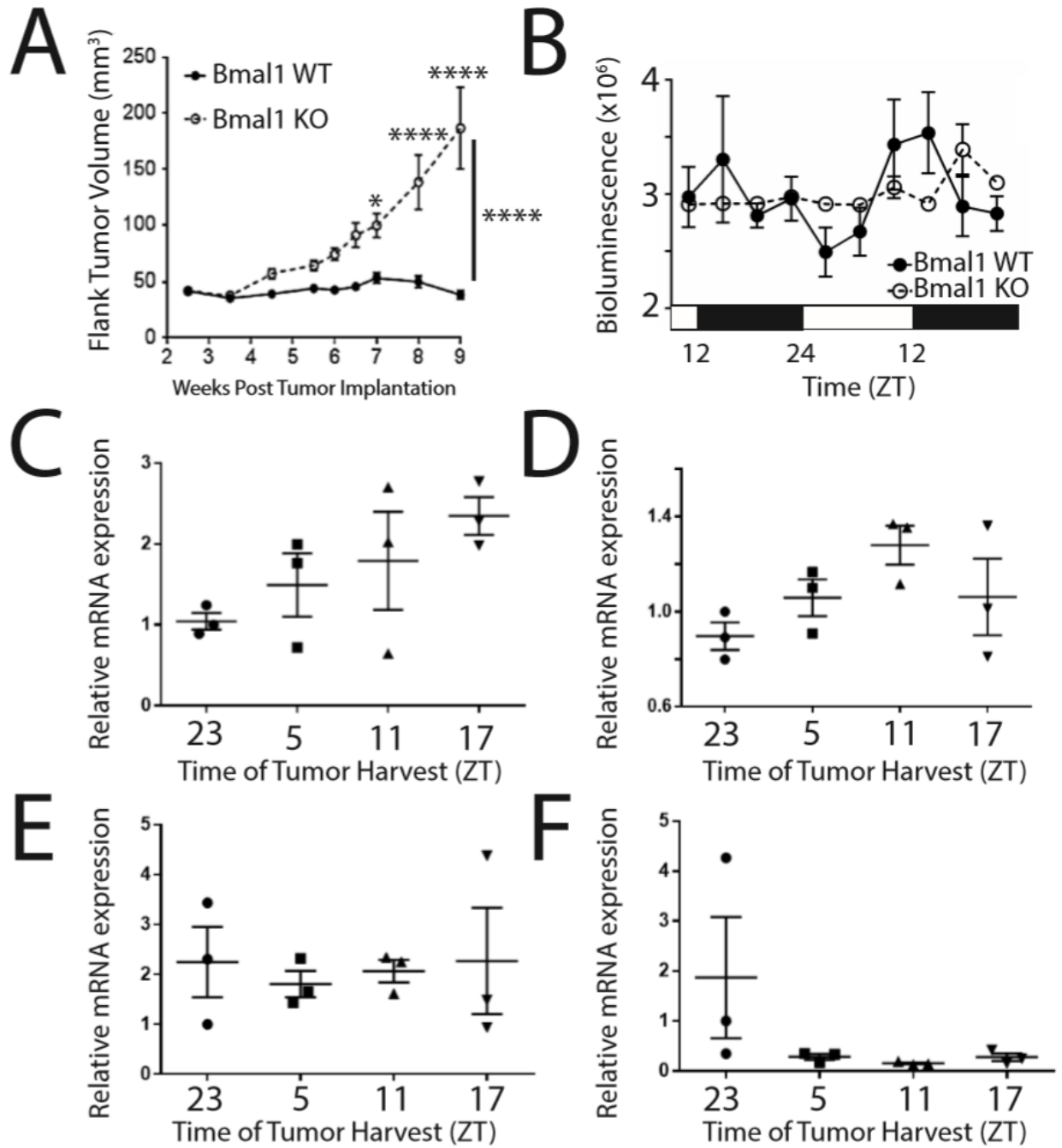


Figure 4.3. *Bmal1* KO flank tumors lose rhythmic clock gene expression and have enhanced tumorigenesis *in vivo*. **A)** Subcutaneous implants of *Bmal1* WT Mes-GBM astrocytes did not form tumors (n = 25). Subcutaneous implantation of *Bmal1* KO Mes-GBM astrocytes led to rapid tumor growth *in vivo* (n = 28). Statistical analyses demonstrate significant difference in flank tumor size between *Bmal1* WT and KO (**** = p<0.0001), and significant growth from 2.5 weeks to 7 weeks (* = p<0.05), 8 and 9 weeks (**** = p<0.0001). **B)** *Bmal1* WT Mes-GBM

astrocytes had circadian rhythms in median *Per2-luc* bioluminescence across 36 hours, reaching peak expression at ZT 15 (10 pm) (JTK Cycle, p-value < 0.05, n = 10). *Bmal1* KO Mes-GBM astrocytes had arrhythmic *Per2-luc* bioluminescence (JTK Cycle, p-value > 0.05 n = 8). **C-F** RT-qPCR of mRNA levels in *Bmal1* KO tumors harvested in triplicate every 6 hours across zeitgeber time (ZT) showed no significant difference in mRNA expression levels across time for *Per2* (**C**), *beta-actin* (**D**), *Atm* (**E**), or *Ppp1r3c* (**F**) using the delta-delta Cq method (One-way ANOVA, p > 0.05, n = 3 per time point).

Bmal1* KO Mes-GBM tumors lack a circadian rhythm in TMZ sensitivity *in vivo

After demonstrating dysregulated clock-controlled gene expression in the *Bmal1* KO tumors, we tested the hypothesis that *Bmal1* KO Mes-GBM tumors would lack rhythmic TMZ sensitivity *in vivo*. As we have demonstrated previously [138], TMZ treatment causes a brief plateau in GBM growth *in vivo*. To test whether the timing of TMZ treatment would alter the duration of TMZ-induced growth inhibition, we treated nude mice with TMZ or DMSO (12AM or 12PM) four weeks after subcutaneous Mes-GBM astrocyte implantation. Flank tumor volumes were measured 2-3 times per week after treatment. Cohort 1 (**Figure 4.4A**) showed a brief plateau in flank tumor growth that was greater in the 12PM TMZ treatment group compared to 12AM TMZ. In contrast, Cohort 2 showed no difference in growth between the two treatment groups (**Figure 4.4B**). There was no significant difference in tumor growth between DMSO- and TMZ-treated *Bmal1* KO tumors in Cohort 1 (**Figure 4.4C**). However, in Cohort 2 the growth rates of the TMZ-treated *Bmal1* KO tumors was significantly less than the growth of the DMSO-treated tumors (**Figure 4.4D**, ANOVA, $p < 0.05$). Overall, there was no consistent difference in long-term *Bmal1* KO tumor growth following treatment at 12AM versus 12PM.

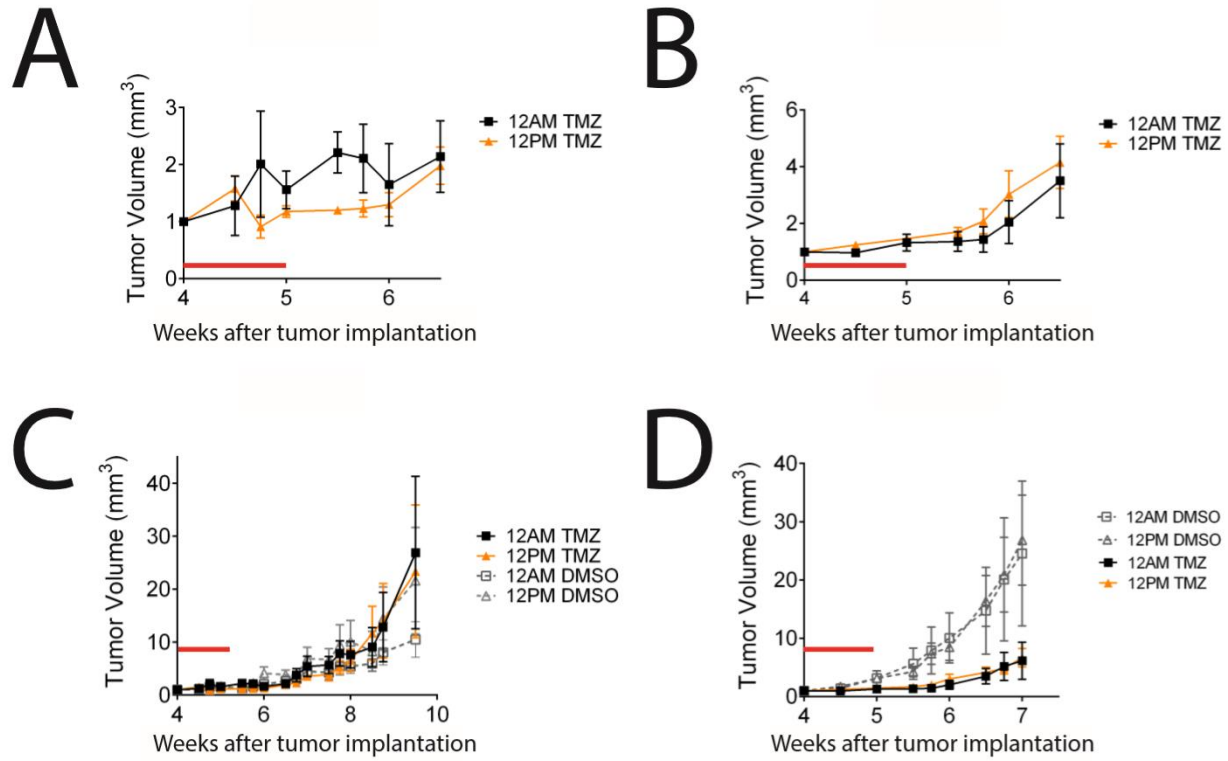


Figure 4.4. Long-term Mes-GBM *Bmal1* KO flank tumor growth after TMZ

chronotherapy *in vivo*. TMZ-induced growth inhibition of flank tumors was measured by digital caliper measures. The first 1.5 weeks after treatment for cohort 1 (**A**) and cohort 2 (**B**) are shown with 12AM TMZ-treated tumors in black and 12PM TMZ-treated tumors in orange, with the red bar representing 5 days of TMZ treatment (n=3 per group). Long-term growth curves of cohort 1 (**C**) and cohort 2 (**D**) show four treatment groups: 12AM TMZ (black square), 12PM TMZ (orange triangle), 12AM DMSO (gray open square), and 12PM DMSO (gray open triangle).

We examined acute TMZ sensitivity in the *Bmal1* KO tumors. To test whether the rhythms in H2AX phosphorylation and caspase cleavage we observed *in vitro* persist *in vivo*, we treated mice bearing *Bmal1* KO Mes-GBM flank tumors with TMZ or DMSO at 2 different times of day: 12AM or 12PM. These times were chosen based on preliminary *Per2-luc* rhythms obtained from *Bmal1* WT Mes-GBM subcutaneous implants, which reached peak *Per2-luc* expression at 2AM (data not shown). Mice were treated once per day, at 12AM or 12PM, for 5 consecutive days. *Bmal1* KO tumor tissue was harvested at 24 h or 36 h after the final treatment. Western blots of histone-extracted tumor tissue were probed for phospho- and total H2AX (Figure 4.5A). Phospho-H2AX was normalized to total H2AX protein for each sample and fold change in H2AX phosphorylation was determined by dividing TMZ-treated tumors by DMSO-treated control tumors. There was no significant difference in TMZ-induced phosphorylation of H2AX between the 12AM and 12PM treatment groups for tissue harvested at 24 h or 36 h post-treatment (Figure 4.5B & C). Westerns of tumor tissue lysate were probed for cleaved caspase-3 and beta-actin (Figure 4.5D). Cleaved caspase-3 was normalized to beta-actin for each sample and fold change in caspase-3 cleavage was determined by dividing TMZ-treated tumor samples by their DMSO-treated controls. There was no significant difference in caspase-3 cleavage between the 12AM and 12PM treatment groups, regardless of the time of tissue harvest (Figures 4.5E & F). These data demonstrate a lack of rhythmicity in acute TMZ sensitivity in *Bmal1* KO Mes-GBM astrocytes *in vivo*.

The clock gene expression in human intracranial U87 xenograft and *Bmal1* WT Mes-GBM flank implants changed in a time of day-dependent manner. Loss of *Bmal1* caused arrhythmic expression of clock-controlled genes in the Mes-GBM astrocytes, *in vivo*. TMZ-induced inhibition of intracranial U87 and *Bmal1* KO Mes-GBM flank tumor growth did not

vary based on timing of TMZ administration. In both sets of experiments, there was a high degree of variability in tumor growth after treatment. Taken together, these data demonstrate an absence of time of day-dependent TMZ sensitivity of GBM tumors *in vivo*.

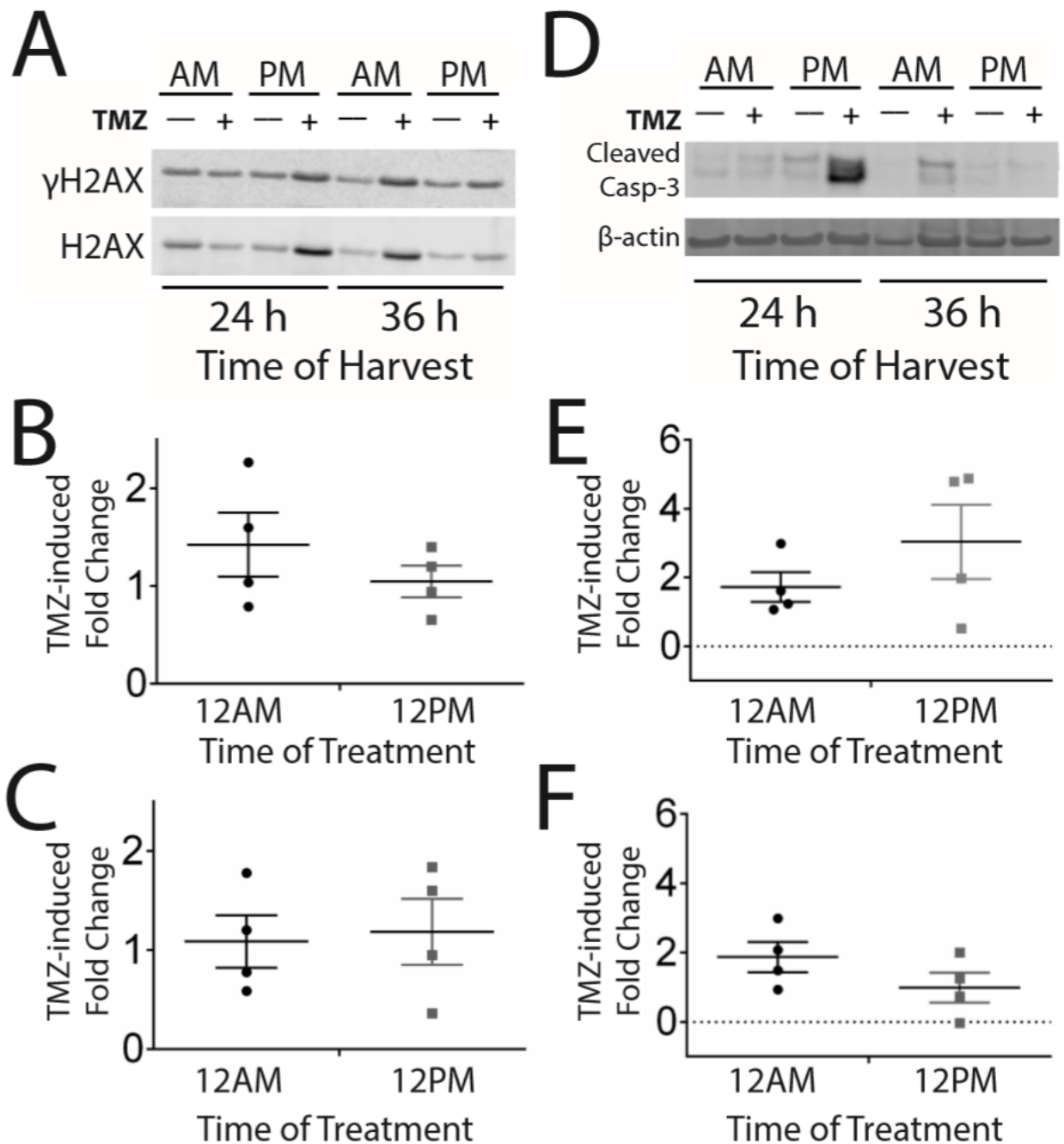


Figure 4.5. Acute DNA damage response and activation of apoptosis does not change with chronotherapy *in vivo*. Representative Western blots of phospho-H2AX (A) and cleaved caspase-3 (D) were quantified in panels B&C and E&F, respectively. B) *Bmal1* KO tumors harvested 24 hours after the fifth and final dose of TMZ showed no difference in

phosphorylation of H2AX between 12AM and 12PM TMZ treatment groups (Student's T-test, $p > 0.05$). **C)** Bmal1 KO tumors harvested 36 hours after the fifth and final dose of TMZ showed no difference in phosphorylation of H2AX (Student's T-test, $p > 0.05$). **E)** TMZ-induced cleavage of caspase-3 was not significantly different between treatment groups for tumors harvested 24 hours after the final TMZ treatment (Student's T-test, $p > 0.05$). **F)** TMZ-induced cleavage of caspase-3 was not significantly different between treatment groups for tumors harvested 36 hours after the final TMZ treatment (Student's T-test, $p > 0.05$).

Discussion

The *in vitro* characterization of the *Bmal1*-dependent rhythms in gene expression and susceptibility to TMZ described in the previous chapters of this thesis has helped us understand more about the molecular clock in glioblastoma, but we also need to understand these rhythms in the context of a more complex *in vivo* system. Does rhythmic clock gene expression persist *in vivo*? If so, are these rhythms *Bmal1*-dependent? Are there times of day-dependent oscillations in TMZ sensitivity *in vivo*? Answering these questions will help us determine how readily our *in vitro* observations can be translated to clinical treatments of GBM patients.

We are the first group to demonstrate circadian rhythms in clock gene expression in glioma cells *in vivo*. We have shown higher *Bmal1-luc* expression at 9am versus 9pm in intracranial U87 xenografts. Alone, the *Bmal1-luc* U87 data do not demonstrate a rhythm, only a morning versus evening difference. With more frequent sampling, we have demonstrated a rhythm in *Per2-luc* expression over time in *Bmal1* WT Mes-GBM astrocytes *in vivo*. Our results are consistent with rhythmic clock gene expression in flank tumor xenografts of a human fibrosarcoma cell line, which also reached peak *Per2-luc* expression during the night [142]. Comas and colleagues showed the phase of *Per2* expression in their tumors was similar to the phases of *Per2* expression in liver, lung and spleen within the same mouse. The rhythmic expression of *Per1-luc* in rat olfactory bulb [143] and *Per2-luc* in mouse olfactory bulb [144] show circadian rhythms in clock gene expression with phases that are consistently in anti-phase with the *Bmal1-luc* expression we showed in the intracranial U87 xenografts. Taken together, these data demonstrate rhythmic clock gene expression in GBM tumors *in vivo*, with peak expression occurring at a time of day consistent with clock gene expression data previously reported in other tissues.

The loss of rhythmic *Per2-luc* bioluminescence in the *Bmal1* KO Mes-GBM flank tumors demonstrates a *Bmal1*-dependent regulation of clock gene expression *in vivo*. RT-qPCR data showing a lack of rhythm in the mRNA expression levels of clock controlled genes (CCGs) *Per2*, *Atm* and *Ppp1r3c* provide further support for the loss of rhythmic expression of CCGs in the *Bmal1* KO Mes-GBM tumors. It is important to recognize that we do not show rhythmic expression of CCGs in *Bmal1* WT Mes-GBM flank tumors. The RT-qPCR data would be stronger if we had demonstrated rhythmic expression of CCGs in *Bmal1* WT tumors and a loss of rhythmic expression in the *Bmal1* KO tumors. However, we did not have enough tissue from the *Bmal1* WT implants to perform RT-qPCR. When we combine the RT-qPCR results with the similarly arrhythmic expression of *Per2-luc* in the *Bmal1* KO flank tumors, we create a stronger argument for the loss of circadian regulation of CCG transcription in the absence of *Bmal1*. This outcome is consistent with our *in vitro* data. However, it conflicts with data from Pando and colleagues, demonstrating a restoration of circadian rhythms in clock gene expression in *Clock/Clock* mutant mouse embryonic fibroblasts implanted subcutaneously in mice with intact circadian rhythms in healthy tissue [145]. The host signal responsible for restoring rhythmic clock gene expression in *Clock/Clock* mutant MEFs is either absent or insufficient to restore rhythms in the *Bmal1* KO Mes-GBM astrocytes. Taken together, these data demonstrate the persistence of rhythmic clock gene expression in the Mes-GBM astrocytes *in vivo*, with *Bmal1*-dependent regulation of rhythmic CCG expression. Further research is needed to help us reconcile the discrepancy between our findings and those of Pando and colleagues.

The TMZ chronotherapy studies in U87 xenograft-bearing mice showed inconsistent anti-tumor activity and no significant changes in overall survival based on the timing of TMZ administration. Intracranial U87 xenografts in two out of three cohorts showed a greater

reduction in tumor burden in mice treated with TMZ at 7AM versus 7PM. Despite these differences in tumor burden, we never saw significant changes in overall survival. It is possible that two cycles of TMZ was insufficient to change overall survival. Additional treatment cycles or higher TMZ doses may alter survival. This outcome is inconsistent with two rodent chronotherapy trials, showing increased tumor regression and improved survival following day time treatment with doxorubicin or early night time treatment with oxaliplatin [134, 135]. Since these trials used different chemotherapies to treat different tumor types, there are many reasons why our data are inconsistent with their outcomes. Based on these data, we cannot conclude a presence or absence of daily rhythms in TMZ anti-tumor activity in GBM *in vivo*. We have demonstrated a lack of change in survival in our U87 intracranial xenograft model of GBM. Future studies should try higher doses of TMZ at a greater variety of treatment times throughout the day to find the optimal benefit of TMZ therapy for GBM.

Following up on these early U87 xenograft studies, we examined the *in vivo* TMZ sensitivity of GBM flank tumors lacking a functional clock. We showed a lack of time of day-dependent TMZ sensitivity in the *Bmal1* KO Mes-GBM flank tumors when measuring acute tumor responses to TMZ and long-term growth inhibition in *BMAL1* KO flank tumors following TMZ chronotherapy. The *Bmal1* WT Mes-GBM flank implants did not form tumors, so we were unable to test the TMZ sensitivity of those GBM cells *in vivo*. Due to the lack of parallel studies in *Bmal1* WT Mes-GBM flank tumors, we cannot conclude that the lack of time of day-dependent sensitivity of *Bmal1* KO Mes-GBM flank tumors is a loss of rhythm. If the *Bmal1* WT flank tumors had grown, they may have also shown no difference in TMZ sensitivity based on the timing of treatment. Two rodent chronotherapy trials demonstrated minimal antitumor activity of cisplatin at all treatment times in a rats with plasmacytoma and mice with pancreatic

adenocarcinoma, regardless of the timing of treatment [135]. We will learn more about the importance of the clock within the tumor by performing future studies in a GBM model system where we can directly compare *Bmal1* WT and *Bmal1* KO TMZ chronotherapy responses *in vivo*.

Very few studies have demonstrated a role for the molecular clock in regulating the sensitivity to chemotherapy *in vivo*. Gorbacheva and colleagues demonstrated time of day-dependent rhythms in cyclophosphamide toxicity in mice. They ablated these daily rhythms in toxicity and increased total toxicity in *Bmal1* KO and *Clock/Clock* mutant mice [146]. Although this study only looked at toxicity in the healthy host tissue, it provides insight into the circadian regulation of chemotherapy. In contrast, overexpression of *Bmal1* in colon cancer flank tumors increased the sensitivity of these flank tumors to oxaliplatin [69]. Together, these data may demonstrate that disruption of the normal oscillations of the clock, through knockout or overexpression, increase sensitivity to chemotherapy.

Chronotherapy has improved clinical outcomes for a variety of cancers. However, this study provides the first application of chronotherapy to brain tumors. These data provide a foundation on which to build a strong case for the application of chronotherapy to brain tumor patients. Our current data suggest a role for *Bmal1* in maintaining circadian oscillations in gene expression *in vivo*. The intracranial and subcutaneous xenograft studies provide insufficient evidence that TMZ chronotherapy will improve tumor growth inhibition or survival in the context of a tumor-bearing host. It is possible that the circadian rhythms we have demonstrated in TMZ sensitivity *in vitro* may not result in improved treatment outcomes in the context of the complex *in vivo* environment. However, we have not proven a lack of rhythm in TMZ sensitivity *in vivo*. Future studies may need to use more sensitive methods of measuring anti-tumor efficacy,

or try treating with higher doses at a greater variety of time points throughout the day in order to discover the optimal timing of TMZ therapy.

Acknowledgements

Special thanks for technical assistance from Erin Smith, Najla Kfoury, Nicole Warrington, Stacey Ward, and Tatiana Simon. Constructive critiques and helpful scientific discussions were provided by many members of the Rubin and Herzog labs. Thanks to Daniel Granados-Fuentes, Luciano Marpegan, Tao Sun, Stacey Ward and Nicole Warrington for expert advice. Thanks to Michael Hughes for helpful advice and for providing JTK Cycle software (University of Missouri- St. Louis, St. Louis, MO). Shondra Miller and the Genome Engineering Center for consultation and gRNA Cas9-CRISPR design and production. Andrew Liu provided the *Bmal1::dLuc* and *Per2::dLuc* lentiviruses.

REFERENCES

1. Stupp, R., et al., *Radiotherapy plus concomitant and adjuvant temozolomide for glioblastoma*. N Engl J Med, 2005. **352**(10): p. 987-96.
2. Beale, P., et al., *Effect of gastric pH on the relative oral bioavailability and pharmacokinetics of temozolomide*. Cancer Chemother Pharmacol, 1999. **44**(5): p. 389-94.
3. Grossman, R., et al., *Microdialysis measurement of intratumoral temozolomide concentration after cediranib, a pan-VEGF receptor tyrosine kinase inhibitor, in a U87 glioma model*. Cancer Chemother Pharmacol, 2013. **72**(1): p. 93-100.
4. Gupta, S.K., et al., *Discordant in vitro and in vivo chemopotentiating effects of the PARP inhibitor veliparib in temozolomide-sensitive versus -resistant glioblastoma multiforme xenografts*. Clin Cancer Res, 2014. **20**(14): p. 3730-41.
5. Kobayashi, M., P.A. Wood, and W.J. Hrushesky, *Circadian chemotherapy for gynecological and genitourinary cancers*. Chronobiol Int, 2002. **19**(1): p. 237-51.
6. Schmiegelow, K., et al., *Impact of morning versus evening schedule for oral methotrexate and 6-mercaptopurine on relapse risk for children with acute lymphoblastic leukemia*. Nordic Society for Pediatric Hematology and Oncology (NOPHO). J Pediatr Hematol Oncol, 1997. **19**(2): p. 102-9.
7. Levi, F., et al., *Chronomodulation of chemotherapy against metastatic colorectal cancer*. International Organization for Cancer Chronotherapy. Eur J Cancer, 1995. **31A**(7-8): p. 1264-70.
8. Vitaterna, M.H., J.S. Takahashi, and F.W. Turek, *Overview of circadian rhythms*. Alcohol Res Health, 2001. **25**(2): p. 85-93.

9. Reppert, S.M. and D.R. Weaver, *Coordination of circadian timing in mammals*. Nature, 2002. **418**(6901): p. 935-41.
10. Preitner, N., et al., *The orphan nuclear receptor REV-ERB α controls circadian transcription within the positive limb of the mammalian circadian oscillator*. Cell, 2002. **110**(2): p. 251-60.
11. Nakajima, Y., et al., *Bidirectional role of orphan nuclear receptor ROR α in clock gene transcriptions demonstrated by a novel reporter assay system*. FEBS Lett, 2004. **565**(1-3): p. 122-6.
12. Sato, T.K., et al., *A functional genomics strategy reveals Rora as a component of the mammalian circadian clock*. Neuron, 2004. **43**(4): p. 527-37.
13. Bunger, M.K., et al., *Mop3 is an essential component of the master circadian pacemaker in mammals*. Cell, 2000. **103**(7): p. 1009-17.
14. Marpegan, L., et al., *Circadian regulation of ATP release in astrocytes*. J Neurosci, 2011. **31**(23): p. 8342-50.
15. Stevens, R.G., *Circadian disruption and breast cancer: from melatonin to clock genes*. Epidemiology, 2005. **16**(2): p. 254-8.
16. Schernhammer, E.S., et al., *Rotating night shifts and risk of breast cancer in women participating in the nurses' health study*. J Natl Cancer Inst, 2001. **93**(20): p. 1563-8.
17. Van Dycke, K.C., et al., *Chronically Alternating Light Cycles Increase Breast Cancer Risk in Mice*. Curr Biol, 2015. **25**(14): p. 1932-7.
18. Levi, F., et al., *Implications of circadian clocks for the rhythmic delivery of cancer therapeutics*. Adv Drug Deliv Rev, 2007. **59**(9-10): p. 1015-35.

19. Wang, F., et al., *Correlation between deregulated expression of PER2 gene and degree of glioma malignancy*. Tumori, 2014. **100**(6): p. e266-72.
20. Kang, T.H. and S.H. Leem, *Modulation of ATR-mediated DNA damage checkpoint response by cryptochrome 1*. Nucleic Acids Res, 2014. **42**(7): p. 4427-34.
21. Unsal-Kacmaz, K., et al., *Coupling of human circadian and cell cycles by the timeless protein*. Mol Cell Biol, 2005. **25**(8): p. 3109-16.
22. Yang, X., P.A. Wood, and W.J. Hrushesky, *Mammalian TIMELESS is required for ATM-dependent CHK2 activation and G2/M checkpoint control*. J Biol Chem, 2010. **285**(5): p. 3030-4.
23. Kemp, M.G., et al., *Tipin-replication protein A interaction mediates Chk1 phosphorylation by ATR in response to genotoxic stress*. J Biol Chem, 2010. **285**(22): p. 16562-71.
24. Smith, K.D., M.A. Fu, and E.J. Brown, *Tim-Tipin dysfunction creates an indispensable reliance on the ATR-Chk1 pathway for continued DNA synthesis*. J Cell Biol, 2009. **187**(1): p. 15-23.
25. Gery, S., et al., *The circadian gene per1 plays an important role in cell growth and DNA damage control in human cancer cells*. Mol Cell, 2006. **22**(3): p. 375-82.
26. Im, J.S., et al., *Per3, a circadian gene, is required for Chk2 activation in human cells*. FEBS Lett, 2010. **584**(23): p. 4731-4.
27. Kang, T.H., et al., *Circadian oscillation of nucleotide excision repair in mammalian brain*. Proc Natl Acad Sci U S A, 2009. **106**(8): p. 2864-7.
28. Fu, L., et al., *The circadian gene Period2 plays an important role in tumor suppression and DNA damage response in vivo*. Cell, 2002. **111**(1): p. 41-50.

29. Matsuo, T., et al., *Control mechanism of the circadian clock for timing of cell division in vivo*. Science, 2003. **302**(5643): p. 255-9.
30. Rana, S., et al., *Deregulated expression of circadian clock and clock-controlled cell cycle genes in chronic lymphocytic leukemia*. Mol Biol Rep, 2014. **41**(1): p. 95-103.
31. Feillet, C., et al., *Coupling between the Circadian Clock and Cell Cycle Oscillators: Implication for Healthy Cells and Malignant Growth*. Front Neurol, 2015. **6**: p. 96.
32. Granda, T.G., et al., *Experimental chronotherapy of mouse mammary adenocarcinoma MA13/C with docetaxel and doxorubicin as single agents and in combination*. Cancer Res, 2001. **61**(5): p. 1996-2001.
33. Granda, T.G. and F. Levi, *Tumor-based rhythms of anticancer efficacy in experimental models*. Chronobiol Int, 2002. **19**(1): p. 21-41.
34. Hori, K., et al., *Timing of cancer chemotherapy based on circadian variations in tumor tissue blood flow*. Int J Cancer, 1996. **65**(3): p. 360-4.
35. Warrington, N.M., et al., *Spatiotemporal differences in CXCL12 expression and cyclic AMP underlie the unique pattern of optic glioma growth in neurofibromatosis type 1*. Cancer Res, 2007. **67**(18): p. 8588-95.
36. Sun, T., et al., *Sexually dimorphic RB inactivation underlies mesenchymal glioblastoma prevalence in males*. J Clin Invest, 2014. **124**(9): p. 4123-33.
37. Tu, H.C., et al., *The p53-cathepsin axis cooperates with ROS to activate programmed necrotic death upon DNA damage*. Proc Natl Acad Sci U S A, 2009. **106**(4): p. 1093-8.
38. Liu, A.C., et al., *Redundant function of REV-ERB α and β and non-essential role for Bmal1 cycling in transcriptional regulation of intracellular circadian rhythms*. PLoS Genet, 2008. **4**(2): p. e1000023.

39. Zhang, E.E., et al., *A genome-wide RNAi screen for modifiers of the circadian clock in human cells*. Cell, 2009. **139**(1): p. 199-210.
40. Ramanathan, C., et al., *Monitoring cell-autonomous circadian clock rhythms of gene expression using luciferase bioluminescence reporters*. J Vis Exp, 2012(67).
41. Yang, L., et al., *Blocking CXCR4-mediated cyclic AMP suppression inhibits brain tumor growth in vivo*. Cancer Res, 2007. **67**(2): p. 651-8.
42. Goldhoff, P., et al., *Targeted inhibition of cyclic AMP phosphodiesterase-4 promotes brain tumor regression*. Clin Cancer Res, 2008. **14**(23): p. 7717-25.
43. Livak, K.J. and T.D. Schmittgen, *Analysis of relative gene expression data using real-time quantitative PCR and the 2(-Delta Delta C(T)) Method*. Methods, 2001. **25**(4): p. 402-8.
44. Gross, S. and D. Piwnica-Worms, *Real-time imaging of ligand-induced IKK activation in intact cells and in living mice*. Nat Methods, 2005. **2**(8): p. 607-14.
45. Hughes, M.E., J.B. Hogenesch, and K. Kornacker, *JTK_CYCLE: an efficient nonparametric algorithm for detecting rhythmic components in genome-scale data sets*. J Biol Rhythms, 2010. **25**(5): p. 372-80.
46. Rubin, J.B., et al., *A small-molecule antagonist of CXCR4 inhibits intracranial growth of primary brain tumors*. Proc Natl Acad Sci U S A, 2003. **100**(23): p. 13513-8.
47. Comas, M., et al., *Daily rhythms are retained both in spontaneously developed sarcomas and in xenografts grown in immunocompromised SCID mice*. Chronobiol Int, 2014. **31**(8): p. 901-10.
48. Abraham, U., et al., *Independent circadian oscillations of Period1 in specific brain areas in vivo and in vitro*. J Neurosci, 2005. **25**(38): p. 8620-6.

49. Miller, J.E., et al., *Vasoactive intestinal polypeptide mediates circadian rhythms in mammalian olfactory bulb and olfaction*. J Neurosci, 2014. **34**(17): p. 6040-6.
50. Pando, M.P., et al., *Phenotypic rescue of a peripheral clock genetic defect via SCN hierarchical dominance*. Cell, 2002. **110**(1): p. 107-17.
51. Gorbacheva, V.Y., et al., *Circadian sensitivity to the chemotherapeutic agent cyclophosphamide depends on the functional status of the CLOCK/BMAL1 transactivation complex*. Proc Natl Acad Sci U S A, 2005. **102**(9): p. 3407-12.
52. Zeng, Z.L., et al., *Overexpression of the circadian clock gene Bmal1 increases sensitivity to oxaliplatin in colorectal cancer*. Clin Cancer Res, 2014. **20**(4): p. 1042-52.

Chapter 5: Discussion

The poor prognosis of GBM has motivated a number of scientists and clinicians to seek novel therapeutic strategies to fight these high grade gliomas. The addition of temozolomide (TMZ) increased median survival by 2.5 months over surgery and radiation alone. Additional lengthening of median survival by an additional 2.5 months or more would be a breakthrough in GBM treatment. Improvement of clinical outcomes in the treatment of other cancers has been achieved by timing the administration of chemotherapy to biological rhythms, a technique known as chronotherapy. This thesis extends the application of chronotherapy to gliomas for the first time in order to enhance treatment outcomes using temozolomide, a drug currently used as standard therapy for high grade gliomas. In light of the success of chronotherapy for other cancers, this thesis attempts to answer four questions: 1) What are the characteristics of the molecular clock in glioma cells? If there is an intact clock in glioma cells, 2) Is there a time of day-dependent oscillation in TMZ sensitivity? 3) If a rhythm exists, is it dependent upon a functional molecular clock? 4) If we identify rhythms in TMZ sensitivity *in vitro*, will those rhythms persist *in vivo*? Through a series *in vitro* and *in vivo* experiments, this study demonstrates circadian rhythms in clock gene expression. This study also demonstrates a *Bmal1*-dependent GBM tumor cell-intrinsic sensitivity to temozolomide (TMZ) that oscillates in a time of day-dependent manner *in vitro*. However, our current studies do not demonstrate a persistence of this rhythmic sensitivity *in vivo*. Further work needs to be done to evaluate the circadian rhythms in TMZ sensitivity of GBM *in vivo*.

Circadian oscillations in clock gene expression in GBM *in vitro* and *in vivo*

Daily oscillations in *Per2* and *Bmal1* luciferase reporters in U87 and Mes-GBM

astrocytes demonstrated that glioma cells have an intact molecular clock *in vitro*. Many human cancer cell lines that have been tested do not have rhythmic clock gene expression (Robert Dallman and John Hogenesch, personal communication). Clock gene expression in U87 cells and Mes-GBM astrocytes had average periods of 24.5 h and 23.3 h, respectively, showing reliable near-24 hour rhythms in clock gene expression *in vitro*. Anti-phase oscillations of *Per2-luc* and *Bmal1-luc*, with peaks occurring 12.1 hours apart on average, demonstrate canonical regulation of the molecular clock within the U87 cells. In contrast, the average time between *Bmal1* and *Per2* peaks in Mes-GBM astrocyte cultures is 8.8 ± 2.1 h, demonstrating that *Bmal1* and *Per2* are often, but not always, expressed in anti-phase *in vitro*. This imperfect phase relationship between the positive and negative arms of the molecular clock may have contributed to variations between replicate experiments. Overall, these data demonstrate reliable circadian oscillations in gene expression in two different glioma cultures *in vitro*.

Bioluminescence imaging of *Bmal1* and *Per2* reporters showed diurnal rhythms in clock gene expression in two *in vivo* GBM models. We demonstrated higher *Bmal1-luc* expression at 9AM versus 9PM in U87 intracranial xenografts, which only supports a day-night difference in *Bmal1* expression. With more frequent sampling, we demonstrated *Per2-luc* rhythms in *Bmal1* WT Mes-GBM astrocyte subcutaneous implants. By sampling every 4 hours across 36 hours, we were able to demonstrate peak *Per2* expression at 10PM (ZT 15) on two consecutive days. High *Bmal1* expression in U87 xenografts in the morning and high *Per2* expression at night in Mes-GBM flank implants supports an anti-phase relationship between *Bmal1* and *Per2* expression in GBM *in vivo*. Definitive evidence of an anti-phase relationship between *Bmal1* and *Per2* *in vivo*

would require imaging *Bmal1-luc* and *Per2-luc*-expressing GBM tumors simultaneously *in vivo*. These data support reliable diurnal rhythms in clock gene expression in two models of GBM *in vivo*. To define these clock gene expression rhythms as circadian we would need to house the mice in constant darkness before measuring *Per2-luc* expression *in vivo*. Our results are consistent with rhythmic clock gene expression in flank tumor xenografts of a human fibrosarcoma cell line, which also reached peak *Per2* expression during the night [142]. Together, these data demonstrate a diurnal rhythm in clock gene expression in GBM cells *in vivo*.

We next examined the phase relationships of clock gene expression in the GBM cells to neighboring tissues *in vivo*. The rhythmic expression of *Per1-luc* in rat olfactory bulb [143] and *Per2-luc* in mouse olfactory bulb [144] show circadian rhythms in clock gene expression with phases that are consistently in anti-phase with the *Bmal1-luc* expression we showed in the intracranial U87 xenografts. We have also demonstrated *Per2* rhythms in the skin of *Per2-luc* knock-in mice with peak expression at 11PM (ZT16), near the time of peak *Per2* expression in the *Bmal1* WT tumors. These data are consistent with a publication showing similar phases of *Per2* expression in colon cancer cell flank tumors and liver, lung and spleen within the same mouse [142]. Taken together, these data demonstrate similar phases of clock gene expression in GBM cells and neighboring healthy host cells *in vivo*.

The phase relationship we observe between GBM cells and host tissue suggests, but does not prove that GBM cells entrain to host rhythms. To test the hypothesis that GBM cells entrain to host rhythms, future studies would need to house GBM tumor-bearing mice in shifting lighting schedules. If the GBM cells entrain to host rhythms, a shift in the lighting schedule would shift clock gene expression rhythms in the tumor. Comas and colleagues were able to shift

Bmal1 and *Per2* expression in fibrosarcoma flank tumors by entraining the mice to a restricted feeding schedule [142]. We could adopt their protocol and restrict feeding to the day (rest) time for the mice and assess rhythms in *Per2-luc* after their activity rhythms have entrained to the new feeding schedule. Current evidence suggests GBM rhythms are synchronized to the host, but further research is required to determine whether GBM rhythms in clock gene expression can be entrained to host rhythms.

The loss of rhythmic *Per2-luc* expression in the *Bmal1* KO Mes-GBM flank tumors demonstrates a *Bmal1*-dependent regulation of clock gene expression *in vivo*. RT-qPCR data showing a lack of rhythm in the mRNA expression levels of clock controlled genes (CCGs) *Per2*, *Atm* and *Ppp1r3c* provided further support for the loss of rhythmic expression of CCGs in the *Bmal1* KO Mes-GBM tumors. It is important to recognize that we do not show rhythmic expression of CCGs in *Bmal1* WT Mes-GBM flank tumors. The RT-qPCR data would be stronger if we had demonstrated rhythmic expression of CCGs in *Bmal1* WT tumors and a loss of rhythmic expression in the *Bmal1* KO tumors. However, we did not have enough tissue from the *Bmal1* WT implants to perform RT-qPCR. When we combine the RT-qPCR results with the similarly arrhythmic expression of *Per2-luc* in the *Bmal1* KO flank tumors, we create a stronger argument for the loss of circadian regulation of CCG transcription in the absence of *Bmal1*. This outcome is consistent with our *in vitro* data, demonstrating a loss of *Per2-luc* rhythms in *Bmal1* KO Mes-GBM astrocytes. However, it conflicts with data from Pando and colleagues, demonstrating a restoration of circadian rhythms in clock gene expression in *Clock/Clock* mutant mouse embryonic fibroblasts (MEFs) implanted subcutaneously in mice with intact circadian rhythms in healthy tissue [145]. The host signal responsible for restoring rhythmic clock gene expression in *Clock/Clock* mutant MEFs is either absent or insufficient to restore rhythms in the

Bmall KO Mes-GBM astrocytes. Taken together, these data demonstrate the persistence of rhythmic clock gene expression in the Mes-GBM astrocytes *in vivo*, with *Bmall*-dependent regulation of rhythmic CCG expression. Further research is needed to help us reconcile the discrepancy between our findings and those of Pando and colleagues.

Time of day-dependent rhythms in response to temozolomide treatment *in vitro*

This thesis demonstrates cell-intrinsic circadian rhythms in sensitivity of a human U87 glioblastoma cell line and a mouse model of glioblastoma (*Nf1*^{-/-};*DNp53* astrocytes) to temozolomide (TMZ). The amount of TMZ-induced growth inhibition varied based on the time of day of treatment, achieving greatest growth inhibition at the peak of *Bmall* expression in both GBM models. Consistent with these findings, we also demonstrated a circadian rhythm in activation of apoptosis in Mes-GBM astrocytes, achieving greatest induction of apoptosis when treating at the *Bmall* peak. This is consistent with data demonstrating reduced apoptosis following *Bmall* knockdown in colon cancer cell lines *in vitro* [68]. Demonstrating a rhythm in TMZ-induced cell death was a promising start, which led us to search for rhythms in response to TMZ treatment at a higher level of the DNA damage response pathway.

We knew TMZ treatment exerted its cytotoxicity through the formation of double strand breaks (DSBs), so we examined phosphorylation of histone H2AX at serine 139, an early step in the cellular response to DSB formation. We have identified circadian rhythms in TMZ-induced phosphorylation of H2AX in both GBM models *in vitro*. At any point in time, the level of H2AX phosphorylation reflects the balance between the sensing of DSBs, which recruits DNA repair proteins to sites of damage near phosphorylated H2AX, and DNA repair, which causes dephosphorylation of H2AX. With this in mind, there are several potential interpretations of the

data. First, the oscillations in phospho-H2AX may reflect a daily rhythm in the number of DSBs induced by TMZ. Second, these oscillations may result from rhythms in ATM-induced phosphorylation of H2AX following induction of DNA damage. Third, these oscillations may reflect a time of day-dependent rhythm in the kinetics of DNA repair and dephosphorylation of H2AX. It is also possible that the rhythm we measure is a combination of rhythms in two or more of these processes. There are currently no publications demonstrating a circadian rhythm in H2AX phosphorylation. However, there are studies supporting the enhanced ATM-dependent phosphorylation of Chk2 following overexpression of Per1 or Per3 [70, 71]. It is possible that the enhanced interactions of ATM with Chk2 reduce the availability of ATM to phosphorylate H2AX, but there is currently no evidence to support this hypothesis. Further studies are needed to understand how components of the core molecular clock regulate H2AX phosphorylation.

At every level where we have tested for rhythms in TMZ sensitivity, we have found them. We have seen a consistent correlation between the peak of *Bmal1* and the maximal measures of H2AX phosphorylation, caspase activity and growth inhibition. Consistent with our studies, Dulong and colleagues demonstrated an endogenous circadian rhythm in irinotecan-induced cytotoxicity in colon cancer cells with greatest cytotoxicity occurring at the peak of *Bmal1* expression *in vitro*. Taken together, these studies correlate *Bmal1* expression with sensitivity to DNA damaging agents in tumor cells.

Where does the cell-intrinsic rhythm in TMZ response originate?

We have characterized the circadian rhythm in TMZ sensitivity in our GBM model system, but we have not yet identified a specific mechanism that creates the rhythm. One possible explanation of the consistent rhythms measured at the levels of DNA repair, apoptosis and growth inhibition is that the molecular clock could directly regulate the DNA damage

response at many levels simultaneously. Or, we could interpret our observations of a rhythm at the levels of DNA repair and apoptosis as the reflections of a rhythm created at a single point early in the pathway. These rhythms could originate at the level of DNA repair, but we cannot draw that conclusion based on current results.

We have not yet ruled out the possibility that rhythms in the amount of DNA damage induced by TMZ at different times of day may underlie the circadian rhythms we have observed in TMZ sensitivity. *Clock* knockdown increased the amount of radiation-induced DNA damage in U87 cells [147]. In contrast, *Bmal1* knockdown reduced cisplatin-induced DNA damage in colon cancer cell lines [68]. Despite the conflicting results from these two studies, both demonstrated links between the molecular clock and induction of DNA damage. A rhythm in cell cycle regulation could create an oscillation in the number of TMZ-induced DNA double strand breaks. In future studies, quantifying EdU incorporation at each of the 4 circadian times of treatment would tell us whether or not there is a rhythm in cell cycle progression through S phase. If this experiment identifies a rhythm in EdU incorporation, it would provide an opportunity for more double strand breaks to occur at the time of day when the largest percentage of tumor cells are in S phase. Several cell cycle regulators have already been identified as clock controlled genes. So, it is possible that circadian rhythms exist in the regulation of cell cycle progression in the Mes-GBM astrocytes. Another possible mechanism underlying rhythmic TMZ sensitivity is the TMZ concentration within tumor cells at different times of day. Rhythms in the expression or activity of drug efflux pumps could alter intracellular TMZ concentrations, causing a rhythm in the amount of TMZ-induced DNA damage. Dulong and colleagues recently demonstrated a rhythm in pharmacokinetics of irinotecan underlying circadian sensitivity to the drug *in vitro* [94]. Further evaluation is required to determine whether

the rhythm in TMZ sensitivity exists at the level of DNA damage induction or regulation of the response to DNA damage.

Role of *Bmal1* in temozolomide sensitivity

To test whether the circadian oscillation in TMZ-induced growth inhibition was created by a rhythm in cell death, we examined the activation of the apoptotic pathway in response to TMZ treatment at different times of day. TMZ-induced DNA damage led to a time of day-dependent rhythm in apoptosis in the Mes-GBM astrocytes. The bioluminescent caspase 3/7 activity reporter used in Figure 4 shows highest caspase 3 activity at the peak of *Bmal1* expression. Because caspases 3 and 7 are downstream effector caspases in the apoptotic pathway, their activation irreversibly leads to programmed cell death [148]. Therefore, the time of day-dependent oscillation observed in TMZ-induced caspase 3 and 7 activity demonstrates a circadian rhythm in apoptotic cell death. The loss of rhythmic activation of apoptosis in *Bmal1* KO Mes-GBM astrocytes demonstrated that *Bmal1* was required for creating this rhythm. All evidence in the literature supporting circadian regulation of apoptosis involves genetic manipulation of clock gene expression. These findings are consistent with reports of reduction in etoposide-induced apoptosis of colon cancer cells after *Bmal1* knockdown [68]. *Bmal1* knockdown also led to reduced irinotecan-induced apoptosis [94]. In contrast, a number of studies have demonstrated increased expression of Period genes with increased apoptosis. *Per1* overexpression increased the rate of apoptosis in response to ionizing radiation [70] and *Per2* and *Per3* overexpression induced increased apoptosis in the absence of DNA-damaging agents [71, 81]. Taken together, these data show that components of the core molecular clock are capable of regulating apoptosis; however, the conflicting outcomes of genetic manipulation of cancer cells

in these studies demonstrates the need for further evaluation of the interactions between the circadian and apoptotic pathways.

Future studies could manipulate Bmal1 expression and function to further characterize the role of Bmal1 in DNA damage response. Overexpression of Bmal1 increases sensitivity of colon cancer cells to oxaliplatin [69]. Overexpression of Bmal1 in the Mes-GBM astrocytes would test the sufficiency of Bmal1 for the induction of high levels of activation of apoptosis. To test whether the transcription factor activity of Bmal1 is responsible for regulating TMZ sensitivity, we could express Bmal1 with a mutated DNA binding domain in *Bmal1* KO Mes-GBM astrocytes. If the binding domain-mutated Bmal1 does not rescue the *Bmal1* KO phenotype, then we could conclude DNA binding activity of Bmal1 is required for its regulation of TMZ sensitivity, likely through the transcriptional activation of one or more clock controlled genes. Manipulation of Bmal1 expression and transcriptional activity may provide clues to the mechanism that creates circadian oscillations in TMZ sensitivity.

Bmal1 protein-protein interactions should also be tested to determine if Bmal1 regulates susceptibility to TMZ through a DNA binding-independent mechanism. Immunoprecipitation of Bmal1 followed by identification of proteins in complex with Bmal1 would provide a list of candidates potentially involved in regulating the DNA damage response. There are currently no published reports of DNA damage response-related proteins interacting with Bmal1. However, a high throughput screen identified Clock as a modulator of DNA damage-induced ATR signaling and demonstrated co-localization of *CLOCK* with phospho-H2AX [149]. This was the first report of a direct interaction of the transcription factor Clock with proteins involved in DDR. Many studies have assumed that *CLOCK* and *BMAL1* exert their regulation of the response to DNA damage solely through transcriptional activity, but that may not be the case. Identification

of *BMAL1* protein binding partners after induction of DNA damage may help elucidate the key regulators of the *Bmal1*-dependent regulation of TMZ sensitivity rhythms.

It is possible that the *Bmal1* KO phenotype is related solely to *Bmal1*'s role as a transcription factor, not necessarily as a regulator of the molecular clock. To test the role of the molecular clock more directly, we could delete *CRY1* and *CRY2* to abolish circadian rhythms in transcriptional activation of clock-controlled genes. This would get rid of the daily rhythms of the molecular clock without hindering the activity of *Bmal1*. If the results of the *CRY1/2* DKO studies corroborate the results of our *Bmal1* KO studies, it will provide even stronger evidence that the *Bmal1* -dependent TMZ sensitivity is a molecular clock-dependent rhythm.

Based on *Bmal1* knockout studies performed in other cell types [60, 64, 65], we predicted that loss of *Bmal1* would lead to loss of daily oscillations in *Per2* expression. We have demonstrated rhythmic expression of the *Per2-luc* bioluminescent reporter *in vitro*. Loss of *Bmal1* leads to arrhythmic expression of *Per2-luc in vitro*. We use the *Per2-luc* reporter as a way to detect and measure oscillations in clock-controlled genes. The loss of rhythm in TMZ sensitivity in the *Bmal1* KO Mes-GBM astrocytes provides an output supporting this assumption. It will be important for future studies to identify specific clock-controlled genes contributing to the *Bmal1* -dependent rhythmicity in TMZ sensitivity in GBM. Comparing microarray data from *Bmal1* WT and *Bmal1* KO Mes-GBM astrocytes harvested every 2 hours across 48 hours will reveal genes with *Bmal1* -dependent rhythms in expression. Within the resulting list of genes, there are likely to be some genes with known functions related to the DNA damage response. These will be candidates for key regulators of the mechanism underlying the circadian regulation of TMZ sensitivity observed in Mes-GBM astrocytes in this study.

Chronotherapy has improved clinical outcomes for a variety of cancers. However, this study provides the first application of chronotherapy to brain tumors. These results provide a foundation on which to build a strong case for the application of chronotherapy to brain tumor patients.

Role of *Bmal1* in GBM tumorigenesis *in vivo*

We observed enhanced tumorigenesis in the *Bmal1* KO Mes-GBM astrocytes *in vivo*. The *Bmal1* WT Mes-GBM astrocytes implanted subcutaneously survived for the duration of our studies, but did not form tumors. In contrast, the *Bmal1* KO Mes-GBM astrocytes formed rapidly growing tumors in two independent cohorts of mice. These data are consistent with a study showing accelerated growth of colorectal cancer flank tumors with reduced *Bmal1* expression [68]. Zeng and colleagues also demonstrated that *Bmal1* knockdown increased proliferation of colorectal cancer cells *in vitro* [68]. In line with these observations, overexpression of *Bmal1* reduced colorectal cancer flank tumor growth [69]. Taken together, these data demonstrate a role for *Bmal1* in suppressing cancer cell proliferation and tumorigenesis.

Temozolomide chronotherapy of GBM *in vivo*

The *in vitro* characterization of the *Bmal1*-dependent rhythms in gene expression and susceptibility to TMZ has helped us understand more about the molecular clock in glioblastoma, but we also need to understand these rhythms in the context of a more complex *in vivo* system. Using two mouse models of GBM, we tested whether the rhythms in TMZ sensitivity we identified *in vitro* persisted *in vivo*.

The TMZ chronotherapy studies in U87 xenograft-bearing mice showed inconsistent anti-tumor activity and no significant changes in overall survival based on the timing of TMZ administration. Intracranial U87 xenografts in two out of three cohorts showed a greater

reduction in tumor burden in mice treated with TMZ at 7AM versus 7PM. Despite these differences in tumor burden, we never saw significant changes in overall survival. It is possible that two cycles of TMZ was insufficient to change overall survival. Additional treatment cycles or higher TMZ doses may alter survival. This outcome is inconsistent with two rodent chronotherapy trials, showing increased tumor regression and improved survival following day time treatment with doxorubicin or early night time treatment with oxaliplatin [134, 135]. Since these trials used different chemotherapies to treat different tumor types, there are many reasons why our data are inconsistent with their outcomes. Based on these data, we cannot conclude a presence or absence of daily rhythms in TMZ anti-tumor activity in GBM *in vivo*. We have demonstrated a lack of change in survival in our U87 intracranial xenograft model of GBM. Future studies should try higher doses of TMZ at a greater variety of treatment times throughout the day to find the optimal benefit of TMZ therapy for GBM.

Following up on these early U87 xenograft studies, we examined the *in vivo* TMZ sensitivity of GBM flank tumors lacking a functional clock. We showed a lack of time of day-dependent TMZ sensitivity in the *Bmal1* KO Mes-GBM flank tumors when measuring acute tumor responses to TMZ and long-term growth inhibition in *Bmal1* KO flank tumors following TMZ chronotherapy. The *Bmal1* WT Mes-GBM flank implants did not form tumors, so we were unable to test the TMZ sensitivity of those GBM cells *in vivo*. Due to the lack of parallel studies in *Bmal1* WT Mes-GBM flank tumors, we cannot conclude that the lack of time of day-dependent sensitivity of *Bmal1* KO Mes-GBM flank tumors is a loss of rhythm. If the *Bmal1* WT flank tumors had grown, they may have also shown no difference in TMZ sensitivity based on the timing of treatment. Two rodent chronotherapy trials demonstrated minimal antitumor activity of cisplatin at all treatment times in a rats with plasmacytoma and mice with pancreatic

adenocarcinoma, regardless of the timing of treatment [135]. We will learn more about the importance of the clock within the tumor by performing future studies in a GBM model system where we can directly compare *Bmal1* WT and *Bmal1* KO TMZ chronotherapy responses *in vivo*.

Very few studies have demonstrated a role for the molecular clock in regulating the sensitivity to chemotherapy *in vivo*. Gorbacheva and colleagues demonstrated time of day-dependent rhythms in cyclophosphamide toxicity in mice. They ablated these daily rhythms in toxicity and increased total toxicity in *Bmal1* KO and *Clock/Clock* mutant mice [146]. Although this study only looked at toxicity in the healthy host tissue, it provides insight into the circadian regulation of chemotherapy. In contrast, overexpression of *Bmal1* in colon cancer flank tumors increased the sensitivity of these flank tumors to oxaliplatin [69]. Together, these data may demonstrate that disruption of the normal oscillations of the clock, through knockout or overexpression, increase sensitivity to chemotherapy.

Chronotherapy has improved clinical outcomes for a variety of cancers. However, this study provides the first application of chronotherapy to brain tumors. These data provide a foundation on which to build a strong case for the application of chronotherapy to brain tumor patients. Our *in vivo* GBM studies provide insufficient evidence that TMZ chronotherapy will improve tumor growth inhibition or survival in the context of a tumor-bearing host. It is possible that the circadian rhythms we have demonstrated in TMZ sensitivity *in vitro* may not result in improved treatment outcomes in the context of the complex *in vivo* environment. However, we have not proven a lack of rhythmicity in TMZ sensitivity *in vivo*. Future studies may need to use more sensitive methods of measuring anti-tumor efficacy, or treating at a greater variety of time points throughout the day in order to discover the optimal timing of TMZ therapy.

Clinical Applications of Chronotherapy for Brain Cancer

Through these studies, we provide a foundation for future applications of chronotherapy to brain tumors in additional mouse models and in human GBM patients. Using GBM as a model system, we have characterized the role of tumor cell-intrinsic circadian rhythms in response to chronomodulated chemotherapy. The results of our studies can be applied to a variety of other tumor types in future studies.

Concepts tested in this thesis can be applied to TMZ treatment of GBM patients in the clinic. Based on these studies, we will perform a retrospective study to review chart information from GBM patients treated with TMZ in the morning or the evening. We recently discovered that two neuro-oncologists at Barnes-Jewish Hospital advised their patients to take their TMZ at two different times of day: early in the morning, or at night before bed. We have received IRB approval to perform a chart review of these patients. We will compare hematologic toxicity and survival in these patients to see if there are statistically significant differences in clinical outcomes based on the time of day of treatment. Retrospective studies have some disadvantages; the inability to randomize patients to treatment groups creates selection bias in the study, we rely on notes in the chart to be detailed and accurate for each patient and we have no way of confirming that the patients took the TMZ at the times of day recommended by their neuro-oncologist. Retrospective studies are not perfect, but they help us gather preliminary information to lay the groundwork for future prospective studies. We have also put together a prospective trial for future GBM patients at Barnes-Jewish Hospital. The patients will be randomized to morning or evening adjuvant TMZ treatments (after the completion of radiation therapy and concomitant TMZ). We will monitor quality of life, hematologic toxicity, tumor response, and survival in these patients to see if timing of TMZ therapy alters any of these clinical outcomes.

We will also monitor daily rest-activity rhythms to correlate the behavioral circadian rhythms of these patients to clinical outcomes. This prospective clinical trial will gather information to lay the groundwork for larger trials that could be created in the future.

The outcomes of these studies could be applied to the use of other DNA damaging agents in the future, including ionizing radiation. Rahn and colleagues published a study reporting greater survival of patients with brain metastases of non-small cell lung cancer following gamma knife radiosurgery in the morning compared to afternoon [150]. If the principles underlying the circadian regulation of DNA damage response can be applied to all treatments that induce DNA double strand breaks, then this study provides the basis for applications to a variety of cancer types and treatment types. To determine how generalizable the findings of this study might be, it will be important to test for circadian regulation of DNA damage response in a variety of cell types. It will also be important to test a variety of DNA-damaging agents. The pharmacokinetics of other chemotherapies may guide the optimal timing of treatment, but the immediate formation of double strand breaks following ionizing radiation makes radiation therapy a logical next step in testing the generalizability of chronomodulation of therapeutic DNA-damaging agents in the treatment of GBM, and other cancers.

Conclusions

The mechanism by which daily oscillations occur in TMZ sensitivity to glioblastoma remains unclear; however, we were able to demonstrate for the first time a Bmal1-dependent rhythm in sensitivity to DNA damaging chemotherapy in GBM *in vitro*. Our study extends the chronotherapy literature to a new class of chemotherapy, DNA alkylators. The consistency of our findings with the findings of other studies evaluating the circadian regulation of tumor response to DNA damage demonstrates a common outcome among different cancer cell types and different DNA-damaging agents. This suggests that the mechanism of cellular response to DNA damage may be the common pathway regulated in response to a variety of chemotherapies. Future studies are necessary to identify the specific mechanism of circadian regulation of DNA damage response. Identification of such a mechanism would allow us to extend the application of chronotherapy to even more chemotherapies and cancer types.

References

1. Agnihotri, S., et al., *Glioblastoma, a brief review of history, molecular genetics, animal models and novel therapeutic strategies*. Arch Immunol Ther Exp (Warsz), 2013. **61**(1): p. 25-41.
2. Ferguson, S. and M.S. Lesniak, *Percival Bailey and the classification of brain tumors*. Neurosurg Focus, 2005. **18**(4): p. e7.
3. Louis, D.N., et al., *The 2007 WHO classification of tumours of the central nervous system*. Acta Neuropathol, 2007. **114**(2): p. 97-109.
4. Karsy, M., et al., *Established and emerging variants of glioblastoma multiforme: review of morphological and molecular features*. Folia Neuropathol, 2012. **50**(4): p. 301-21.
5. Ostrom, Q.T., et al., *CBTRUS statistical report: Primary brain and central nervous system tumors diagnosed in the United States in 2006-2010*. Neuro Oncol, 2013. **15 Suppl 2**: p. ii1-56.
6. Ostrom, Q.T., et al., *CBTRUS statistical report: primary brain and central nervous system tumors diagnosed in the United States in 2007-2011*. Neuro Oncol, 2014. **16 Suppl 4**: p. iv1-63.
7. Sturm, D., et al., *Paediatric and adult glioblastoma: multiform (epi)genomic culprits emerge*. Nat Rev Cancer, 2014. **14**(2): p. 92-107.
8. Qaddoumi, I., I. Sultan, and A. Gajjar, *Outcome and prognostic features in pediatric gliomas: a review of 6212 cases from the Surveillance, Epidemiology, and End Results database*. Cancer, 2009. **115**(24): p. 5761-70.
9. Sanders, R.P., et al., *High-grade astrocytoma in very young children*. Pediatr Blood Cancer, 2007. **49**(7): p. 888-93.
10. Huse, J.T. and M.K. Rosenblum, *The Emerging Molecular Foundations of Pediatric Brain Tumors*. J Child Neurol, 2015.
11. Morokoff, A., et al., *Molecular subtypes, stem cells and heterogeneity: Implications for personalised therapy in glioma*. J Clin Neurosci, 2015. **22**(8): p. 1219-26.
12. Ohgaki, H. and P. Kleihues, *Population-based studies on incidence, survival rates, and genetic alterations in astrocytic and oligodendroglial gliomas*. J Neuropathol Exp Neurol, 2005. **64**(6): p. 479-89.
13. Dunn, G.P., et al., *Emerging insights into the molecular and cellular basis of glioblastoma*. Genes Dev, 2012. **26**(8): p. 756-84.
14. Sun, T., N.M. Warrington, and J.B. Rubin, *Why does Jack, and not Jill, break his crown? Sex disparity in brain tumors*. Biol Sex Differ, 2012. **3**: p. 3.
15. Phillips, H.S., et al., *Molecular subclasses of high-grade glioma predict prognosis, delineate a pattern of disease progression, and resemble stages in neurogenesis*. Cancer Cell, 2006. **9**(3): p. 157-73.
16. Verhaak, R.G., et al., *Integrated genomic analysis identifies clinically relevant subtypes of glioblastoma characterized by abnormalities in PDGFRA, IDH1, EGFR, and NF1*. Cancer Cell, 2010. **17**(1): p. 98-110.
17. Huse, J.T., E. Holland, and L.M. DeAngelis, *Glioblastoma: molecular analysis and clinical implications*. Annu Rev Med, 2013. **64**: p. 59-70.
18. Frankel, S.A. and W.J. German, *Glioblastoma multiforme; review of 219 cases with regard to natural history, pathology, diagnostic methods, and treatment*. J Neurosurg, 1958. **15**(5): p. 489-503.
19. Maher, E.A., et al., *Malignant glioma: genetics and biology of a grave matter*. Genes Dev, 2001. **15**(11): p. 1311-33.
20. Shapiro, W.R., et al., *Randomized trial of three chemotherapy regimens and two radiotherapy regimens in postoperative treatment of malignant glioma. Brain Tumor Cooperative Group Trial 8001*. J Neurosurg, 1989. **71**(1): p. 1-9.

21. Stupp, R., et al., *Radiotherapy plus concomitant and adjuvant temozolomide for glioblastoma*. N Engl J Med, 2005. **352**(10): p. 987-96.
22. Hirose, Y., et al., *Delayed repletion of O6-methylguanine-DNA methyltransferase resulting in failure to protect the human glioblastoma cell line SF767 from temozolomide-induced cytotoxicity*. J Neurosurg, 2003. **98**(3): p. 591-8.
23. Hegi, M.E., et al., *MGMT gene silencing and benefit from temozolomide in glioblastoma*. N Engl J Med, 2005. **352**(10): p. 997-1003.
24. Wick, W., et al., *MGMT testing--the challenges for biomarker-based glioma treatment*. Nat Rev Neurol, 2014. **10**(7): p. 372-85.
25. Kitange, G.J., et al., *Induction of MGMT expression is associated with temozolomide resistance in glioblastoma xenografts*. Neuro Oncol, 2009. **11**(3): p. 281-91.
26. Ohka, F., A. Natsume, and T. Wakabayashi, *Current trends in targeted therapies for glioblastoma multiforme*. Neurol Res Int, 2012. **2012**: p. 878425.
27. Levi, F. and A. Okyar, *Circadian clocks and drug delivery systems: impact and opportunities in chronotherapeutics*. Expert Opin Drug Deliv, 2011. **8**(12): p. 1535-41.
28. Rivard, G.E., et al., *Maintenance chemotherapy for childhood acute lymphoblastic leukaemia: better in the evening*. Lancet, 1985. **2**(8467): p. 1264-6.
29. Rivard, G.E., et al., *Circadian time-dependent response of childhood lymphoblastic leukemia to chemotherapy: a long-term follow-up study of survival*. Chronobiol Int, 1993. **10**(3): p. 201-4.
30. Schmiegelow, K., et al., *Impact of morning versus evening schedule for oral methotrexate and 6-mercaptopurine on relapse risk for children with acute lymphoblastic leukemia*. Nordic Society for Pediatric Hematology and Oncology (NOPHO). J Pediatr Hematol Oncol, 1997. **19**(2): p. 102-9.
31. Petit, E., et al., *Circadian rhythm-varying plasma concentration of 5-fluorouracil during a five-day continuous venous infusion at a constant rate in cancer patients*. Cancer Res, 1988. **48**(6): p. 1676-9.
32. Lincoln, D.W., 2nd, W.J. Hrushesky, and P.A. Wood, *Circadian organization of thymidylate synthase activity in normal tissues: a possible basis for 5-fluorouracil chronotherapeutic advantage*. Int J Cancer, 2000. **88**(3): p. 479-85.
33. Harris, B.E., et al., *Relationship between dihydropyrimidine dehydrogenase activity and plasma 5-fluorouracil levels with evidence for circadian variation of enzyme activity and plasma drug levels in cancer patients receiving 5-fluorouracil by protracted continuous infusion*. Cancer Res, 1990. **50**(1): p. 197-201.
34. Zhang, R., et al., *Relationship between circadian-dependent toxicity of 5-fluorodeoxyuridine and circadian rhythms of pyrimidine enzymes: possible relevance to fluoropyrimidine chemotherapy*. Cancer Res, 1993. **53**(12): p. 2816-22.
35. Levi, F., et al., *Chronomodulation of chemotherapy against metastatic colorectal cancer*. International Organization for Cancer Chronotherapy. Eur J Cancer, 1995. **31A**(7-8): p. 1264-70.
36. Kobayashi, M., P.A. Wood, and W.J. Hrushesky, *Circadian chemotherapy for gynecological and genitourinary cancers*. Chronobiol Int, 2002. **19**(1): p. 237-51.
37. Paschos, G.K., et al., *The role of clock genes in pharmacology*. Annu Rev Pharmacol Toxicol, 2010. **50**: p. 187-214.
38. Schernhammer, E.S., et al., *Night work and risk of breast cancer*. Epidemiology, 2006. **17**(1): p. 108-11.
39. Lie, J.A., J. Roessink, and K. Kjaerheim, *Breast cancer and night work among Norwegian nurses*. Cancer Causes Control, 2006. **17**(1): p. 39-44.

40. Van Dycke, K.C., et al., *Chronically Alternating Light Cycles Increase Breast Cancer Risk in Mice*. *Curr Biol*, 2015. **25**(14): p. 1932-7.
41. Davis, S. and D.K. Mirick, *Circadian disruption, shift work and the risk of cancer: a summary of the evidence and studies in Seattle*. *Cancer Causes Control*, 2006. **17**(4): p. 539-45.
42. Davis, S., D.K. Mirick, and R.G. Stevens, *Night shift work, light at night, and risk of breast cancer*. *J Natl Cancer Inst*, 2001. **93**(20): p. 1557-62.
43. Hansen, J., *Increased breast cancer risk among women who work predominantly at night*. *Epidemiology*, 2001. **12**(1): p. 74-7.
44. Schernhammer, E.S., et al., *Rotating night-shift work and lung cancer risk among female nurses in the United States*. *Am J Epidemiol*, 2013. **178**(9): p. 1434-41.
45. Gu, F., et al., *Total and cause-specific mortality of U.S. nurses working rotating night shifts*. *Am J Prev Med*, 2015. **48**(3): p. 241-52.
46. Schernhammer, E.S., et al., *Rotating night shifts and risk of skin cancer in the nurses' health study*. *J Natl Cancer Inst*, 2011. **103**(7): p. 602-6.
47. Schernhammer, E.S., et al., *Rotating night shifts and risk of breast cancer in women participating in the nurses' health study*. *J Natl Cancer Inst*, 2001. **93**(20): p. 1563-8.
48. Papantoniou, K., et al., *Night shift work, chronotype and prostate cancer risk in the MCC-Spain case-control study*. *Int J Cancer*, 2014.
49. Bhatti, P., et al., *Nightshift work and risk of ovarian cancer*. *Occup Environ Med*, 2013. **70**(4): p. 231-7.
50. Hahn, R.A., *Profound bilateral blindness and the incidence of breast cancer*. *Epidemiology*, 1991. **2**(3): p. 208-10.
51. Feychting, M., B. Osterlund, and A. Ahlbom, *Reduced cancer incidence among the blind*. *Epidemiology*, 1998. **9**(5): p. 490-4.
52. Straif, K., et al., *Carcinogenicity of shift-work, painting, and fire-fighting*. *Lancet Oncol*, 2007. **8**(12): p. 1065-6.
53. Levi, F., et al., *Wrist actimetry circadian rhythm as a robust predictor of colorectal cancer patients survival*. *Chronobiol Int*, 2014. **31**(8): p. 891-900.
54. Vitaterna, M.H., J.S. Takahashi, and F.W. Turek, *Overview of circadian rhythms*. *Alcohol Res Health*, 2001. **25**(2): p. 85-93.
55. McClung, C.R., *Plant circadian rhythms*. *Plant Cell*, 2006. **18**(4): p. 792-803.
56. Dunlap, J.C., *Molecular bases for circadian clocks*. *Cell*, 1999. **96**(2): p. 271-90.
57. Golden, S.S., et al., *Cyanobacterial Circadian Rhythms*. *Annu Rev Plant Physiol Plant Mol Biol*, 1997. **48**: p. 327-354.
58. Gallego, M. and D.M. Virshup, *Post-translational modifications regulate the ticking of the circadian clock*. *Nat Rev Mol Cell Biol*, 2007. **8**(2): p. 139-48.
59. Ramanathan, C., et al., *Monitoring cell-autonomous circadian clock rhythms of gene expression using luciferase bioluminescence reporters*. *J Vis Exp*, 2012(67).
60. Bunger, M.K., et al., *Mop3 is an essential component of the master circadian pacemaker in mammals*. *Cell*, 2000. **103**(7): p. 1009-17.
61. DeBruyne, J.P., D.R. Weaver, and S.M. Reppert, *CLOCK and NPAS2 have overlapping roles in the suprachiasmatic circadian clock*. *Nat Neurosci*, 2007. **10**(5): p. 543-5.
62. Vitaterna, M.H., et al., *Differential regulation of mammalian period genes and circadian rhythmicity by cryptochromes 1 and 2*. *Proc Natl Acad Sci U S A*, 1999. **96**(21): p. 12114-9.
63. Zheng, B., et al., *Nonredundant roles of the mPer1 and mPer2 genes in the mammalian circadian clock*. *Cell*, 2001. **105**(5): p. 683-94.

64. Marpegan, L., et al., *Circadian regulation of ATP release in astrocytes*. J Neurosci, 2011. **31**(23): p. 8342-50.
65. Vollmers, C., S. Panda, and L. DiTacchio, *A high-throughput assay for siRNA-based circadian screens in human U2OS cells*. PLoS One, 2008. **3**(10): p. e3457.
66. Shi, S., et al., *Circadian clock gene Bmal1 is not essential; functional replacement with its paralog, Bmal2*. Curr Biol, 2010. **20**(4): p. 316-21.
67. Fu, L., et al., *The circadian gene Period2 plays an important role in tumor suppression and DNA damage response in vivo*. Cell, 2002. **111**(1): p. 41-50.
68. Zeng, Z.L., et al., *Effects of the biological clock gene Bmal1 on tumour growth and anti-cancer drug activity*. J Biochem, 2010. **148**(3): p. 319-26.
69. Zeng, Z.L., et al., *Overexpression of the circadian clock gene Bmal1 increases sensitivity to oxaliplatin in colorectal cancer*. Clin Cancer Res, 2014. **20**(4): p. 1042-52.
70. Gery, S., et al., *The circadian gene per1 plays an important role in cell growth and DNA damage control in human cancer cells*. Mol Cell, 2006. **22**(3): p. 375-82.
71. Im, J.S., et al., *Per3, a circadian gene, is required for Chk2 activation in human cells*. FEBS Lett, 2010. **584**(23): p. 4731-4.
72. Lee, J.H. and A. Sancar, *Circadian clock disruption improves the efficacy of chemotherapy through p73-mediated apoptosis*. Proc Natl Acad Sci U S A, 2011. **108**(26): p. 10668-72.
73. Brown, E.J. and D. Baltimore, *Essential and dispensable roles of ATR in cell cycle arrest and genome maintenance*. Genes Dev, 2003. **17**(5): p. 615-28.
74. Unsal-Kacmaz, K., et al., *Coupling of human circadian and cell cycles by the timeless protein*. Mol Cell Biol, 2005. **25**(8): p. 3109-16.
75. Chou, D.M. and S.J. Elledge, *Tipin and Timeless form a mutually protective complex required for genotoxic stress resistance and checkpoint function*. Proc Natl Acad Sci U S A, 2006. **103**(48): p. 18143-7.
76. Lemar, A.R., et al., *Human Timeless and Tipin stabilize replication forks and facilitate sister-chromatid cohesion*. J Cell Sci, 2010. **123**(Pt 5): p. 660-70.
77. Kang, T.H. and S.H. Leem, *Modulation of ATR-mediated DNA damage checkpoint response by cryptochrome 1*. Nucleic Acids Res, 2014. **42**(7): p. 4427-34.
78. Kang, T.H., et al., *Circadian oscillation of nucleotide excision repair in mammalian brain*. Proc Natl Acad Sci U S A, 2009. **106**(8): p. 2864-7.
79. Gaddameedhi, S., et al., *Control of skin cancer by the circadian rhythm*. Proc Natl Acad Sci U S A, 2011. **108**(46): p. 18790-5.
80. Matsuo, T., et al., *Control mechanism of the circadian clock for timing of cell division in vivo*. Science, 2003. **302**(5643): p. 255-9.
81. Hua, H., et al., *Circadian gene mPer2 overexpression induces cancer cell apoptosis*. Cancer Sci, 2006. **97**(7): p. 589-96.
82. Ogura, K., et al., *Initial and cumulative recurrence patterns of glioblastoma after temozolomide-based chemoradiotherapy and salvage treatment: a retrospective cohort study in a single institution*. Radiat Oncol, 2013. **8**: p. 97.
83. Stupp, R., et al., *Effects of radiotherapy with concomitant and adjuvant temozolomide versus radiotherapy alone on survival in glioblastoma in a randomised phase III study: 5-year analysis of the EORTC-NCIC trial*. Lancet Oncol, 2009. **10**(5): p. 459-66.
84. Levi, F., et al., *Implications of circadian clocks for the rhythmic delivery of cancer therapeutics*. Adv Drug Deliv Rev, 2007. **59**(9-10): p. 1015-35.
85. Jiang, G., et al., *Strategies to improve the killing of tumors using temozolomide: targeting the DNA repair protein MGMT*. Curr Med Chem, 2012. **19**(23): p. 3886-92.

86. Marpegan, L., T.J. Krall, and E.D. Herzog, *Vasoactive intestinal polypeptide entrains circadian rhythms in astrocytes*. J Biol Rhythms, 2009. **24**(2): p. 135-43.
87. Prolo, L.M., J.S. Takahashi, and E.D. Herzog, *Circadian rhythm generation and entrainment in astrocytes*. J Neurosci, 2005. **25**(2): p. 404-8.
88. Beaulé, C., et al., *In vitro circadian rhythms: imaging and electrophysiology*. Essays Biochem, 2011. **49**(1): p. 103-17.
89. Liu, A.C., et al., *Redundant function of REV-ERB α and beta and non-essential role for Bmal1 cycling in transcriptional regulation of intracellular circadian rhythms*. PLoS Genet, 2008. **4**(2): p. e1000023.
90. Zhang, E.E., et al., *A genome-wide RNAi screen for modifiers of the circadian clock in human cells*. Cell, 2009. **139**(1): p. 199-210.
91. Bonner, W.M., et al., *GammaH2AX and cancer*. Nat Rev Cancer, 2008. **8**(12): p. 957-67.
92. Collins, A.R., *The comet assay for DNA damage and repair: principles, applications, and limitations*. Mol Biotechnol, 2004. **26**(3): p. 249-61.
93. Mozaffarieh, M., et al., *Comet assay analysis of single-stranded DNA breaks in circulating leukocytes of glaucoma patients*. Mol Vis, 2008. **14**: p. 1584-8.
94. Dulong, S., et al., *Identification of circadian determinants of cancer chronotherapy through in vitro chronopharmacology and mathematical modeling*. Mol Cancer Ther, 2015.
95. Oklejewicz, M., et al., *Phase resetting of the mammalian circadian clock by DNA damage*. Curr Biol, 2008. **18**(4): p. 286-91.
96. Hong, C.I., J. Zamborszky, and A. Csikasz-Nagy, *Minimum criteria for DNA damage-induced phase advances in circadian rhythms*. PLoS Comput Biol, 2009. **5**(5): p. e1000384.
97. Papp, S.J., et al., *DNA damage shifts circadian clock time via Hausp-dependent Cry1 stabilization*. Elife, 2015. **4**.
98. Friedman, H.S., et al., *Methylator resistance mediated by mismatch repair deficiency in a glioblastoma multiforme xenograft*. Cancer Res, 1997. **57**(14): p. 2933-6.
99. Stevens, M.F., et al., *Antitumor activity and pharmacokinetics in mice of 8-carbamoyl-3-methylimidazo[5,1-d]-1,2,3,5-tetrazin-4(3H)-one (CCRG 81045; M & B 39831), a novel drug with potential as an alternative to dacarbazine*. Cancer Res, 1987. **47**(22): p. 5846-52.
100. Newlands, E.S., et al., *Phase I trial of temozolomide (CCRG 81045; M&B 39831; NSC 362856)*. Br J Cancer, 1992. **65**(2): p. 287-91.
101. Beale, P., et al., *Effect of gastric pH on the relative oral bioavailability and pharmacokinetics of temozolomide*. Cancer Chemother Pharmacol, 1999. **44**(5): p. 389-94.
102. Grossman, R., et al., *Microdialysis measurement of intratumoral temozolomide concentration after cediranib, a pan-VEGF receptor tyrosine kinase inhibitor, in a U87 glioma model*. Cancer Chemother Pharmacol, 2013. **72**(1): p. 93-100.
103. Gupta, S.K., et al., *Discordant in vitro and in vivo chemopotentiating effects of the PARP inhibitor veliparib in temozolomide-sensitive versus -resistant glioblastoma multiforme xenografts*. Clin Cancer Res, 2014. **20**(14): p. 3730-41.
104. Reppert, S.M. and D.R. Weaver, *Coordination of circadian timing in mammals*. Nature, 2002. **418**(6901): p. 935-41.
105. Preitner, N., et al., *The orphan nuclear receptor REV-ERB α controls circadian transcription within the positive limb of the mammalian circadian oscillator*. Cell, 2002. **110**(2): p. 251-60.
106. Nakajima, Y., et al., *Bidirectional role of orphan nuclear receptor ROR α in clock gene transcriptions demonstrated by a novel reporter assay system*. FEBS Lett, 2004. **565**(1-3): p. 122-6.

107. Sato, T.K., et al., *A functional genomics strategy reveals Rora as a component of the mammalian circadian clock*. *Neuron*, 2004. **43**(4): p. 527-37.
108. Stevens, R.G., *Circadian disruption and breast cancer: from melatonin to clock genes*. *Epidemiology*, 2005. **16**(2): p. 254-8.
109. Wang, F., et al., *Correlation between deregulated expression of PER2 gene and degree of glioma malignancy*. *Tumori*, 2014. **100**(6): p. e266-72.
110. Yu, C., et al., *Hypoxia disrupts the expression levels of circadian rhythm genes in hepatocellular carcinoma*. *Mol Med Rep*, 2015. **11**(5): p. 4002-8.
111. Rana, S., et al., *Deregulated expression of circadian clock and clock-controlled cell cycle genes in chronic lymphocytic leukemia*. *Mol Biol Rep*, 2014. **41**(1): p. 95-103.
112. Sahar, S. and P. Sassone-Corsi, *Circadian clock and breast cancer: a molecular link*. *Cell Cycle*, 2007. **6**(11): p. 1329-31.
113. Lin, Y.M., et al., *Disturbance of circadian gene expression in hepatocellular carcinoma*. *Mol Carcinog*, 2008. **47**(12): p. 925-33.
114. Yang, X., P.A. Wood, and W.J. Hrushesky, *Mammalian TIMELESS is required for ATM-dependent CHK2 activation and G2/M checkpoint control*. *J Biol Chem*, 2010. **285**(5): p. 3030-4.
115. Kemp, M.G., et al., *Tipin-replication protein A interaction mediates Chk1 phosphorylation by ATR in response to genotoxic stress*. *J Biol Chem*, 2010. **285**(22): p. 16562-71.
116. Smith, K.D., M.A. Fu, and E.J. Brown, *Tim-Tipin dysfunction creates an indispensable reliance on the ATR-Chk1 pathway for continued DNA synthesis*. *J Cell Biol*, 2009. **187**(1): p. 15-23.
117. Feillet, C., et al., *Coupling between the Circadian Clock and Cell Cycle Oscillators: Implication for Healthy Cells and Malignant Growth*. *Front Neurol*, 2015. **6**: p. 96.
118. Warrington, N.M., et al., *Spatiotemporal differences in CXCL12 expression and cyclic AMP underlie the unique pattern of optic glioma growth in neurofibromatosis type 1*. *Cancer Res*, 2007. **67**(18): p. 8588-95.
119. Sun, T., et al., *Sexually dimorphic RB inactivation underlies mesenchymal glioblastoma prevalence in males*. *J Clin Invest*, 2014. **124**(9): p. 4123-33.
120. Tu, H.C., et al., *The p53-cathepsin axis cooperates with ROS to activate programmed necrotic death upon DNA damage*. *Proc Natl Acad Sci U S A*, 2009. **106**(4): p. 1093-8.
121. Galban, S., et al., *Imaging proteolytic activity in live cells and animal models*. *PLoS One*, 2013. **8**(6): p. e66248.
122. Livak, K.J. and T.D. Schmittgen, *Analysis of relative gene expression data using real-time quantitative PCR and the 2(-Delta Delta C(T)) Method*. *Methods*, 2001. **25**(4): p. 402-8.
123. Brennan, C.W., et al., *The somatic genomic landscape of glioblastoma*. *Cell*, 2013. **155**(2): p. 462-77.
124. Cancer Genome Atlas Research, N., et al., *Integrated genomic characterization of endometrial carcinoma*. *Nature*, 2013. **497**(7447): p. 67-73.
125. Robinson, D., et al., *Integrative clinical genomics of advanced prostate cancer*. *Cell*, 2015. **161**(5): p. 1215-28.
126. Cancer Genome Atlas Research, N., *Integrated genomic analyses of ovarian carcinoma*. *Nature*, 2011. **474**(7353): p. 609-15.
127. Cancer Genome Atlas Research, N., *Comprehensive genomic characterization of squamous cell lung cancers*. *Nature*, 2012. **489**(7417): p. 519-25.
128. Cancer Genome Atlas, N., *Comprehensive molecular portraits of human breast tumours*. *Nature*, 2012. **490**(7418): p. 61-70.
129. Cancer Genome Atlas, N., *Comprehensive molecular characterization of human colon and rectal cancer*. *Nature*, 2012. **487**(7407): p. 330-7.

130. Cancer Genome Atlas Research, N., *Comprehensive molecular characterization of clear cell renal cell carcinoma*. *Nature*, 2013. **499**(7456): p. 43-9.
131. Cancer Genome Atlas Research, N., *Genomic and epigenomic landscapes of adult de novo acute myeloid leukemia*. *N Engl J Med*, 2013. **368**(22): p. 2059-74.
132. Giacchetti, S., et al., *Sex moderates circadian chemotherapy effects on survival of patients with metastatic colorectal cancer: a meta-analysis*. *Ann Oncol*, 2012.
133. Rogakou, E.P., et al., *Megabase chromatin domains involved in DNA double-strand breaks in vivo*. *J Cell Biol*, 1999. **146**(5): p. 905-16.
134. Granda, T.G., et al., *Experimental chronotherapy of mouse mammary adenocarcinoma MA13/C with docetaxel and doxorubicin as single agents and in combination*. *Cancer Res*, 2001. **61**(5): p. 1996-2001.
135. Granda, T.G. and F. Levi, *Tumor-based rhythms of anticancer efficacy in experimental models*. *Chronobiol Int*, 2002. **19**(1): p. 21-41.
136. Hori, K., et al., *Timing of cancer chemotherapy based on circadian variations in tumor tissue blood flow*. *Int J Cancer*, 1996. **65**(3): p. 360-4.
137. Yang, L., et al., *Blocking CXCR4-mediated cyclic AMP suppression inhibits brain tumor growth in vivo*. *Cancer Res*, 2007. **67**(2): p. 651-8.
138. Goldhoff, P., et al., *Targeted inhibition of cyclic AMP phosphodiesterase-4 promotes brain tumor regression*. *Clin Cancer Res*, 2008. **14**(23): p. 7717-25.
139. Gross, S. and D. Piwnica-Worms, *Real-time imaging of ligand-induced IKK activation in intact cells and in living mice*. *Nat Methods*, 2005. **2**(8): p. 607-14.
140. Hughes, M.E., J.B. Hogenesch, and K. Kornacker, *JTK_CYCLE: an efficient nonparametric algorithm for detecting rhythmic components in genome-scale data sets*. *J Biol Rhythms*, 2010. **25**(5): p. 372-80.
141. Rubin, J.B., et al., *A small-molecule antagonist of CXCR4 inhibits intracranial growth of primary brain tumors*. *Proc Natl Acad Sci U S A*, 2003. **100**(23): p. 13513-8.
142. Comas, M., et al., *Daily rhythms are retained both in spontaneously developed sarcomas and in xenografts grown in immunocompromised SCID mice*. *Chronobiol Int*, 2014. **31**(8): p. 901-10.
143. Abraham, U., et al., *Independent circadian oscillations of Period1 in specific brain areas in vivo and in vitro*. *J Neurosci*, 2005. **25**(38): p. 8620-6.
144. Miller, J.E., et al., *Vasoactive intestinal polypeptide mediates circadian rhythms in mammalian olfactory bulb and olfaction*. *J Neurosci*, 2014. **34**(17): p. 6040-6.
145. Pando, M.P., et al., *Phenotypic rescue of a peripheral clock genetic defect via SCN hierarchical dominance*. *Cell*, 2002. **110**(1): p. 107-17.
146. Gorbacheva, V.Y., et al., *Circadian sensitivity to the chemotherapeutic agent cyclophosphamide depends on the functional status of the CLOCK/BMAL1 transactivation complex*. *Proc Natl Acad Sci U S A*, 2005. **102**(9): p. 3407-12.
147. Wang, F., et al., *The Circadian Gene Clock Plays an Important Role in Cell Apoptosis and the DNA Damage Response In Vitro*. *Technol Cancer Res Treat*, 2015.
148. Boatright, K.M. and G.S. Salvesen, *Mechanisms of caspase activation*. *Curr Opin Cell Biol*, 2003. **15**(6): p. 725-31.
149. Cotta-Ramusino, C., et al., *A DNA damage response screen identifies RHINO, a 9-1-1 and TopBP1 interacting protein required for ATR signaling*. *Science*, 2011. **332**(6035): p. 1313-7.
150. Rahn, D.A., 3rd, et al., *Gamma knife radiosurgery for brain metastasis of nonsmall cell lung cancer: is there a difference in outcome between morning and afternoon treatment?* *Cancer*, 2011. **117**(2): p. 414-20.